A COMPARISON OF TWO

HYDROLOGIC MODELING APPROACHES

A COMPARISON OF TWO HYDROLOGIC MODELING APPROACHES FOR THE ESTIMATION OF FLOOD FREQUENCY DISTRIBUTIONS

By

MATTHEW SENIOR, B.ENG.SOCIETY

A Thesis

Submitted to the School of Graduate Studies

in Partial Fulfilment of the Requirements

for the Degree

Master of Applied Science

McMaster University

ACKNOWLEDGEMENTS

I wish to thank my thesis supervisor, Dr. Yiping Guo, for his guidance and for his patience in helping me complete this work.

I would also like to thank the Natural Sciences and Engineering Research Council of Canada (NSERC) and McMaster University (in particular the Department of Civil Engineering) for financial support of this work.

I would also like to thank my employer, the Hamilton Conservation Authority, and in particular my supervisor, George Stojanovic, for allowing me the flexibility and time off required to finally finish my thesis.

To my parents I owe thanks for not only financial support, but for their encouragement and love as well.

Last (but definitely not least) to my wonderful wife Leah I owe endless thanks for her patience and support. The excuses for not being able to do housework end now.

TABLE OF CONTENTS

LIST OF FIGURES

LIST OF TABLES

CHAPTER 1: INTRODUCTION

1.1 WATER AND THE HYDROLOGIC CYCLE

The importance of water to man cannot be overstated. It is essential for our daily survival: without adequate drinking water, we dehydrate and ultimately perish. This is clear when one considers that the average adult is in fact composed of approximately 60% water by body weight (Lefever Kee et al., 2004).

We use water in countless other ways as well. We rely on rainwater to irrigate the crops that we eat, and to provide plants with part of the photosynthetic equation that helps produce oxygen for us to breathe. We use water for cleaning, for manufacturing, for navigation and shipping, for generating electricity, and in some cases, for shelter (in the form of snow in igloos and quinzhees).

The water we so depend on is continuously changing forms and locations. The hydrologic cycle describes the processes by which the Earth's water (some 50 billion cubic feet in total) moves (McCuen, 2005). The cycle is driven by the force of gravity and the continuous energy supply of the sun. As the total amount of water is fixed, the hydrologic cycle can be seen as a closed system for the Earth (Viessman, Jr. and Lewis, 2003). As a closed system, the hydrologic cycle has no real beginning or ending, but is rather a continuous loop of processes and sub-processes.

1.2 HYDROLOGIC MODELLING

There are numerous definitions of a model, however a general definition is that a model is a simplified representation of a complex system (Clarke, 1973). In the case of a hydrologic model, the complex system being represented is either part or all of the hydrologic cycle. It is the complexity of the hydrologic cycle that lends itself well to the modelling approach. As Singh (1988a) notes, we cannot hope to understand hydrologic systems in complete detail. Abstraction (replacing the system with a similar, but simplified, model representation) is therefore necessary for understanding and control (Singh, 1988a). With hydrologic models, scientists and engineers are not just limited to analysis using existing hydrologic data, which may be sparse or non-existent. Hydrologic models allow scientists and engineers to examine a variety of different conditions and scenarios, and to model a great variety of different output parameters.

There are a great number of different types of hydrologic models. Each offers a different method of analyzing and understanding the hydrologic cycle. The focus of this thesis is upon a specific group of hydrologic models – deterministic models. Deterministic models are those where the inputs and processes are considered to be known with certainty, and are free of random variation (USACE, 2000). For engineers practicing in the water resources area, these are likely the most commonly applied group of models. As such, they deserve special attention. Specifically, water resources engineers typically

concern themselves with deterministic stormwater models, or what are usually referred to as rainfall-runoff models.

Rainfall-runoff models are a specific group of hydrologic models that are interested with only a portion of the hydrologic cycle. Specifically, they concern themselves with only those processes occurring over land. Detailed atmospheric and oceanic processes are typically not considered in rainfall-runoff models. As the name implies, they use rainfall data as input in order to simulate the runoff response – the outflow caused by the rainfall for a certain drainage area. The majority of these models are deemed to be deterministic, because, as previously defined, their inputs, parameters and processes are considered to be known with certainty (USACE, 2000). Or, put another way, the behaviour of every variable is completely determined by the governing equations (ASCE, 1982). There is a further subdivision of such models into the empirical/component and conceptual/integrated approaches. In terms of rainfall-runoff models, the distinction depends on how the whole process is viewed, and the knowledge base of the underlying formulae. If the rainfall-runoff process is simplified into a direct relationship between input and output, based on experimental or observational data, then the model is deemed to be empirical/component (Fleming, 1979). An example would be the widely used rational method, originally credited to Mulvaney (1850), which relates peak flow to rainfall intensity, drainage basin area, and a runoff coefficient. No attempt is made in such a model to account for the underlying processes which cause the

transformation for rainfall to runoff. If these component processes are accounted for, the rainfall-runoff model is deemed to be a conceptual or integrated model. Conceptual/integrated rainfall-runoff models therefore offer a much more robust and accurate method of hydrologic analysis than empirical/component methods.

Conceptual/integrated rainfall-runoff models have grown in use and popularity since their inception, mainly due to the increased availability of computers. They allow for the integration of the complex processes underlying the rainfall-runoff process, and permit rapid calculations. They allow water resources engineers to simulate runoff hydrographs and examine different scenarios for watersheds, and to design water resources infrastructure. They also allow for more detailed outputs with multiple parameters, such as peak flow and runoff volume. Such conceptual/integrated rainfall-runoff models are invaluable in addressing many of the issues discussed in Section 1.1, such as analyzing the effects of increased urbanization and deforestation, and assessing flood risks. Numerous computer programs have been written which implement this rainfall-runoff modelling approach. Popular programs include the US Army Corp of Engineers' Hydrologic Modeling System (HEC-HMS), the US Environmental Protection Agency's Storm Water Management Model (SWMM), OTTHYMO, and MIDUSS. Such models are useful and robust tools to water resources engineers.

However, care must be taken in applying these rainfall-runoff models. Serious problems can ensue with both over and under design. Water resources engineers employing such models must thus ensure accuracy in the estimation of values of the various parameters and variables of the model. They must also pay attention to the different methods used within the model, and the underlying assumptions of each. The temporal characteristics of the model are particularly important - the distinction between discrete and continuous models. Discrete models consider only a single storm (typically termed a design storm), with time ranges in the order of hours to days (USACE, 2000). Initial basin moisture conditions must therefore be assumed in discrete models. Processes that occur over longer periods of time, such as groundwater flow and evapotranspiration are typically ignored in these models. Continuous simulation models on the other hand, consider much longer rainfall record series, including periods of zero rain (Fleming, 1979). Basin moisture conditions are continuously calculated in such models, and processes such as evapotranspiration are accounted for.

The choice of the temporal resolution of a model can have a large impact on the accuracy of the model results. Thus, a thorough analysis of the difference between discrete (design storm) methods and continuous simulation methods is warranted.

1.3 OBJECTIVES AND OVERVIEW

The focus of this thesis is an indepth comparison between continuous simulation and design storm hydrologic modeling methods in estimating peak flow frequency distributions. The work in this thesis will attempt to verify what differences exist between the two methods, and whether or not design storms can effectively duplicate continuous simulation results. The analysis will involve varying different parameters such as basin type, storm duration, antecedent moisture conditions, and basin complexity to examine the differences. The focus is on peak flow frequency distributions, as this is the most common application of design storm methods. Peak flow is a very commonly used design variable, particularly in designing stormwater management infrastructure. With the exception of one section, hydrograph volume and timing are not considered in the comparison.

Chapter 2 of this thesis consists of a literature review which discusses the two approaches in more detail, as well as previous comparison studies, and a justification for the work done in this thesis.

Chapter 3 discusses the theory and set-up of the hydrologic model and parameters used for the comparison. A number of different design storm distributions used in the analysis are also discussed. Thus, parts of this chapter could also be viewed as contributing to the literature review.

Chapter 4 discusses the results of the comparison on individual basins. Factors such as land use type (urban/rural) and design storm duration are examined, as well as a detailed examination of antecedent moisture conditions.

Chapter 5 compares the two methods on a much more complex watershed system. The results are analyzed at several different basin junction nodes to determine how the comparison is affected by increasing the number of hydrologic elements and contributing drainage area.

Chapter 6 examines how the two methods compare when detention ponds are involved. Two ponds, one with a linear storage-discharge function and another with a non-linear function, were considered.

Chapter 7 summarizes the work and major findings of this thesis, as well as suggesting avenues for future research on the subject.

CHAPTER 2: LITERATURE REVIEW

2.1 INTRODUCTION AND THEORY

As suggested in the introduction, hydrologic modeling (rainfall-runoff modelling in this case) is performed in one of two ways with respect to temporal characteristics: event-based modeling or continuous simulation.

A continuous simulation approach performs a long term simulation of streamflows. As such, these models perform a much more in-depth accounting of the movement of water within the study area. Processes such as evaporation and transpiration, groundwater flow and infiltration are generally accounted for, as continuous simulation models account for much more of the hydrologic cycle. Continuous simulation models can track changes in soil moisture deficits, which is an important parameter in determining the amount of rainfall available for runoff. To use a continuous simulation model, a long-term record of recorded rainfall (along with other required data) is fed into the model of the study area, which in turn generates a long-term output record of flows. These flows can then be analyzed statistically to determine, among other things, flood frequency distributions. One of the earliest and most well-known continuous simulation models was the Stanford watershed model (Crawford and Linsley, 1966), now available as the EPA's HSPF program. Many current hydrologic models offer continuous simulation capabilities, such as the EPA's SWMM program, and the

U.S. Army Corps of Engineer's HEC-HMS program, among others. With the increase in modern computing power, additional and more in-depth models continue to be developed and employed in hydrologic studies. Because of the complex nature of this method, it is typically applied for larger drainage area studies. It is also a preferred option when analyzing storage elements or addressing water quality issues, as discussed later.

Event-based simulations on the other hand, perform a much more limited simulation of single rainfall events only. As such, many processes that act gradually over a longer period of time (such as evaporation) are neglected, as their impact on a single storm is limited. However, this means that initial conditions for the model (such as antecedent moisture conditions) must be specified, as the model is not designed to calculate them. Once the initial conditions are specified, a single rainfall event of interest is fed into the model of the study area, which in turn produces the response hydrograph. The selection of a representative rainfall event and its properties is of critical importance. In some cases this may a severe historical storm (such as Hurricane Hazel in Southern Ontario), or a theoretical value such as the probable maximum precipitation – the largest amount of precipitation considered physically possible for the local meteorological conditions for a certain duration. In most cases, the rainfall event chosen is what is known as a design storm. A design storm is a synthetic hyetograph that is typically (but not always) designed based on the average characteristics of storms that have occurred in the past for a certain area (McCuen, 2005). Marsalek and

Watt (1984) provide an overview of a number of different design storm types in current use. Many of these types are discussed in greater detail in Section 3.4.3. The design storm is usually constructed using data from local intensity-duration-frequency (IDF) curves. The resulting design storm is then typically referred to a T-year storm, where T indicates the return period (inverse of exceedance probability per year) of the chosen value of average rainfall intensity from the IDF data. The properties of the resulting hydrograph (volume, and most often peak flow) are then assumed to hold the same return period as the design storm. By using a series of design storms of varying return periods, a flood frequency distribution can then be generated. The design storm is typically employed in sewer design, as well as generating flood frequency estimates for smaller developments.

The theoretical basis of design storm theory has been known to be flawed for quite some time. As early as 1974 (and perhaps earlier), Linsley and Crawford noted that the return period for a rainfall event is not equal to that of the resulting flow event. This point has been noted by several other authors, more recently by Adams and Howard (1986). In their article, the authors systematically criticize design storm methodology. To summarize their main arguments:

1. A unique frequency or return period cannot be assigned to a rainfall hyetograph. A hyetograph is described by numerous characteristics (average intensity, duration, total volume, etc.) which themselves have

unique frequencies. These frequencies are different for different characteristics, and thus no single overall return period can be assigned to a rainfall hyetograph. The same argument also applies to the runoff hydrograph.

2. The assumption that the return period of the design storm is equal to that of the resulting runoff hydrograph is fundamentally flawed. As noted in the previous point, neither input nor output possess a unique frequency. The assumption that the frequencies of specific characteristics are directly related to one another (typically that the return period of the input average intensity is equal to that of the output peak flow) is also frequently false. Identical storms may result in different flow peaks depending on the specified antecedent moisture conditions in the catchment.
3. Design storm methods cannot adequately examine long-term or dry-weather conditions, nor can they correctly identify return periods for the full range of output parameters (volume, peak flow, etc.).

Given the above failings of the design storm method, the authors suggest the use of continuous analysis methods (such as continuous simulation or probability distribution based methods) which avoids the above-listed pitfalls.

Although it is not the focus of this thesis, it is worth noting that many authors have also shown the failings of the design storm method to properly address environmental and water quality issues. Marsalek (1978) argued that design storms were inappropriate for modelling pollutant loads, given the importance of the antecedent dry-weather period. Medina (1986) showed major discrepancies between design storm and continuous simulation methods in estimating return periods for fecal coliform counts. James (1994) argues that design storm methodology is unethical and potentially destructive to ecosystems. He states that event-based methods, unlike continuous simulation, cannot be easily adapted to examine dry-weather parameters such as overall changes in flow depth and velocities, necessary for fish habitat. Numerous other authors have made arguments against event-based simulation and the design storm method for water quality and environmental applications. These authors have all suggested that continuous simulation types of modelling are a preferable alternative to event-based modelling and the design storm approach.

Despite these criticisms and failings, the design storm approach continues to be used in hydrologic modeling studies. The reasons for this are numerous. Justification for use of the design storm concept was given by Marsalek and Watt (1984). The authors cited numerous reasons, including a lack of data (for frequency analysis, modeling, or calibration purposes), the high cost and extensive work involved with continuous simulation (which may not be warranted for smaller projects), the perception of a uniform and consistent standard, and its

current widespread acceptance in practice. Although many of these reasons are not strictly defensible, they do illustrate many of the practical reasons why the design storm method continues to be used, despite its numerous theoretical failings.

2.2 PREVIOUS COMPARISON STUDIES

To justify the use of design storms, and to verify whether its theoretical failings translate into actual failings, many researchers have attempted to compare design storm modeled flows with observed or continuous simulation-based synthetic values. A review of past research on the subject follows.

In a 1978 research paper, Marsalek examined the accuracy of two types of design storms against actual recorded rainfall data in estimating peak flows for several different catchments. The Chicago storm (discussed in more detail in Section 3.4.3.1) and the Illinois State Water Survey design storm were used in the comparison. The 15 years of actual rainfall data were not used in a continuous simulation, rather those storms that were determined likely to produce high runoff peaks were screened out based on total rainfall depth and intensity, using a 3 hour inter-event time to discretize individual storms. These actual rainfalls were then run as a series of single-event simulations along with the design storm distributions in EPA's well-known SWMM program. Thus, the comparison focused on the difference in rainfall distribution patterns between actual and

design storms only, and not the difference in antecedent moisture conditions between the two methods. Several small catchments (all 130 ha or less) with varying imperviousness, both actual and hypothetical were employed in the comparison. Some catchments were sub-divided into smaller units with pipe connections, however in all cases the focus was on the comparison of the outlet flow only. Marsalek (1978) noted that surcharging was not considered, thus pipe sizes were artificially enlarged to avoid this conditions. Marsalek (1978) found that in all catchments and for all return periods, the design storms predicted higher peak flows than those predicted by the actual rainstorms. The Chicago storm in particular greatly overestimated peaks. In examining correlation coefficients between peak outflows and peak rainfall intensities, Marsalek (1978) also found that only about half of the variation in runoff peaks could be explained by variation in rainfall intensity. This furthered his conclusion that other characteristics of the input rainfall should be considered. Marsalek (1978) also found large discrepancies between design storm and actual storm results in predicting the return periods for runoff event volumes. It was therefore suggested that design storms are inappropriate for volume-based designs such as detention basins.

Urbonas (1979) summarized the work of the Urban Drainage and Flood Control District (UDFCD) of Denver, Colorado in examining the design storm concept and attempting to develop more reliable simulation methods. Using four small (0.56 mi^2 or less) catchments in the Denver area, Urbonas (1979) compared

a partial duration series of rainfalls extracted from a 73-year period of record to design storms generated using data from two different local rainfall atlases. Similarly to Marsalek (1978), a complete continuous simulation was not performed. For the sites chosen however, Urbonas (1979) found that antecedent moisture conditions had little effect on the results, given the semi-arid nature of the climate in the study area, and the highly urbanized nature of the test catchments. The results of the analysis showed significant variations between the historic rainfalls and the design storms. The predominant trend was for design storms to again overestimate peak flows. Different design storm distributions were then developed by the UDFCD based on rainfall atlas and partial duration series data, and were found to show much better agreement with peak flows generated using actual storm data.

Packman and Kidd (1980) examined how sensitivity analysis could be used in single-event simulations to more accurately determine parameters such as antecedent moisture conditions, and thus to more accurately model flood return periods. A number of different small catchments (two actual and three imaginary, all 142 ha or less) in the UK were used for the analysis. These catchments featured varying area, imperviousness, slopes, and number of pipe connections. Using continuous simulation with actual rainfall records, a synthetic peak flood flow frequency distribution was generated for the five different catchments, using two different rainfall series (depending on catchment location – 98 years of data for one, and 34 years for the other). It should be noted that a pre-screening

analysis was employed to extract out those events deemed likely to cause the largest floods, along with the corresponding antecedent moisture conditions. These synthetic flood frequency distributions were also generated for 10 points within the pipe network of each catchment. Pipe surcharging was accounted for in the model used. The generated synthetic frequency distributions were found to have good agreement with observed distributions. Comparison of modeled hydrographs for individual storms also showed good agreement with observed data, indicating that the synthetic data were representative of actual data. Packman and Kidd (1980) then examined the data using sensitivity analysis to determine ideal conditions for a design storm analysis that could accurately reproduce the synthetic flood frequency distributions generated in the previous step. A single storm distribution with depth/volume determined from local depth-duration-frequency curves was used. Several different storm durations were attempted in order to determine the ideal length. The major focus of the sensitivity analysis was to examine the effect of varying what the authors termed the "urban catchment wetness index" (UCWI), essentially the antecedent moisture conditions. By performing a number of simulation runs for different locations, return periods, and UCWI values, peak flows were generated which could in turn be compared to the synthetic values. Mean relative errors were then calculated between mean flood values for different UCWIs at all locations. The ideal UCWI for the catchment is then determined as the value where the error is minimal (i.e. zero). When this calculated UCWI was used in the event-based analysis, very

good agreement with the synthetic flood frequency distribution was achieved for all locations, up until about the 10 year return period mark, after which the design storm method tended to overestimate peaks. Results were only given for the downstream outlet, not for the other points within the pipe network, although it was suggested in the paper that the results were similar. The authors also found that there was a relationship between the UCWI and average annual rainfall for the two rainfall series used, which could be used in future design and potentially eliminate the need for a detailed sensitivity analysis.

Beaudoin et al (1983) performed a comparative study between design storm and continuous simulation results in estimating peak flow frequency distributions. A single urban catchment of 8.63 km^2 on the island of Montréal, Québec, was used in the analysis. The model used in the study was not designed to handle pipe surcharging, thus the model was run under a mode in which the network is redesigned to handle increased flow and to avoid surcharging. A 10-year rainfall record was employed for the continuous simulation run. Because the model employed by the authors was a single-event one, a pre-screening of rainfall events similar to previous authors was performed, whereby rainstorms with a return period of 0.25 years or greater were extracted along with the five-day antecedent rainfall total. For the design storm data, both a Chicago-type and 2^{nd} quartile Huff-type design storm were employed, which were run with both dry and saturated antecedent moisture conditions. The authors found that the Chicago storm with dry antecedent conditions agreed well with actual storm

results, as did the 2nd quartile Huff storm with saturated antecedent conditions. As such, the authors concluded that design storm modeled flood frequency distributions can reasonably approximate those calculated using actual storms/continuous simulation methods. They noted however that results are significantly affected by the choice of storm and antecedent conditions, as both storms did not perform nearly as well when the alternate antecedent moisture conditions were employed.

Wenzel Jr. and Voorhees (1984) evaluated the accuracy and sensitivity of several different design storms. Three different small (5.9 - 9.4 ha) urbanized catchments in the US were employed which included numerous sewer reaches. Pipe surcharging was not accounted for. Long-term recorded rainfall data (25-34 years in length) were used as input for continuous simulation modeling. As with previous works, a screening procedure was used to identify rain storms with depths greater than 60% of the 1-year return period value. Antecedent moisture conditions were however accounted for in a separate, fully continuous module. Several different design storms were employed: a uniform intensity storm, a Huff 1st quartile storm, and two different triangular hyetographs. The authors examined how the design storm results were affected by the type of storm distribution used, the choice of storm duration, and the choice of antecedent moisture conditions, in comparison to the continuous simulation results. With regards to storm distributions, they found that when average antecedent moisture conditions were used, the triangular and Huff distributions tended to overestimate

peaks, or roughly approximate the continuous simulation data. The uniform distribution consistently underestimated peak flows. The ideal design storm duration was found to be roughly equal to the time of concentration, or slightly longer. Variation of the antecedent moisture conditions (both dry and saturated conditions) for the design storms led to significant deviations from the continuous simulation modeled flood frequency distribution. The authors therefore recommended using a local average moisture deficit. In general, the authors found that design storms can effectively reproduce the flood frequency distributions generated by continuous simulation. However, they strongly cautioned that this is only the case when an appropriate distribution, duration, and antecedent moisture conditions are selected. If this is not the case, then large discrepancies between design storm and continuous simulation results can occur.

Petrovic and Despotovic (1998) examined the accuracy of using different pre-screening methods on historical data for continuous simulation in comparison to actual and design storm results. In this way, both the accuracy of pre-screening, as well as the impact of different rainfall distribution parameters on accurately predicting peak flows could be examined. Historical rainfall data were screened in several different ways, based on storm depth, peak intensity, and duration. These screened datasets of rainfall were then run through a rainfall-runoff model, along with the full historical record for a study catchment in Belgrade, Serbia. The study area consists of a small 7.14 ha subcatchment in a residential urban area, which contains a rain gauge as well as a flow gauge with

13 years of data. No details are provided in the paper on the chosen antecedent moisture conditions for these simulations. In addition to the historical data, design storms were also run with the test catchment: a constant-intensity storm, along with a temporally distributed storm based on one of the authors previous work (Vukmirovic and Despotovic, 1984). Again, no details were provided on antecedent moisture conditions. All modeled results were then compared to observed peak flows. It was found that all modeled flood frequency distributions gave lower peaks than the observed distribution. Of the screened datasets, those screened by depth and peak intensity gave almost identical results to the full historical datasets, suggesting that data could successfully be screened by using those parameters in order to reduce the computational workload. The data screened by storm duration greatly underestimated peaks, leading the authors to conclude that storms should not be screened by this parameter, nor should design storm duration be selected purely on the basis of the basin's time of concentration, particularly when this value is short as it was for the test catchment. Design storm results also underestimated flows, with the uniform-intensity storms greatly underestimating, and the temporally varying storm coming much closer to the historical and observed results.

Nnadi et al. (1999) examined how accurately a number of different design storm distributions modeled peak flow frequency distributions as compared to continuous simulations results for a number of different catchments and rainfall datasets in the state of Florida. Four different rainfall datasets from throughout

the state were used in the analysis for the continuous simulation model input, as well as to generate IDF data for the design storms. Four different relatively small (0.004 to 3.04 km^2) hypothetical watersheds were also employed. Losses were calculated using a modified Horton equation (1940) approach. The continuous simulation model incorporated a recovery coefficient which allowed for soil drying between rainfalls. Values of initial conditions and basin parameters (area, time of concentration, imperviousness and infiltration rate) for each of the four watersheds were optimized to maximize peak flow for a different duration regulatory design storm (known as the FDOT storm). In addition to the individual regulatory design storm, three other SCS design storms (including the SCS Type-II distribution) were also tested on each catchment and with each set of rainfall data. These storms were compared against continuous simulation results, which were first fit with a frequency distribution that best matched the data. A modified version of the Horton equation was used to estimate infiltration and rainfall abstraction. In general, the authors found that the continuous simulation results matched reasonably well with the different design storm results. Individual results varied depending on catchment, rainfall data, and storm type, with both overestimation and underestimation occurring. The SCS Type-II distribution, with the exception of one of the rainfall datasets, tended to overestimate peaks as compared to continuous simulation.

2.3 JUSTIFICATION FOR FURTHER STUDY

After reviewing the previous research on the comparison of continuous simulation and design storm methodologies, a few observations were made. In particular, some of the shortcomings of the previous studies and avenues for potential research were examined. It is worth noting that all of these previous studies assumed that continuous simulation results offer the best estimate of flood frequency distributions. This is not necessarily true – continuous simulation has limitations, and cannot always provide the required solution for certain design cases either. In keeping with the work of previous authors however, this study also assumes that continuous simulation results are the true estimate of flood frequency distributions.

As a first observation on previous studies, no definitive conclusions can be drawn by examining their overall results. In some studies, authors reported that design storms tended to overestimate peak flows, while in another, they underestimated. Others found that design storms provided a good comparison, provided that appropriate parameters were selected. Thus, comparison results are still inconclusive. Given that design storms are widely used in practice, this issue deserves further study. There is also a lack of current research on the topic – many of the papers reviewed on this subject are 20-30 years old. A new approach with current modeling methods is therefore warranted.

Second, all of the previous studies involved relatively small urbanized basins. Although this is typically the purview of the design storm, these studies fail to verify whether or not this should be the case – can the design storm reasonably duplicate continuous simulation results on undeveloped rural-type basins as well? If the design storm is to be used to estimate pre-development as well as post-development peak flows, this should be verified. Further, using highly urbanized basins neglects or minimizes the importance of antecedent moisture conditions in the comparison between the two methods due to limited contribution of runoff from pervious areas. By focusing on smaller basins with short times of concentration and short duration design storms, previous comparison studies further limit the comparison. Study is therefore warranted on larger and more rural basins, as well as an examination of using longer duration design storms.

Third, the majority of previous study areas were modeled as single lumped catchments. Those studies that did involve sub-catchments and pipe connections still only presented comparison results at the outlet of the whole catchment. This not only makes it difficult to fairly compare previous studies that used these different approaches, it also blurs the importance of routing reaches and multiple basin connections. None of the previous studies examined how the two methods compared as more sub-catchments are added and the basin system becomes more complex. Nor did any of the previous studies verify the comparison through

storage components such as detention basins. As such, further study is warranted in this area.

Last, with the exception of Marsalek (1978), all of the previous authors employed study areas with very different characteristics than the local area. The semi-arid climate of Denver (Urbonas, 1979) and the humid sub-tropical climate of Florida (Nnadi et al., 1999) have little in common with Southern Ontario. Similarly, the basin characteristics chosen (particularly for hypothetical ones) may have little similarity to typical local soils and land uses. The types of design storms used were also in many cases inapplicable to the local area. By using an actual local study area and frequently used design storm distributions this research is made more valuable to local practitioners while adding to the different climate and location types used in comparison studies.

Therefore, for the reasons discussed in this section further study of the comparison between design storm and continuous simulation in modeling flood frequency distributions is warranted. This thesis will therefore attempt to perform an indepth comparison addressing the issues raised by previous studies.

CHAPTER 3: MODEL AND DATA

3.1 STUDY AREA AND MODEL IMPLEMENTATION

In order to further examine and compare design storm and continuous simulation methodologies, it is first necessary to create a watershed model. As such, a study basin area is required. An actual watershed was deemed preferable to a hypothetical one for a few reasons. First, using actual basin parameters makes the model much more realistic, and therefore makes the results much more credible. Second, with an actual watershed with recorded flows, the results can be calibrated and verified before testing.

The study area chosen for this thesis is located in the Town of Ancaster, which is now part of the City of Hamilton, Ontario, Canada. The majority of Ancaster lies on the Haldimand Clay Plain, with 50% sand, 30% silt, and 20% clayey silt (Philips, 1987). Part of Ancaster also lies on the edge of the Niagara Escarpment, a prominent rocky ridgeline that runs throughout Southern Ontario. However, for the area under study, bedrock is located at depths of 3 metres or greater, and the escarpment edge is not reached by water courses included in this study (Philips, 1987). Thus, this feature does not impact this study.

The majority of Ancaster is drained by two sub-watersheds: the Ancaster Creek sub-watershed, and the Tiffany Creek sub-watershed (a small portion is also drained by the Sulphur Creek sub-watershed). These two creeks eventually

join together below the escarpment, however within the Ancaster area, they are separate. There have been various studies undertaken of these two areas, and thus a variety of different watershed boundary delineations. Figure 3.1 shows the delineation of basins and sub-basins from the Town of Ancaster's 1987 Master Drainage Plan (Philips, 1987).

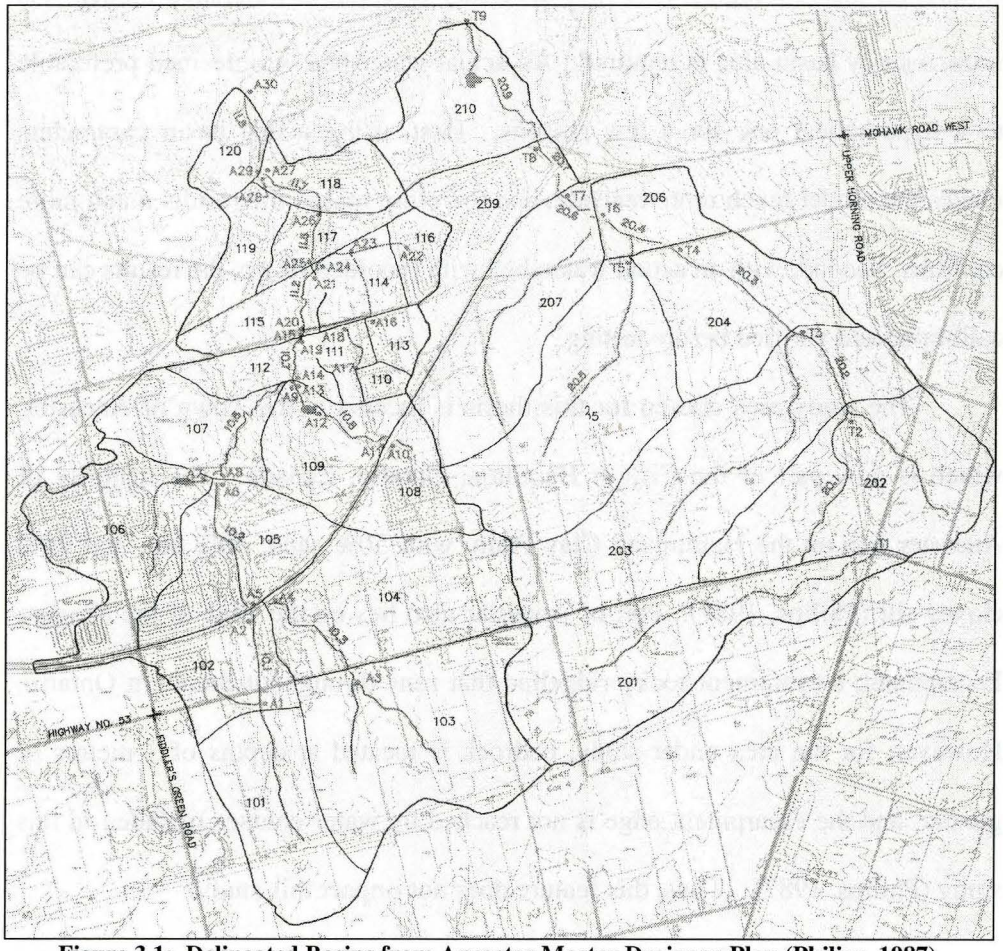

Figure 3.1: Delineated Basins from Ancaster Master Drainage Plan (Philips, 1987)

Figure 3.1 illustrates both delineated sub-watershed boundaries, and the creeks themselves. The basin on the left (with 100 series sub-basins) is the Ancaster Creek sub-watershed. The basin on the right (with 200 series sub-basins) is the Tiffany Creek sub-watershed. Each is approximately 850 hectares in size (Philips, 1987). The outlets for both sub-watersheds are at the north end – the top of Figure 3.1.

For this thesis, the Ancaster Creek sub-watershed was chosen as a more appropriate study basin for a few reasons. First, it offers a greater variety in land use than the Tiffany Creek sub-watershed, with agricultural, urban, and recreational (there is a large golf course in the centre of the sub-watershed) areas. At the time of the study report, the Tiffany Creek watershed was almost entirely undeveloped, with primarily rural land use and small, ephemeral streams. Thus, the Ancaster Creek sub-watershed allows for a more varied and robust comparison. Second, a stream level gauge exists for the Ancaster Creek sub-watershed at junction A29, allowing for calibration and verification of the model (in fact two gauges are operated at the same location – one by Water Survey Canada, and one by the Hamilton Conservation Authority). For these reasons, the Ancaster Creek sub-watershed was chosen.

In order to create a rainfall-runoff model for the Ancaster Creek sub-watershed area, the relationships between sub-basins must be understood. A schematic diagram is included in the Town of Ancaster's 1987 Master Drainage

Plan, which indicates how the sub-basins are connected with one another (Philips). It is reproduced below in Figure 3.2 (Philips, 1987).

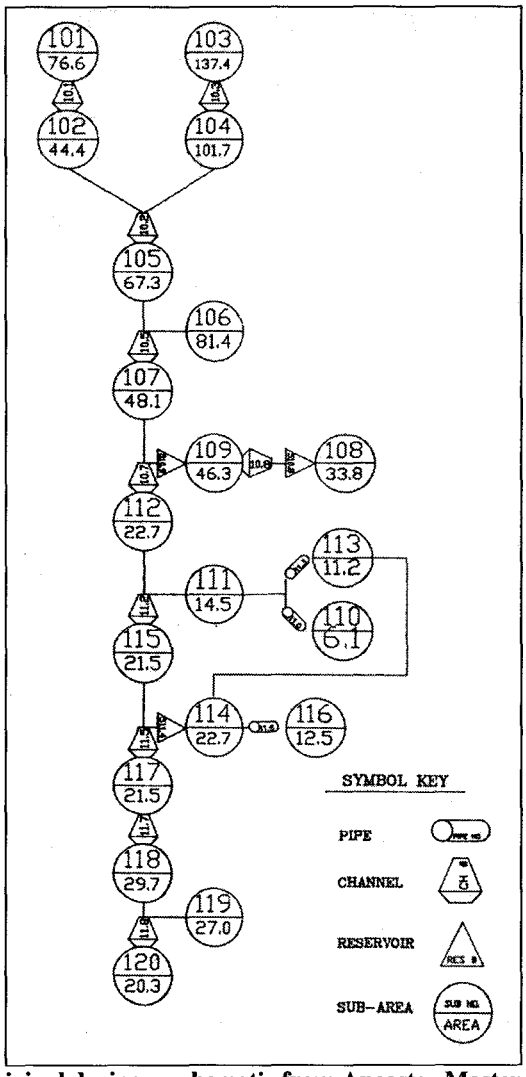

Figure 3.2: Original drainage schematic from Ancaster Master Drainage Plan (Philips, 1987)

Figure 3.2 shows the connections between the various hydrologic elements of the sub-watershed. Sub-basins are represented as circles, which give the sub-

basin name as well as the drainage area in hectares. Routing reaches (channels) are indicated by trapezoids. Reservoirs are given as triangles, while pipe connections are given by cylinders. Lines indicate a connection between upstream and downstream elements. It should be noted that the orientation of Figure 3.2 is opposite to that of Figure 3.1, in that the most downstream element (sub-basin 120) is given at the bottom of the page, not the top.

In order to more easily implement the relationships of Figure 3.2 into a rainfall-runoff model, some alterations were made. First, Basin 120 and the channel reach connecting to it, Channel 11.8, were omitted. This was due to the location of the stream gauge used for calibration, which was located immediately upstream of these elements. It seemed more logical to calibrate the model using the final output of the sub-watershed. As such, Basin 120 and Channel 11.8 were unnecessary additions. Second, the three reservoirs shown in Figure 3.2 were omitted. This was due to a lack of information. No data on any of the properties of these detention ponds could be found in any reports, nor were they known to Hamilton Conservation Authority staff. None of the ponds appeared to be of any significant magnitude either, thus it was assumed that their omission would have a negligible impact on the model accuracy. Third, modifications were made to the arrangement of basins 110, 111, 113, 114, and 116. Figure 3.2 shows a connection from sub-basin 113 to both basin 111 (via a pipe) and to basin 114. There is no information on what percentage of flow is diverted in which direction. There is also no information on the various pipe connection properties. Given

this, and given the relatively small drainage areas of these sub-basins, a simplification was made. It was assumed that the flow from sub-basin 113 did not connect to sub-basin 114, and that all flow went instead in the direction of 111. Also, to eliminate the problem with pipe connections, sub-basins 110, 111, and 113 were lumped into a single sub-basin, and sub-basins 114 and 116 were lumped into another separate sub-basin. Sub-basin properties were appropriately averaged out for the new amalgamated sub-basins.

Thus, the final sub-basin relationships and flow paths used for the rainfall-runoff model in this thesis are slightly different than those presented in Figure 3.2. The modified relationships were implemented into a popular hydrologic rainfall-runoff simulation program known as HEC-HMS (Hydrologic Engineering Center's Hydrologic Modeling System). The result, when combined with GIS data of the sub-basin boundaries and creek location, is the screenshot shown in Figure 3.3 below.

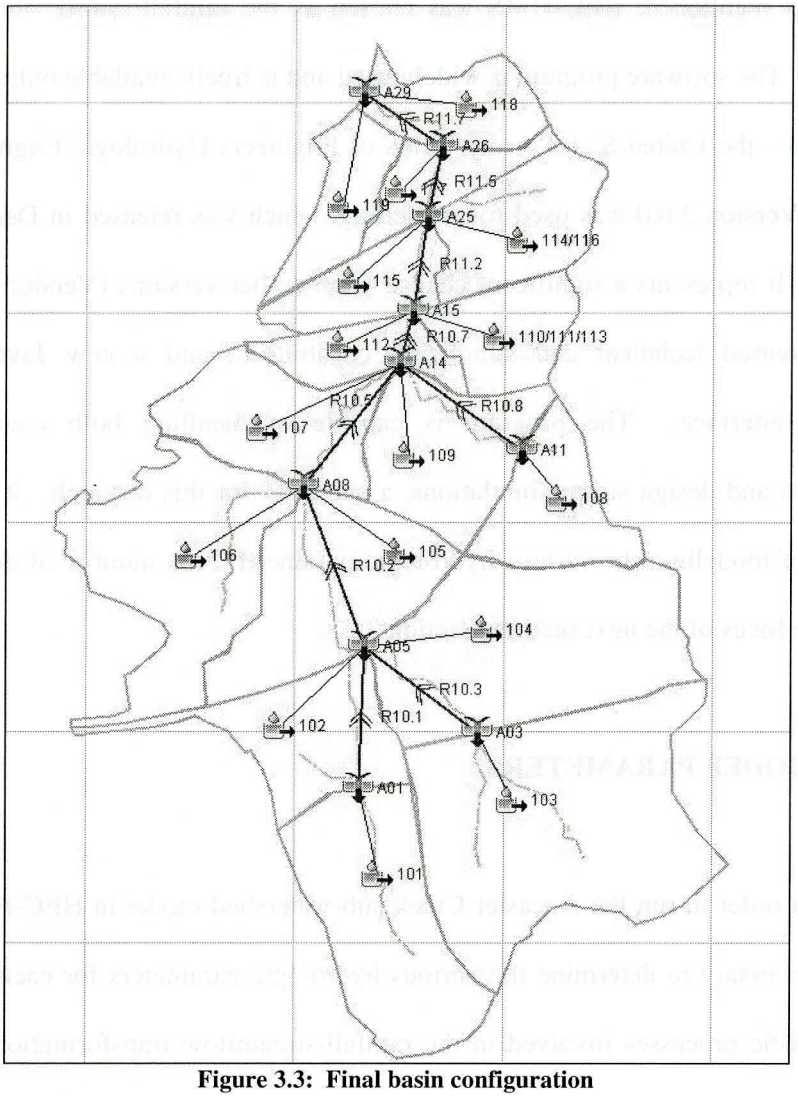

Figure 3.3: Final basin configuration

Sub-basins follow the same numbering order in Figures 3.1 and 3.2 (100 series numbers). Junctions are indicated by codes beginning with A, while routing reaches are indicated by codes beginning with R. Details of parameter values can be found in Tables B1 – B6 of Appendix B.

As mentioned, HEC-HMS was chosen as the rainfall-runoff simulation program. The software program is widely used and is freely available online from the author - the United States Army Corps of Engineers Hydrologic Engineering Center. Version 3.0.0 was used for modelling, which was released in December of 2005. It represents a significant change from earlier versions (Version 2.2.2), with increased technical and simulation capabilities, and a new Java-based program interface. The program is capable of handling both continuous simulation and design storm simulations, a necessity for this research. It is also capable of modelling the various hydrologic parameters in a number of different ways, the focus of the next section, Section 3.2.

3.2 MODEL PARAMETERS

In order to run the Ancaster Creek sub-watershed model in HEC-HMS, it is first necessary to determine the various hydrologic parameters for each of the deterministic processes involved in the rainfall-streamflow transformation. The methods used to model these processes, and the parameters chosen, are discussed in the following sub-sections. Parameter values can be found in Tables B1-B6 of Appendix B, and are again based on the previously mentioned study (Philips, 1987). It should be noted that watershed conditions are assumed to be stationary throughout. Although this would not be the case in reality for the watershed, it is

a necessary simplification in order to fairly compare continuous simulation and design storm results.

3.2.1 LOSS AND INFILTRATION

The first deterministic process involved in the rainfall-runoff system is the process of abstraction and loss. This process is required to calculate how much of the input rainfall is lost to the sub-processes of interception and storage, soil infiltration and initial loss, and evapotranspiration. Thus, this process calculates how much of the input rainfall is available to become runoff.

In the report on which this model is based (Philips, 1987), losses for sub-basins were estimated using the well-known US Soil Conservation Service's (SCS) Curve Number Method (1964, 1986), along with imperviousness percentages. These values were provided for two different development scenarios, something which is discussed in more detail in Section 3.3.

A curve number is a number between 0 and 100 which describes the relationship between rainfall and runoff for a basin, based on soil group, cover complex, and the antecedent moisture conditions (McCuen, 2005). This value is then used, along with initial abstraction, rainfall, and the maximum potential soil moisture retention (S), in the well known SCS equation to calculate runoff. Initial abstraction is usually estimated as 0.2 of S, thus to calculate the cumulative runoff at any time increment, all that is required is the cumulative rainfall and the

maximum potential retention of the soil, which is in turn, defined as a function of the curve number by another SCS equation.

The SCS curve number method can therefore be used to calculate cumulative runoff for the pervious portion of the sub-basin knowing only cumulative rainfall and the curve number. For the impervious portion (if it exists), all rainfall is assumed to become runoff. Total cumulative runoff is then the sum of these two components. For storms of varying rainfall intensities, incremental runoffs are simply calculated by calculating cumulative runoffs at each time step, and then subtracting previous runoff quantities.

The SCS method in this case would be appropriate for design storm simulation, as it satisfies all restrictions of the method as given by Viessman Jr. and Lewis (2003). To summarize, all sub-basins are homogenous in curve number (urban, rural, and recreational areas are separated in the delineation of sub-basins in Figure 3.1), all curve numbers are above 50, and (as discussed in more detail in Section 3.2.2) the time of concentration for all sub-basins, as well as the entire basin, are between 0.1 hours and 10 hours. The SCS method is also designed to be applicable to smaller urbanizing watersheds, as is the case in many of the basins here (SCS, 1986).

However, although the SCS method is appropriate for design storm and other single storm methods, it is inappropriate for continuous simulation work. All calculations are cumulative values based on the assumption of a single storm. There is no mechanism to account for soil drying in between storms, thus

subsequent storms would assume erroneously high saturation levels, no matter what the time delay between storms, or no matter how high actual evapotranspiration rates were.

Thus, an alternative method of modeling watershed loss process is required – one that is adaptable to both design storm and continuous simulation modeling. HEC-HMS offers several different methods of event-based loss methods (Initial and constant-rate, exponential loss rate, Green and Ampt, SCS Curve Number) and continuous simulation methods (Deficit and constant-rate, Soil Moisture Accounting). In order to ensure a fair comparison between the two, the assumptions and processes of each should be similar. Given the complexities of the Soil Moisture Accounting method for continuous simulation, and the fact that no design storm method can match its processes, the Deficit and constant-rate method was chosen for continuous simulation modeling. Its event-based parallel, the Initial and constant-rate method, was then chosen for design storm modeling. The two methods are very similar in nature, and can both be described by Equation 3.1 (USACE, 2000):

$$\begin{aligned} pe_t &= 0, && \text{if } \sum p_i < I_a \\ pe_t &= (p_t - f_c) && \text{if } \sum p_i > I_a \text{ and } p_t > f_c \\ pe_t &= 0, && \text{if } \sum p_i > I_a \text{ and } p_t < f_c \end{aligned} \qquad \text{(Equation 3.1)}$$

where pe_t represents the excess precipitation at time t, p represents precipitation, I_a, represents the initial abstraction, and f_c represents the constant rate of infiltration. Thus, the initial abstraction must be satisfied before runoff can begin. Once the abstraction has been satisfied, runoff is equal to the rainfall minus the constant rate of infiltration loss (unless the rate of rainfall is less than the constant rate, in which case runoff is zero). The difference between the two methods lies in how the initial abstraction is calculated. In the initial and constant-rate method, the initial abstraction is a user-specified parameter for the single storm being analyzed. In the deficit and constant-rate method, the abstraction is continuously calculated by considering the soil layer as a simple reservoir. An initial abstraction (or deficit) is specified for the beginning of the simulation period. The deficit level is then continuously updated during the simulation. Input precipitation will raise the level, up to the top of the reservoir to a deficit of zero, whereby runoff can begin. The level will also drop (deficit increase) over time between storms due to evapotranspiration, to a maximum specified deficit. Thus in addition to the initial and constant-rate parameters (initial deficit, constant infiltration rate, imperviousness %), the deficit and constant-rate method also requires a maximum deficit, as well as evapotranspiration rates.

Parameters for the initial and constant-rate and deficit and constant-rate methods were largely estimated using the aforementioned SCS curve number data and procedures (except for imperviousness percentages, which are directly transferable). The maximum deficit parameter was estimated as being equal to

the maximum potential retention parameter S given by the SCS equation. Initial loss was also generally assumed to be 0.2 of S, however some tests on this parameter are discussed in Section 4.2. The constant rate of infiltration was estimated using available soil classification data of the various sub-basins (Philips, 1987). The data uses the SCS soil classification method, which classifies soils into four groups (A, B, C, or D) depending on their infiltration rate – A type sandy soils with high infiltration rates to D type clays with low infiltration rates (SCS, 1986). There are also intermediate soil groups (AB, BC, and CD) for soils that fit between the main classifications. Numerous authors have provided infiltration rate estimates for these different soil classes, e.g. Maidment (1992). In this case, the infiltration values recommended by the USACE (2006) will be employed, which are the values suggested by Skaggs and Khaleel (1982). Because infiltration rates are provided as a range, the values were averaged to provide estimates for each of the four major soil classes. Infiltration rates for the intermediate soil groups were then found by further averaging the surrounding major soil class estimates. The constant rate of infiltration was then calculated using these infiltration estimates and the percentage classification for each sub-basin. Calculations can be seen in Tables B1 and B2 of Appendix B.

In addition to these parameters, evapotranspiration data are required for the deficit and constant-rate method in order to continuously adjust the soil water deficit. HEC-HMS offers two different methods of modelling evapotranspiration: the Priestly Taylor method (1972), and the monthly average method. Given the

large data requirements of the Priestly Taylor method (continuous gauge data for crop coefficients, temperature, and solar radiation), the monthly average method was chosen for simplicity. The monthly average method simply requires an average monthly evapotranspiration rate – this amount is used to find the constant evapotranspiration rate for each time step for the month. A pan coefficient is also used, which is multiplied by the monthly average rate to calculate the actual rate of evapotranspiration.

No evapotranspiration data were available from the report on which this model is based (Philips, 1987). However, lake evaporation data are available for Environment Canada's Hamilton RBG climate station (Climate ID 6153300) from their online climate data site at http://climate.weatheroffice.ec.gc.ca/climateData/canada_e.html. The station has average daily lake evaporation rates, averaged out for the months of April to October for the 1971-2000 period. This time frame is acceptable, since the continuous simulation is run only during these non-winter months (the reasons for which are discussed more fully in Section 3.3). The Environment Canada data were therefore used as the monthly evapotranspiration rate – these data can be seen in Table B3 of Appendix B. Determining the pan coefficient parameter was more difficult.

The pan coefficient parameter was used to adjust evapotranspiration rates to more accurately reflect yearly evapotranspiration variation. There are numerous estimates of the portion that evaporation and transpiration play in the

overall balance of the hydrologic cycle. According to Singh (1988b), nearly 75 percent of the total annual precipitation on land surfaces is returned to the atmosphere by evaporation and transpiration. According to Viessman Jr. and Lewis (2003), about two-thirds (or 66.7 percent) of precipitation is evaporated and transpired back to the atmosphere. McCuen (2005) indicates that approximately 70% of temperate climate precipitation returns to the atmosphere due to evaporation and transpiration. Thus, averaging out these various estimates, evapotranspiration is roughly equal to 70% of total precipitation. As such, pan coefficients were calculated for each simulation year by using this desired ratio, the Environment Canada monthly rates and yearly total, and the April-October rainfall total for that year. Therefore, the monthly variation given by the Environment Canada data remains the same, however the evapotranspiration rates are scaled using the pan coefficient, such that the total evapotranspiration for April to October is about 70% of the total rainfall for this same period.

After determining all the necessary moisture loss and infiltration parameters, it is next necessary to examine the rainfall-runoff transformation parameters.

3.2.2 RAINFALL-RUNOFF TRANSFORMATION

The second deterministic process involved in the rainfall-runoff system is the runoff transformation. After calculating loss and infiltration (as was discussed

in the previous section), and subtracting it from total precipitation, we are left with excess precipitation – the amount of extra rainfall available to create runoff. This excess precipitation is given in units of depth per unit of time – the same units as the starting precipitation data. Excess precipitation in this form is not particularly useful. Water resources engineers are ultimately interested in streamflow – the watercourse flow produced by the excess precipitation. Thus, a runoff transformation process is required to convert excess precipitation into streamflow from a basin. In HEC-HMS, the runoff transformation is accomplished through one of two methods.

The first method is an empirical approach known as the Unit Hydrograph method, originally credited to Sherman (1932). A Unit Hydrograph (UH) is defined as the hydrograph response of a watershed to a unit (typically 1 inch) of excess rainfall falling in a spatially and temporally uniform manner over the watershed over some specified period of time. UHs are defined for different durations of rainfall excess (a 1-hour unit hydrograph, a 2-hour unit hydrograph, etc.) and for different watersheds. UH theory assumes that the ordinates of the UH can be used to find the ordinates of the direct runoff hydrograph of a watershed due to a storm of equal duration but with a different amount of excess rainfall. The ordinates of the direct runoff hydrograph are simply equal to the UH ordinates multiplied by the ratio of $P/1$, where P is equal to the amount of excess precipitation of the storm in question (in inches). This is known as the assumption of linearity, because it assumes a linear relation between excess

rainfall and runoff ordinates – hydrographs for excess precipitation amounts other than 1 inch are simple multiples of the original UH. This also assumes that excess rainfalls of equal durations but different amounts will generate direct runoff hydrographs with identical time bases – thus intensity does not affect the hydrograph duration. It is also assumed that the hydrologic response of a watershed given by the UH is true regardless of when the storm occurs or prior watershed conditions.

For storms of varying intensities (such as design storms), the process of convolution is used, which assumes the linear addition and superposition of hydrographs. For continuous excess rainfall, the integral form of convolution is applied. For discrete excess rainfall (which is more commonly the case), the discrete or summation form of convolution can be used, which is given by (USACE, 2000):

$$Q_n = \sum P_m \, U_{n-m+1} \qquad \text{(Equation 3.2)}$$

where the summation in this case is from m=1 to $n \leq M$, where M represents the total number of discrete intervals. In terms of the variables, Q_n represents the ordinate of the total direct runoff hydrograph at interval n, P_m represents the rainfall excess at interval m, and U_{n-m+1} represents the UH ordinate at that particular interval. Thus, by using a UH along with the discrete form of the

convolution integral given by Equation 3.2, direct runoff hydrographs can be found for a given excess rainfall pattern.

The second available rainfall runoff transformation method is a conceptual approach known as the Kinematic Wave method. This approach views each sub-basin as a large open channel, with the excess precipitation calculated in the previous step as input to the side channel planes. The output runoff hydrograph is generated through an approximate solution of the St. Venant equations of continuity and momentum for the representative channel. This method is more theoretically accurate than the UH approach, since it attempts to conceptually model the runoff process, rather than making the simplifying assumption of linearity. However, the kinematic wave method is fairly data intensive, requiring data on the dimensions and roughness parameters of the planes as well as the main channel. Given the lack of guidance in this area from the report on which this model is based (Philips, 1987), a simpler method is preferable. The UH approach is also a very common method used by practicing water resources engineers. Assuming proper calibration and verification (Section 3.3) for the model, the difference should be negligible.

Therefore, the UH approach was employed for both continuous simulation and design storm modeling. Within HEC-HMS, there are several different UH models – Snyder, Clark, SCS, and user-specified. With the exception of the user-specified UH option, all of these models are synthetic UHs – the dimensions of the UH are determined through the synthesis of different parameters. The choice

was made to use the SCS UH as the runoff transformation for this model, as it is a popular method based on an analysis of a large number of different watersheds, varying both in size and location (SCS, 1972a). It is also simple to use, and can be used in conjunction with available SCS curve number data, as is discussed further on in the section. All conditions of the SCS UH were also satisfied, such as time step duration, as is discussed in Section 3.3.

The SCS UH is a dimensionless hydrograph: it does not specify peak discharge or the time to peak discharge. Rather it specifies the UH shape, as ordinates of the UH are given as a ratio to peak discharge and time to peak discharge. Thus to determine the runoff ordinates for a given amount of excess precipitation, we need to know t_p (the time from the beginning of rise to the peak flow) and q_p (the peak discharge). By approximating the SCS UH by a triangular UH with the same peak discharge and total volume (1 unit of excess rainfall times the area), we can relate q_p to t_p through a calculation of area. In general terms, this relation is given as (USACE, 2000):

$$q_p = C\,(A/t_p) \qquad \text{(Equation 3.3)}$$

where A represents the watershed area and C is a conversion factor depending on the units involved. It is therefore left to determine the time to peak in order to generate the hydrograph. Through several other relations specified by the SCS (1972a, 1972b), the time to peak can be related to the basin time of concentration,

t_c (the time required for runoff from the most hydraulically distant point in the basin to reach the outlet (SCS, 1972b).

There are numerous methods of estimating the time of concentration for a basin. In his review of empirical time of concentration equations, Zhuge (2005) lists twenty different methods. Different methods are used depending on basin characteristics, and on the dominant route of runoff flow, be it overland, channel, or mixed. Most equations are based on four types of input: flow resistance, watershed size, slope, and water input (McCuen et al., 1984). The SCS developed an empirical equation for estimating the time of concentration based on the first three of these inputs (1972b)

$$t_c = 0.000877\, L^{0.8}\, ((1000/CN) - 9)^{0.7}\, S_p^{-0.5} \qquad \text{(Equation 3.4)}$$

where L represents the hydraulic length (longest flow path for the basin) in feet, CN is the SCS Curve Number, and S_p represents the average watershed slope in percentage. Equation 3.4 is known as the SCS lag equation. The lag equation is intended for use in homogeneous subbasins with areas of 2,000 acres or less, conditions satisfied in this case. The method is also meant for basins where overland flow dominates, which is likely in this case, given that subbasin areas are relatively large compared to creek segment sizes. Although the lag equation was originally developed for non-urban watersheds, McCuen et al. (1984) showed that the equation on average gave relatively good estimates of t_c over a test of 48 urban

watersheds. Thus, the lag equation was chosen to estimate t_c for the subbasins in this case, given its applicability and the availability of CN data.

Since CN data are already available, it remains to estimate the length and slope parameters for each subbasin. This was accomplished by using Canadian Digital Elevation Data from Geobase, an organization run by the Canadian Council on Geomatics. A 1:50,000 scale tile (30M04) containing digital elevation data were downloaded for the study area from Geobase's online site at http://www.geobase.ca/geobase/en/data/cded1.html. The elevation data are given to the nearest 0.1 m. By overlaying GIS data of the subbasin boundaries, it was possible to find elevations for points within each subbasin, as well as calculate lengths. By trying different measurements from the outlet of each subbasin (the lowest elevation point for each subbasin), it was possible to estimate the hydraulic length as the longest straight-line distance in the subbasin. The average watershed slope for each subbasin was estimated by averaging the slope over the hydraulic length along with slopes from two other lengths from the outlet to points on the boundary of each subbasin.

Once these data were obtained, Equation 3.4 was used to estimate the time of concentration, and then accordingly the SCS unit hydrograph for each sub-basin. By employing the UH in conjunction with direct rainfall data from the previous step, and the convolution of Equation 3.2, the end result is a direct runoff hydrograph. In order to make these data comparable to observed flows, it is necessary to add in the baseflow component.

3.2.3 BASEFLOW

Another deterministic process involved in modelling basin outflow is the baseflow component. The calculations of the previous two sections yield the direct runoff hydrograph: the basin outflow from excess precipitation only. To properly model total outflow (and be able to compare it to recorded flow records), one must include the baseflow component. Baseflow represents the component of streamflow from groundwater discharge as a result of the accumulation of water in the soil from previous storms. Baseflow is what sustains watercourse flow during periods of dry weather. The combination of baseflow and the direct runoff flow form the total outflow of a basin.

HEC-HMS offers a few different methods of modelling baseflow. The first option is a constant monthly flow, where a constant rate of baseflow is specified for each month. As this is a great oversimplification of baseflow, this method was not used. The second option is the linear reservoir method, in which baseflow is linearly related to the groundwater storage from input infiltration. One or two layers can be specified, as well as multiple routing reservoirs for each layer. The linear reservoir method is primarily intended to be used with the Soil Moisture Accounting (SMA) infiltration method discussed briefly in Section 3.2.1. Given that the SMA method was not used in this model, it did not seem appropriate to use the linear reservoir method. The third option uses the baseflow

recession method. The baseflow recession method models the gradual depletion of groundwater flow as an exponential function:

$$q_t = q_0 K_r^t \qquad \text{(Equation 3.5)}$$

where q_t represents the flow at time t, q_0 represents the initial discharge, and K_r is a recession constant (here defined as the ratio of baseflow at time t to baseflow one day earlier). A shortcoming of this method is that it is an empirical method, and does not use any of the infiltration data calculated by the loss method discussed in Section 3.2.1. However, the recession approach is commonly used and accepted for modelling baseflow, and can be adapted to both design storm and continuous simulation modelling. Given this, along with the inappropriateness of the other baseflow choices within HEC-HMS, the recession method was chosen for use.

The recession method of Equation 3.5 is implemented in several forms in HEC-HMS. One option is the bounded recession method, where monthly baseflow limits are specified, so that baseflow cannot recess beyond this value. The problem with this method is that it does not reset itself after a storm event – a necessity for continuous simulation. It does not account for the soil moisture replenishment after a storm event, and the related increase in baseflow – flow is defined solely by Equation 3.5 until it reaches the limiting value. The other recession option in HEC-HMS accounts for this by using a defined threshold. A

threshold value defines where recession begins again after a storm event. After this threshold, total flow is then defined by Equation 3.5. Baseflow is then calculated indirectly, as total flow minus direct runoff flow. As the threshold is usually defined as direct runoff is close to ending, baseflow quickly approaches total flow. The threshold value can either be defined as a set flow value, or a ratio to peak can be specified (the threshold flow is equal to some percentage of the peak flow). Given the variation in storm magnitudes and durations, as well as pre-storm conditions, it seems more logical to employ the ratio to peak threshold approach rather than a fixed flow rate. With this choice of baseflow method, it is necessary to estimate three parameters: an initial baseflow for the beginning of simulation q_0, the recession constant K_r, and the ratio to peak.

Given that the time frame for continuous simulation is April – October (as discussed more in Section 3.3), the initial baseflow amount was based on April values. This same value was employed for design storm simulation as well. Flow data from the Ancaster Creek gauge at the watershed outlet (the same data used for calibration discussed in Section 3.3) was used to estimate initial baseflow in the form of daily flow averages from Water Survey Canada's 1987-88 April data (there are no available data for April for 1986). This time period was chosen so as to match the time period of the report these study data are based on (Philips, 1987). The data were screened against rainfall data from Environment Canada's Hamilton Airport gauge. Those days with over 1 cm recorded rainfall were eliminated from the analysis, to ensure a better estimate of true baseflow. The

remaining flows were averaged, to produce an average baseflow for April at the outlet of 0.0975 m^3/s. By dividing this flow by the total contributing area of the basin, we get an approximate initial baseflow of 0.01 $m^3/s/km^2$. It was assumed that baseflow contribution was relatively constant for the basin, thus this value was used as initial baseflow for each individual subbasin.

The recession constant was estimated by examining 10 minute flow data from the Hamilton Conservation Authority gauge for the same period and location. The method of Viessman Jr. and Lewis (2003) for estimating the recession constant was employed, which uses a linear trendline fit to a plot of flow recession data. The results are shown below in Figure 3.4.

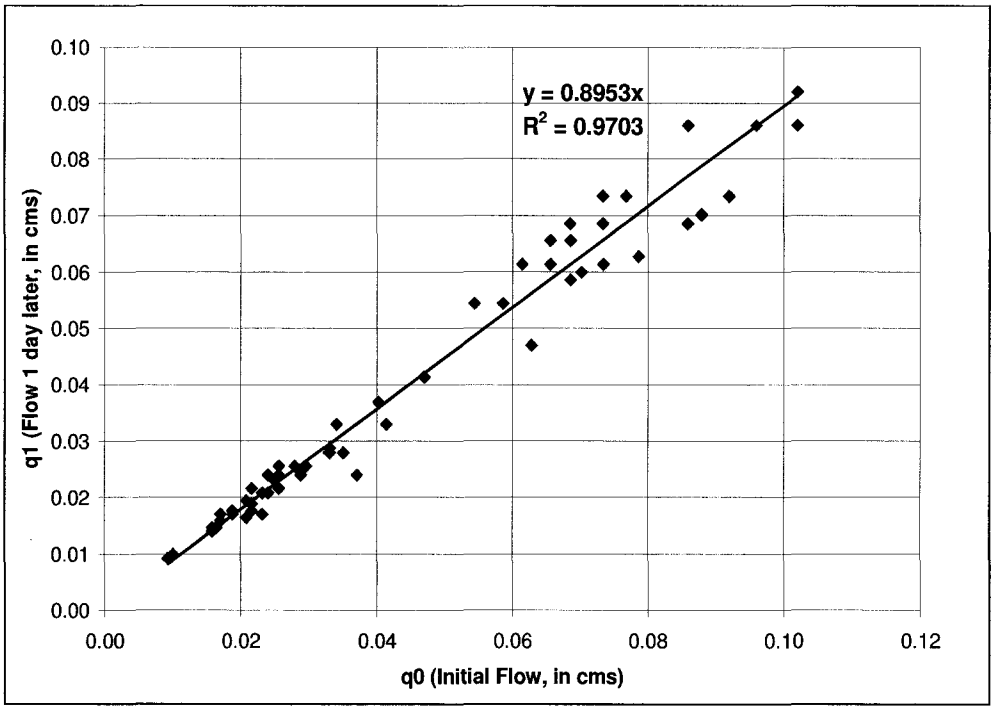

Figure 3.4: Calculation of baseflow recession constant

From Figure 3.4, the slope of the best fit line is 0.8953, or approximately 0.90. This value of K_r can also be obtained by averaging the K_r value for the individual data points. This value approximates the baseflow recession factor K_r for the basin. The high R^2 value for the fit line of Figure 3.4 indicates a good fit to the data.

The ratio to peak value was also estimated from an analysis of 10 minute flow data from the Ancaster gauge. According to the USACE (2000), the threshold value can be estimated by finding the point at which the recession limb of a storm hydrograph is approximated well by a straight line. Four major storm hydrographs (those with the highest peak flows for that year) were chosen for each year in the 1986-1988 period. The threshold value for each hydrograph was approximated using the USACE's definition. The ratio to peak was then simply calculated as the ratio of threshold flow to the peak flow for each storm hydrograph. The average ratio to peak of 0.07 was then assumed to reasonably represent the recession characteristics of the watershed.

With the estimation of these three parameters, baseflow can be estimated on both a discrete and continuous basis for each subbasin. The addition of this flow to the direct runoff calculated previously yields the total outflow hydrograph for a basin.

3.2.4 CHANNEL ROUTING

In addition to modelling the overland runoff flow of sub-basins, it is also necessary to model how that flow moves once it reaches the sub-basin outlet and enters the water course. It is necessary to account for both the travel time and storage effects of the river upon the flow.

HEC-HMS offers a number of different methods of channel routing, including both empirical and conceptual approaches. The empirical approaches (Lag and Straddle Stagger routing methods) use simple time inputs to represent the translation and attenuation effects of reaches. The conceptual approaches (Kinematic Wave, Modified Puls, Muskingum, and Muskingum-Cunge) offer different approximations of the fundamental St. Venant equations of continuity and momentum. The choice of a conceptual approach was deemed preferable, given that they are based on the fundamental equations of flow, and tend to utilize quantifiable physically-based parameters. The difficulty is in determining which conceptual method is the most appropriate. The Muskingum routing method (McCarthy, 1938) was chosen for use in this model. Although not as theoretically robust as the Kinematic Wave and Muskingum Cunge methods, the Muskingum method is simpler to apply (does not directly require channel roughness information, which was not available) while still retaining a reasonable conceptual basis. According to Ponce (1989) the Muskingum method is the most widely used method of hydrologic stream channel routing. The method is based on an

average finite difference approximation of the continuity equation for a cross-section, along with a linear weighted storage function:

$$S_r = K\,[XI + (1\text{-}X)\,O] \qquad \text{(Equation 3.6)}$$

where I represents inflow, O represents outflow, S_r represents storage, K represents the storage time constant for the reach, and X is a weighting factor between 0 and 0.5. The combination of Equation 3.6 and the continuity equation allow for the calculation of outflow at any time step given the initial outflow.

The Muskingum parameters K and X do not have a strict physical meaning. K is usually assumed to be equal to the wave travel time of the reach, while X is simply a weighting factor which affects the degree of flow attenuation (0 being the most attenuation, and 0.5 being no attenuation). HEC-HMS also requires the number of sub-reaches, which further affects attenuation. The number of sub-reaches defines over how many intervals within the reach the equations are applied.

The report on which this model is based (Philips, 1987) included channel cross-sections along the Ancaster Creek along with chainages from the downstream end, which allowed for accurate length measurements for each reach segment. As mentioned, K is usually interpreted as the wave travel time of the reach. Thus, if the reach lengths (L_r) are known, K can be estimated by (USACE, 2000):

$$K = L_r / v_w \qquad \text{(Equation 3.7)}$$

where v_w represents the flood wave velocity. The flood wave velocity can be estimated in a number of different ways. Because measured flow data were only available for the basin outlet, this point was used for estimating velocities. It was assumed that velocity was identical for all other reach sections.

The USACE (2000) recommends estimating the wave velocity by using Seddon's Law (Seddon, 1900) which states

$$v_w = 1/B\ (dQ/dy) \qquad \text{(Equation 3.8)}$$

where B is the top width of the channel, and dQ/dy is the derivative of the stage-discharge curve. The top width of the channel was again calculated using the available cross-section geometry along with recorded water levels at each time interval. The derivative term was calculated from polynomial trend lines which were fitted in three segments to the stage-discharge curve for the creek and then evaluated at each time step. Three segments were necessary, as a single trend line was unable to adequately cover the full curve, particularly at lower stages (below 0.2 m). The stage-discharge curve is shown below in Figure 3.5.

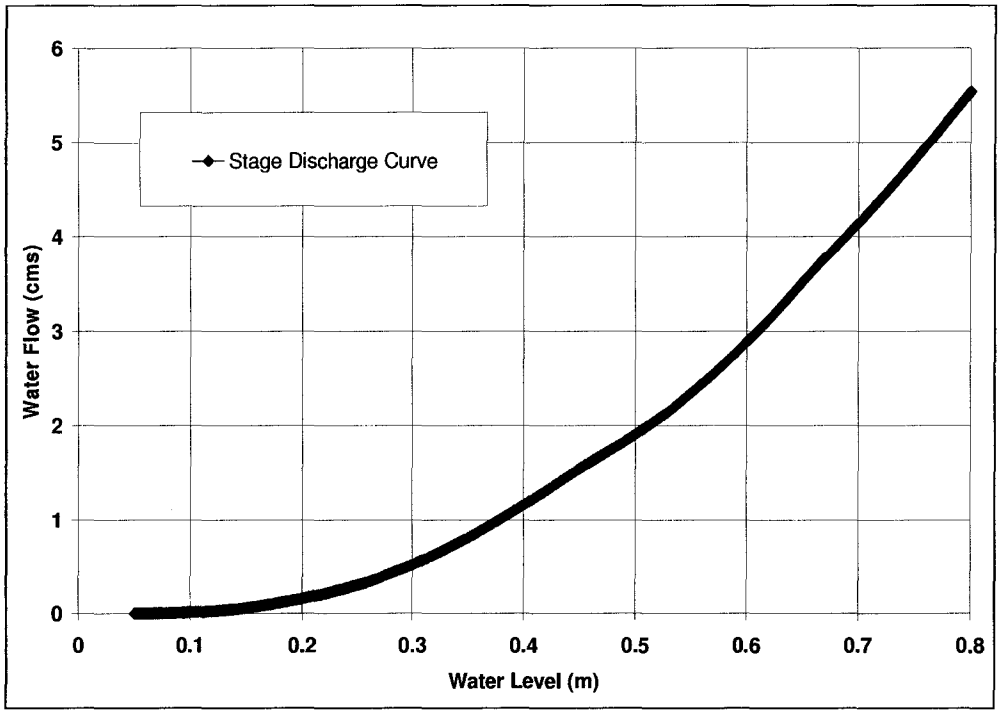

Figure 3.5: Stage-discharge curve

Thus, wave velocities were calculated at each time step of the available data for the 1986-1988 period. These results were again averaged to obtain an average wave velocity estimate of 0.274 m^3/s.

As mentioned, wave velocity was assumed constant for all reach segments. K was then calculated for each reach segment according to Equation 3.7 with the respective lengths of each reach segment, based on chainage information. The estimation of the other parameters in the Muskingum routing method (X, as well as the number of sub-reaches) were dependent upon the stability criteria summarized by the USACE (2000). Because these criteria are dependent upon the value of K, as well as the time step interval (which is in turn

dependent upon other factors such as the SCS UH method described in Section 3.2.2), the final determination of these parameters is described along with the calibration process in Section 3.3.

3.3 MODEL TESTING

In order to properly implement the model parameters described in the previous section, it is necessary to compare it against observed data for the same area. The flow and rainfall data used for this purpose, as well as the consideration of time intervals, and the calibration and verification procedure, are described in the following sub-sections. It should again be noted that the assumption of stationary watershed conditions is made in the calibration and verification of this model. Thus, the final watershed model does not account for changes in land use over time which would affect the magnitude of calculated flows. As noted previously, this simplification is necessary in order to fairly compare design storm and continuous simulation results. As the watershed model is being used for this purpose only, and not to provide the actual historic flood frequency distribution for the watershed, this assumption is justified.

3.3.1 RAINFALL AND FLOW DATA

In order to perform a calibration, two sets of data are needed: rainfall and flow data. This section details what data were available, and how they were used.

Flow data in this study came in the form of 10-minute water level data from the Hamilton Conservation Authority for the 1986 – 1988 period. The gauge is located at the outlet of the modified watershed used in this study, junction A29 in Figure 3.3. The level data were irregular, with many missing periods, which limited some of the later calibration work. Along with these level data, a stage-discharge curve was also provided by the Hamilton Conservation Authority (as was shown in Figure 3.5), which allowed the transformation of levels into flows.

In addition to this main source of flow data, daily flow data from Water Survey Canada were also used (they operate another gauge at the same location). Daily flows from 1987 – 1988 for the month of April were used in estimating initial baseflow was described in Section 3.2.3.

Hourly rainfall data were used in the actual modeling and testing work of this thesis, as discussed in Section 3.4. Thus, hourly rainfall data were also employed for the calibration to ensure consistency. Hourly rainfall data were chosen for use for several reasons. Although rainfall data with a finer temporal resolution (such as 15-minute data) would be preferable, as they more accurately represents actual rainfall patterns, such data are much more difficult to obtain, and

typically have a much shorter record length than hourly rainfall data. Thus, although a better definition of rainfall patterns is gained through the use of 15-minute rainfall data, the ability to more accurately estimate storm return periods is lost. It is also much more computationally intensive to use 15-minute data for long continuous simulation runs, making it much more cumbersome. As such, hourly rainfall data were employed in all modelling work.

For the purposes of calibration only 1986 data were used, as it was felt this would be the most accurate, as this data would be closest to the time frame of the source report (Philips, 1987). Typically a proper calibration and verification should use several years of data. However, the goal of this research is not to create a perfect model of the study watershed – it is to create a reasonably realistic watershed model which can be used as a tool to compare design storm and continuous simulation results. As such, the limited calibration and verification procedure is justified in this case.

Hourly rainfall data from Environment Canada's nearby Hamilton Airport station (Climate ID 6153194) were used as a base. Two missing days were filled using data from nearby stations. In addition, 10-minute rainfall data were available for the Hamilton Conservation Authority's Ancaster rain gauge (located at the same location as the flow gauge). Because this location was closer to the majority of the subwatershed than Environment Canada's gauge, these data were used for major storm events. The 10-minute data were summed into hourly data and replaced the Environment Canada data for the periods of peak flows used in

the calibration discussed in Section 3.3.3. It was felt this would more accurately represent watershed rainfall, given the assumption of an even distribution of rainfall across the watershed.

3.3.2 TIME

Much consideration was also given to the issue of time in this hydrological model – the time duration of the simulation, as well as the time step used for calculations.

The time duration in this case refers to the length of the continuous simulation run. The durations of various design storms are discussed in later sections. Continuous simulations were run between April and October inclusive of each year of available rainfall data. Winter months were not included for several reasons. First, there was a lack of available precipitation data for these months. Gauges were frequently either shut down during these months, or records not kept. Second, not using winter months avoids the problems associated with freezing and snowmelt. Precipitation records are frequently affected by the freezing effects of winter months, as are water level gauges by ice and snow blockages. If the winter months were included, snowmelt calculations would have to be included in order to accurately represent the watershed's characteristics. Since the focus of this thesis is on a comparison of rainfall storm modelling techniques, the inclusion of snowmelt modelling would be an

unnecessarily complicated addition. As such, continuous simulation runs utilize non-winter data only, namely April to October.

The choice of a time step involves a consideration of a number of factors. Although hourly rainfall data were utilized for modelling, the time step need not match this increment. Using such a time step would likely yield very coarse resolution hydrographs, which would likely misrepresent true peak flows. In fact, one of the conditions of using the SCS Unit Hydrograph discussed in Section 3.2.2 is that the time step should be approximately 13% of the time of concentration (t_c), in order to ensure an adequate number of points on the rising limb of the hydrograph. This can be obtained by combining the hydrograph definition of the time to peak (t_p) with the knowledge that for the SCS UH, the time of concentration plus the time step Δt is approximately 1.7 times t_p. Viessman Jr. and Lewis (2003) suggest that the time step can range from this value of 0.13 t_c up to approximately 0.17 t_c. The USACE (2000) recommend that the time step be less than 0.29 the lag time (t_l), which with the SCS assumption that $t_l = 0.6\ t_c$, translates to a time step of 0.174 t_c, very close to the upper limit suggested by Viessman Jr. and Lewis (2003). All of these recommended values were calculated based on individual basin t_c values. Values ranged from a time step of approximately 40 minutes (based on the t_c from the larger agricultural subbasins) to approximately 7 minutes (for the smaller urban subbbasins near the basin outlet). In the end, a time step of 10 minutes was chosen, for a number of reasons. As can be seen from Table B4 in Appendix B (based on the curve

numbers discussed in Section 3.3.3), a 10-minute time step satisfies the conditions of the SCS UH method for all but 3 of the 16 subbasins, which suggested a close, but slightly lower t_c of 7 to 9 minutes. To satisfy this condition of these subbasins, it would have been necessary to reduce the time step to 5 minutes, which would have made computations considerably slower for a negligible improvement in accuracy. A test comparison of hydrographs generated from one of the three subbasins using a 5 minute and then a 10 minute time step showed no discernable difference in the rising limb or magnitude of peak. Thus, a 10 minute time step was determined to be appropriate.

The choice of time step also impacts the Muskingum routing parameters. As a first consideration, the time step should be less than K, in order to have adequate definition of the effects of the routing reach upon the hydrograph. As is shown in the table of routing parameters (Table B5 in Appendix B), all reaches satisfy this condition for all velocities for a time step of 10 minutes. The selection of the other routing parameters are guided by the values of K and the time step. The number of subreaches is estimated by

$$L_r / \Delta x = K / \Delta t \qquad \text{(Equation 3.9)}$$

which is based on combining Equation 3.7 with a substitution of the wave velocity v_w as $\Delta x/\Delta t$. Thus the result of Equation 3.9 was rounded to the nearest integer for each reach segment to determine the number of sub-reaches.

The selection of X, the weighting factor, is also guided by the choice of time step. Besides X being between 0 and 0.5, it must satisfy stability criteria in order to avoid negative flows. As suggested by Hjelmfelt (1985), the criteria is

$$X \leq ((0.5\ \Delta t) / K) \leq 1\text{-}X \qquad \text{(Equation 3.10)}$$

Using these criteria, trial values of X were attempted. It was assumed that all subbasins shared similar characteristics, thus the same value of X was employed for each. A value of X of 0.05 was chosen as a satisfactory value.

Thus after consideration of all affected parameters, a time step of 10 minutes was chosen for computations, which in turn guided the selection of Muskingum routing parameters.

3.3.3 CALIBRATION AND VERIFICATION

After all the previous steps had been taken, and all necessary parameters estimated, it was then necessary to perform a calibration of the hydrologic model, as well as a verification of its output results.

As mentioned briefly in Section 3.2.1, the report on which the data for the model are based (Philips, 1987) provides curve numbers and imperviousness percentages for two different development scenarios. "Existing" refers the state of development in the town of Ancaster as of 1976. The other, "Future" refers to

the state of development as specified in the Town of Ancaster Official Plan for 1986. Curve numbers varied very little between the two scenarios. Imperviousness percentages however, varied quite dramatically between the two different development scenarios, with the "Future" scenario showing a large rise in imperviousness percentages for numerous subbasins.

Given that 1986 flow data were used for calibration purposes, it is more likely that the "Future" development scenario would accurately represent basin conditions at that time. However, these parameters were based on a plan only, and may not have truly represented the conditions at that time – development may have proceeded at a slower pace than anticipated. This would be more significant for the percentage imperviousness, given the small change in curve numbers previously noted. In order to account for this, the percentage imperviousness was employed as a calibration parameter. Because of the small change in values, the "Future" scenario curve numbers were used directly in the model and assumed to be accurate.

As discussed in Section 3.3.1, the calibration was performed for the 1986 year using the modified hourly rainfall data for the area. The rainfall was assumed to be uniformly distributed over all subbasins. All variables were determined as previously discussed, with the imperviousness being varied as part of the calibration process. The calibration and verification was performed against the four highest observed peak flows which occurred in 1986. The highest peak flow was used for verification purposes, while the three lower peaks were used in

the calibration. The results of the calibration comparison using the two different sets of imperviousness values are shown below in Table 3.1.

Table 3.1: Model Calibration Peak Flows

		"Existing" (1976 imperv.)		"Future" (1986 imperv.)		Calibrated	
Date	Observed Peak Flow (cms)	Modeled Peak Flow (cms)	Relative Error (%)	Modeled Peak Flow (cms)	Relative Error (%)	Modeled Peak Flow (cms)	Relative Error (%)
Sep-10	2.842	1.759	38.1	3.856	-35.7	2.457	13.5
Sep-15	1.438	1.290	10.3	2.711	-88.5	1.737	-20.8
Oct-14	1.358	1.073	21.0	2.009	-48.0	1.386	-2.0
Average Relative Error (%)			**23.1**		**-57.4**		**-3.1**

Relative error is used to quantify the difference in peak flow values, where a negative error implies overestimation. As can be seen from the results, the "Existing" imperviousness values underestimate peak flows, while the "Future" imperviousness values greatly overestimate them. From the magnitudes of the errors, one can see that the true imperviousness rates for that period are closer to the "Existing" scenario values (average relative error of 23.1% as compared to -57.4% for the "Future" scenario). Various different linear ratios of the two development scenarios were tried in the calibration process to try and reduce the overall error of peak flow estimates. In the end, the most accurate ratio was found to be 67% of the "Existing" scenario to 33% of the "Future" scenario. As can be seen, relative error is greatly decreased, with an average relative error of only -3.1%. The resulting final impervious percentages, SCS Curve numbers, and related SCS soil moisture parameters are shown in Table B6 of Appendix B.

As a final step, the calibrated hydrologic model should be verified – its ability to accurately predict peak flows checked. The verification was performed against the highest observed peak flow for 1986. The results are shown graphically below in Figure 3.6.

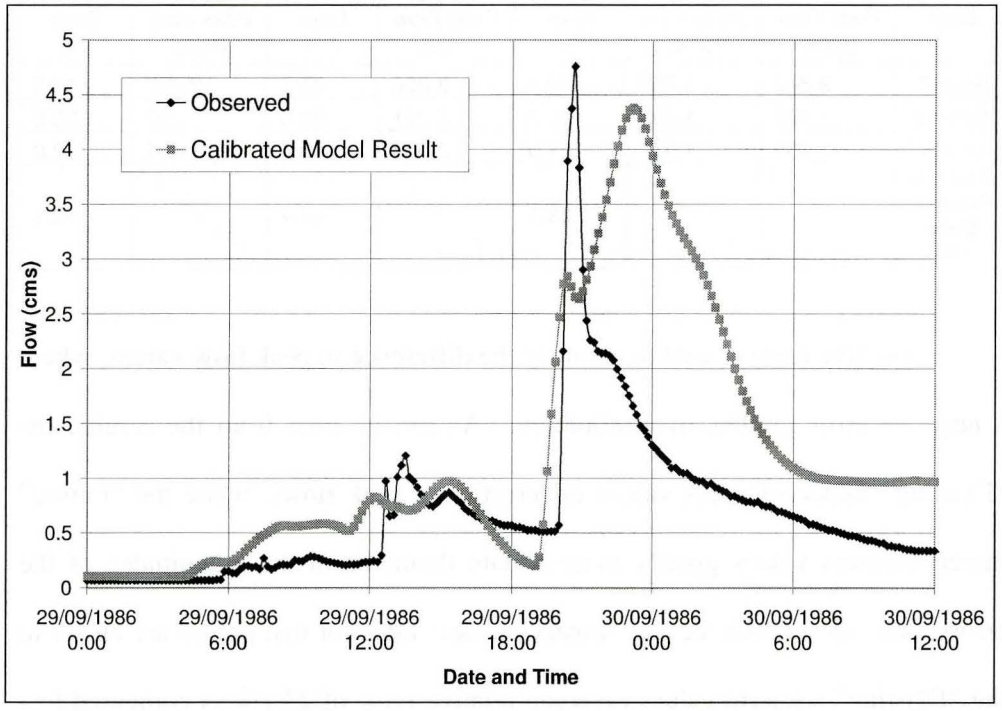

Figure 3.6: Verification results

As can be seen in Figure 3.6, the modeled storm hydrograph is not a perfect match to the observed flow hydrograph. The modeled hydrograph appears to have a larger volume and shows a much slower recession than the observed data. The modeled peak of 4.381 m^3/s is also lower and occurs later than the observed peak of 4.757 m^3/s. These differences could be due to a number of

factors, such as the simplifying assumption of an even rainfall distribution and the use of input rainfall from the Ancaster rainfall gauge only for this storm. The actual drainage pattern in the urban areas may also not match the modeled watershed. Unknown storm sewer outlets and the simplifying basin lumping done in Section 3.1 may have led to discrepancies. Numerous other factors also likely played a role, such as the error in the estimation of other modelling parameters – modeled land use types may not match actual values for the simulated period.

Despite these differences between the two hydrographs, the modelled peak flow is still reasonably close to the observed value: the modelled value has a relative error of only 7.9%. Given that the focus of this thesis is upon the comparison of peak flows, the differences in hydrograph volume and recession, though worth noting, are not that significant. It appears the calibrated hydrologic model can reasonably reproduce peak flows, and thus is appropriate for the comparison modelling undertaken in this thesis.

3.4 MODEL RAINFALL DATA

For the actual modelling performed in this thesis, rainfall input data are required: both continuous simulation and design storm data. Both should be based on the same original rainfall source in order to ensure a fair comparison. An external rainfall record (i.e. outside of the study basin area) was chosen for

use, namely data from Environment Canada's Toronto station (Climate ID 6158350).

The choice to use Toronto over Hamilton rainfall data was made for a few reasons. First and foremost, the Toronto data offered a much longer period of record than the Hamilton data (61 years for Toronto as opposed to 34 years for Hamilton). A longer period of record allows for a much more thorough comparison of design storm and continuous simulation methods. It means a greater chance that high-intensity/low-frequency storms are included in the rainfall record, ensuring a more robust comparison, as well as a much more accurate estimation and comparison of return periods. Second, the Toronto dataset offered a much higher quality than the Hamilton data. The Toronto data had much less missing data, and also had many more nearby rainfall records that could be used to fill gaps.

The use of external rainfall data on the model should have no impact on the results. Hamilton data were used for calibration and verification of the model (Section 3.3.3), in order to verify that the hydrologic model could reasonably model peak flows – thus making the model and the results more realistic and more reliable. Since the accuracy of the hydrologic model was established in Section 3.3.3, the choice of rainfall input source for the actual modelling is immaterial. The built hydrologic model is simply a tool to investigate the hypotheses of this thesis. The two locations should also be quite comparable, as the two sites are only approximately 70 km apart. A comparison of Environment Canada's 1971-

2000 climate normals for the two stations shows differences of less than 10% in average annual precipitation and rainfall totals..

Thus, the use of external Toronto rainfall data in the hydrologic model is both acceptable and advantageous. The following sections discuss how the Toronto rainfall data were adapted for use in both continuous simulation and design storm applications.

3.4.1 CONTINUOUS SIMULATION DATA

As discussed in the previous section, the base for continuous simulation was rainfall data from Environment Canada's Toronto station. As was also discussed in Section 3.3, hourly rainfall data were used, from April to October of each available year.

The raw rainfall data obtained from Environment Canada required editing, as there were many gaps in the data record. The raw data record ranged from 1937-1998. However, several years were missing almost all of their data, and had to be deleted. Filling data for these years from nearby stations was impossible, as these gaps all occurred in the early period of the data, when there were no other nearby rainfall gauges in operation (Toronto Pearson did not begin operation until 1960). Thus, after deletion of incomplete years, the record contained the years 1939, 1941-1955, and 1959-1998 (56 years in total).

This remaining period of data still contained missing data: 412 days in total with some portion missing. The missing data were filled in a variety of ways. Where possible, data gaps were filled using nearby station data. If data from multiple stations were available, the one whose daily total most closely matched that of the target station was used. If nearby station data were not available, the daily precipitation total was used as a guide to fill gaps.

In this manner, a complete hourly rainfall record was created with 56 years worth of data. This dataset was then used to calculate another continuous simulation parameter, evapotranspiration. As discussed in Section 3.2.1, evapotranspiration was assumed to be approximately 70% of precipitation. Thus, pan coefficients were calculated for each year of the Toronto data such that total evapotranspiration was about 70% of annual (April-October) rainfall.

3.4.2 INTENSITY DURATION FREQUENCY CURVES

In addition to the continuous simulation data discussed in the previous section, design storm hyetographs are also required. In order to construct these design storms, statistical rainfall data are required – namely, rainfall intensities corresponding to specified return periods. Typically these are given in the form of IDF (intensity-duration-frequency) curves, which are widely available from a number of sources such as municipalities or Environment Canada. Such IDF curves are available for the Toronto area. However, in order to ensure an accurate

comparison to continuous simulation results, IDF curves should be based on the same original data source. In this way, the frequencies and magnitudes of rainfall intensities should be the same.

Therefore, the formatted continuous simulation data discussed in the previous section were used to generate IDF curves, in order to calculate design storm parameters. This was achieved through the use of a computer program written in MATLAB. An annual maximum series approach was taken, whereby the maximum average rainfall intensity for each year was found for all durations ranging from 1 hour to 24 hours. Average rainfall intensity (i_{avg}) in mm/hr was calculated as

$$i_{avg} = V_p / t \qquad \text{(Equation 3.11)}$$

where V_p represents total rainfall volume (mm) for the specified duration time, t (hours). In order to create IDF curves, a frequency or return period must be assigned to each datum point. Return periods were calculated using the sorted annual maximum series data of average rainfall intensities along with the well-known Weibull plotting position formula

$$T = (n+1) / m \qquad \text{(Equation 3.12)}$$

where T is the return period (years), n is the total number of values in the series, and m is the rank of the value in question within the series. Since in this case there are 56 years of rainfall data, $n = 56$. By using Equation 3.12 in conjunction with the annual maximum series of rainfall intensities, return periods can then be assigned for different average intensities of different time durations. The data are more frequently presented in graphical form, typically for commonly used return periods (2, 5, 10, 25, 50 and 100 years). Because the calculated return periods do not match these even values, the results are presented in an alternative form below in Figure 3.7

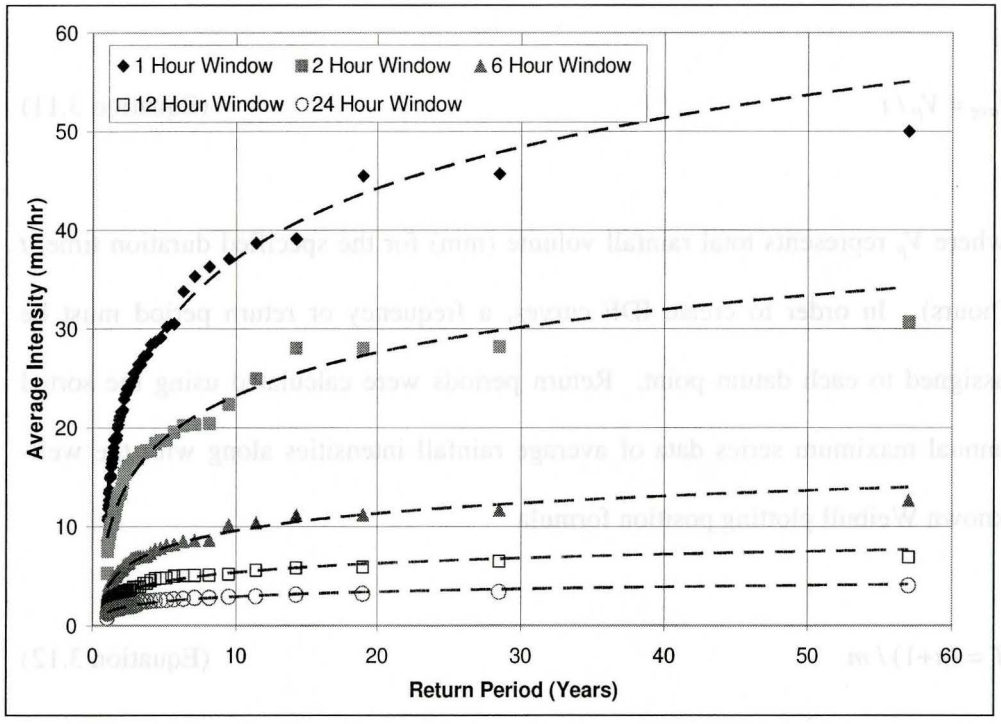

Figure 3.7: Select average intensity data

Figure 3.7 illustrates the results of the IDF analysis for a few common duration times. The data points are fit with logarithmic curves to illustrate general trends. As can be seen in Figure 3.7, in order to use common return periods (2, 5, 10, 25, 50 and 100 years), interpolation between existing data points would be necessary. This would introduce an additional source of error into the analysis. In order to avoid this problem, the calculated data points were used as they were.

Because it would be extremely time-consuming to employ each and every return period in the analysis (and thus construct and model design storms for each and every return period), only select values were employed. Return periods for analysis were selected so as to ensure representation from the complete range of return periods and have reasonably evenly spaced values. Return periods of 57.00, 28.50, 14.25, 8.14, and 3.00 years were selected for use in the analysis. These values are plotted in standard IDF form below in Figure 3.8.

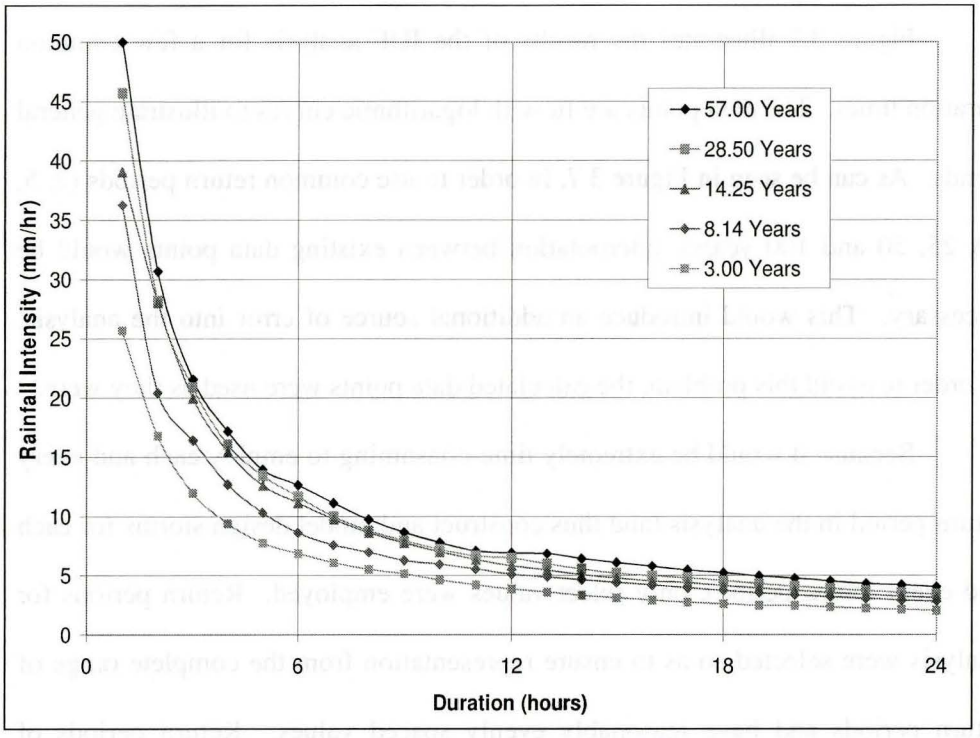

Figure 3.8: Intensity-duration-frequency curves

Figure 3.8 shows that the selected return periods and their associated rainfall intensities are reasonably well-spaced and cover a fairly large range of values. Thus, the five selected return periods can be assumed to be reasonably representative of the full spectrum of IDF curves.

3.4.3 DESIGN STORM TYPES

Once the IDF curves have been calculated, the data they contain can be applied to create a variety of different design storms for comparison with

continuous simulation data. The return period of each design storm is assumed to be equal to the return period of the intensity value used to calculate it – the fundamental assumption of design storm theory, as discussed in Chapter 2. There are numerous types of design storms which can be used, as was also suggested in Chapter 2. Different design storms are based on a wide variety of data and theoretical assumptions, and have widely varying applicability.

As a preliminary guide to design storm selection, the draft version of the City of Hamilton's Criteria and Guidelines for Stormwater Infrastructure Design (Philips, 2004) were employed. In this document, several different types of design storms are suggested for use in the City of Hamilton: the Chicago design storm, the Atmospheric Environment Service (AES) 1-hour and 12-hour design storms, and the U.S. Soil Conservation Service (SCS) Type II design storm. Although not all of these design storm types were used in this thesis, an attempt was made to employ similar design storm types, as discussed in the following sections. A variety of different durations were also employed, in order to try and account for a larger range of possible storms. The storms discussed below used 3, 6, 12 and 24 hour durations unless otherwise specified.

3.4.3.1 ALTERNATING BLOCK STORM

As previously mentioned, one of the design storms recommended in the City of Hamilton's Criteria and Guidelines for Stormwater Infrastructure Design

(Philips, 2004) is the Chicago design storm. This commonly used design storm was introduced by Keifer and Chu (1957) for use in sewer design in the City of Chicago. In the Chicago method, the IDF curve of choice is approximated by the function

$$i_{avg} = a / (t_d^b + c) \qquad \text{(Equation 3.13)}$$

where i_{avg} represents average rainfall intensity, t_d represents the storm duration, and a, b, and c are fitting parameters. The ordinates of the Chicago design storm hyetograph are calculated by

$$i = a[(1\text{-}b)(t_{cb} / r)^b + c] / [(t_{cb} / r)^b + c]^2 \qquad \text{(Equation 3.14)}$$

for the pre-peak period, and by

$$i = a[(1\text{-}b)(t_{ca} / (1\text{-}r))^b + c] / [(t_{ca} / (1\text{-}r))^b + c]^2 \qquad \text{(Equation 3.15)}$$

for the post-peak period. In these equations i represents the intensity ordinate of the hyetograph, t_{cb} represents the time from the point of interest to the peak of the storm (pre-peak period), t_{ca} represents the time from the peak of the storm to the point of the interest (post-peak period), and r represents "the advanceness of the storm pattern" (Keifer and Chu, 1957), calculated as

$$r = t_p / t_d \qquad \text{(Equation 3.16)}$$

where t_p represents the time to peak and t_d represents the total duration of the storm.

A key property of the Chicago storm is that the distribution described by Equations 3.14 and 3.15 contains all of the average intensities of the rainfall source IDF curve for all durations. The Chicago method is typically used for shorter storms (usually 1 and 3 hour durations), which necessitates short time steps. Because hourly rainfall data are used in this thesis, the 1-hour storm is not appropriate, nor is the temporal resolution sufficiently fine to appropriately use Equations 3.14 and 3.15. However, the principles of the Chicago storm can be employed in a similar design storm method, usually referred to as the synthetic block or alternating block storm method.

In the alternating block storm method, the storm also contains all the average intensities of the given IDF curve for all durations – the same principle behind the Chicago storm. The construction method is summarized by Akan and Houghtalen (2003). The chosen IDF curve is analyzed to extract the average intensities at integer multiples of the time step (i.e. for an hourly time step, the 1-hour, 2-hour, 3-hour... intensities). Average intensity is then multiplied by duration to get precipitation depths. The differences between subsequent depths are calculated, and then these values are divided by the time step to get a series of

incremental intensities. The location for the peak intensity is chosen, and then the remaining intensities are distributed on alternating sides of the peak until all values are distributed. The end result is an alternating block storm, a discrete hyetograph with the same principles as the Chicago storm (contains all the average intensities of the source IDF curve for all durations).

The decision on where to place the peak intensity is of some importance in determining the characteristics of the resulting hyetograph. This parameter corresponds to r in the Chicago method – the time to peak divided by the storm duration. Akan and Houghtalen (2003) state that a general rule of thumb is to place the peak between one third and one half of the total duration. Yen and Chow (1983) presented suggested values of r for the United States based on an extensive analysis of recorded rainstorms. Although they do not present results for Canada, an examination of their figures shows that the study area roughly corresponds to an r value of 0.35 based on values in nearby areas of the United States. This value was therefore used as a guide to the placement of the peak in the alternating block method.

The decision on which direction to alternate subsequent rainfall intensities is also of some importance in determining the characteristics of the resulting hyetograph. In this case, alternating began to the right of the peak rainfall. This results in a slightly lower peak runoff than if alternating began to the left, which helps to counteract the overestimation inherent in the Chicago/alternating block storm type. As noted by Marsalek and Watt (1984) the assumption that a storm

would contain all rainfall maxima for a particular return period within its distribution results in an underestimation of the true return period (and thus an overestimation of storm volume/intensity). By alternating to the right after the peak, this may help reduce some of the overestimation inherent in this storm type.

3.4.3.2 AES DESIGN STORMS

As previously mentioned, another of the recommended design storms in the City of Hamilton's Criteria and Guidelines for Stormwater Infrastructure Design (Philips, 2004) is the AES storm – both the 1 and 12 hour versions. Given the use of hourly rainfall data in this thesis, only the 12 hour AES design storm was appropriate for use.

AES design storms are based on a paper by Hogg (1980), who analyzed recorded 1 hour (5-minute time step) and 12 hour (1-hour time step) rain events at 35 different locations across Canada for the 25 year period of 1951-75. Rainfall events were analyzed by expressing their distributions as cumulative percentages of storm totals. These results were then analyzed to create cumulative probability distributions. The results were lumped for four different areas of Canada, including Southern Ontario.

For each of these different geographic areas, cumulative probability distributions are given for 10%, 30%, 50%, 70%, and 90% probabilities. These probabilities represent the percentage of storm events which deposit rainfall in the

manner indicated by the curve. For instance, the 10% probability curve indicates that 10% of the rainfall events analyzed deposited at least 85% of their total 12-hour rainfall in the first 2 hours.

The AES design storm distributions are easily applied to generate 12-hour design storms. IDF curves are analyzed to find the average intensities corresponding to a 12-hour duration for different return periods. These average intensities are multiplied by the duration to get depths. These depths are then used in conjunction with the AES cumulative distributions to obtain the design storm hyetograph.

The only other factor is the decision of which probability to use. Because of the focus on peak flow estimation, storms with higher peak intensities were deemed more appropriate. These storms are indicated by sharp rises in the cumulative probability distribution. Thus, the 10% and 30% AES design storms were chosen for use.

3.4.3.3 SCS DESIGN STORMS

The final design storm type recommended in the City of Hamilton's Criteria and Guidelines for Stormwater Infrastructure Design (Philips, 2004) is the SCS Type II design storm.

This 24-hour design storm was developed by the United States Soil Conservation Service (1986). They developed four different dimensionless

rainfall distributions for different regions of the United States – Type I, IA, II, and III. Type II represents the majority of the non-coastal areas of the continental US, and is thus appropriate for use in the study area. For Type II areas, the storm peak was found to be roughly at the centre of the distribution. The storm distributions were developed using volume-duration-frequency data from the US Weather Bureau. An incremental approach, similar to that used in the Chicago and Alternating Block storm methods was used in the development of the SCS storms. Thus the SCS design storm contains nested rainfall intensities of shorter durations.

In addition to the 24-hour duration design storm, the SCS (now the Natural Resource Conservation Service) has also developed a time-dimensionless design storm, primarily for use in Earth Dam design (2005). Little detail is given on the development of the dimensionless design storm in the source paper (NRCS, 2005). However, it is assumed it was developed in a similar manner to the SCS 24 hour storm. For this dimensionless storm, 6 and 12 hour durations were used. A 3-hours storm was not used given the excessively coarse discretization of the source distribution required.

The SCS dimensionless storm distributions were then applied to design storm creation in the same manner described in previous sections – through the use of IDF data.

3.4.3.4 HUFF DESIGN STORMS

Although not suggested in the City of Hamilton's Criteria and Guidelines for Stormwater Infrastructure Design (Philips, 2004), Huff design storms are another widely used design storm in practice.

The origins of the method lie in a paper by Huff (1967) in which he presented a number of different rainfall time distributions. Huff analyzed 11 years of rainfall data (1955-66) from 49 rain gauges in east central Illinois. Rain storms were separated by defining them as a rain period separated from preceding and succeeding rainfall by 6 hours or more (Huff, 1967). These rainfall events were then analyzed in a manner similar to the AES method previously mentioned (in fact, Hogg (1980) references Huff's method in his paper). In Huff's method, rainfall events were analyzed by expressing their distributions as cumulative percentages of storm totals for different probabilities (the probability that at least that specified percentage of storm total will have occurred for that given time). Huff (1967) also went further, by expressing the time axis as a cumulative percentage of total storm duration, and by sorting storms by whether their peak occurred in the first, second, third, or fourth quartile.

The choice of quartile, probability, and duration will have a definite effect upon the characteristics of the Huff design storm. Although Huff (1967) provided probabilities from 10 to 90%, he states that the 50% level is likely the most useful statistic. In many reproductions (such as Akan and Houghtalen, 2003), the 50%

curve is the only one given. Thus, the 50% probability curve was chosen for use. Because of the interest in peak flows, late peaking storms were chosen for use – 3rd and 4th quartile Huff 50% storms. These storms allow time for the soil to fill moisture deficits prior to peak intensity, resulting in higher peak flows. 1st and 2nd quartile Huff storms result in much lower peaks. 6, 12, and 24 hour duration storms were employed for these storms. Similarly to the SCS distribution, a 3-hour storm was not employed, given the coarse discretization that would result.

Huff's dimensionless storm distributions were then applied to design storm creation in the same manner described in previous sections – through the use of IDF data.

3.4.3.5 TRIANGULAR DESIGN STORMS

A simple design storm construction method was suggested by Yen and Chow (1980), among others. They proposed using a simple triangular approximation to the design storm hyetograph. A storm duration is first specified. The corresponding average intensity is then found using the given IDF curves for different return periods. Then, the peak intensity is simply equal to

$$i_p = 2(i_{avg}) \qquad \text{(Equation 3.17)}$$

In Yen and Chow (1980), Equation 3.17 is arrived at by using moment equations. Equation 3.17 can also be found by using the geometric properties of a triangular hyetograph.

The only other unknown in this method is the location of the peak. This can be found using the methods discussed in Section 3.4.3.1 in relation to the Chicago design storm. As was discussed in that section, the work of Yen and Chow (1983) suggests an r value of 0.35. Thus, that value was also employed in the construction of triangular design storms.

Because of the discrete nature of the time step (hourly increments) of rainfall used in this thesis, the continuous triangular hyetograph had to be approximated. Once the ordinates of the triangular design storm have been found, the continuous intensities for each time increment (hourly) were replaced by a constant average intensity, such that the resulting rainfall depths were still equal for the time period. This approximation was necessary given the format of rainfall data used in this thesis.

The resulting discrete triangular design storms were calculated for 3, 6, and 12 hour durations. 24 hour duration storms were not used, as they result in storms with very low peak intensities.

CHAPTER 4: SINGLE BASIN COMPARISON

Before comparing design storm and continuous simulation methods for a complex watershed, it is first necessary to examine a simpler case: a single basin. In this way, factors that could have influence on the results of a more complex system can be more easily controlled, and analyzed in a simpler case scenario. There are numerous such factors. As mentioned in Section 3.4.3, numerous design storm types were initially chosen for use. However, it is likely that not all will be appropriate. By examining the results for a single basin first, we can more easily determine which storm types compare well with continuous simulation results for simple cases. This will likely lead to more meaningful results in the complex basin analysis of Chapter 5. Similarly, moisture conditions are another important factor, and a critical distinction between design storm and continuous simulation methods. While the initial moisture value for continuous simulation is not critical (given the long period of simulation and continuous moisture calculation), it is extremely important in the design storm method. Thus, similarly to the choice of an appropriate design storm, the choice of an appropriate initial moisture condition will yield a better comparison at the single basin level, and likely better results in the complex basin analysis. These factors are much more easily examined at the single basin level.

Two different individual basins were examined in order to evaluate another factor, the distinction between rural and urban basins. These basins were both chosen from the overall watershed model shown in Figure 3.3, the characteristics of which can be found in Tables B1-B6 of Appendix B. For a rural basin, basin 101 was chosen, and for an urban one, basin 106 was chosen. As can be seen from Tables B4 and B6, basin 101 has a low imperviousness (1%) and a fairly long time of concentration (3.98 hours), which leads to a much longer flow hydrograph with a lower peak, typical characteristics of a rural basin. Basin 106 on the other hand, has a fairly high imperviousness (50.3%), and a much shorter time of concentration (1.60 hours), which results in a short hydrograph with a large peak, typical of an urban basin. The two basins also have approximately the same drainage area, however as the final peak flows are corrected for this, this factor should have no influence on the results. As an initial value, the initial moisture deficit for each basin was calculated as 0.2 of the maximum soil water storage (S), in keeping with the SCS method described in Section 3.2.1. This parameter is further analyzed later in this chapter.

The two basins were therefore used for continuous simulation and design storm modeling with the model parameters described in Chapter 3. As mentioned in previous sections, the focus of this thesis is on the output peak flow only, other hydrograph parameters such as volume and timing parameters were not analyzed. The comparison results given in this section also assume that continuous simulation results are the truer estimate of flood frequency distributions, which as

noted in previous sections, may not necessarily be the case. The simplifying assumption of stationary watershed conditions should be kept in mind.

4.1 GENERAL RESULTS

Peak flow rates were therefore obtained for each run, and the results used in a frequency analysis of return periods. In the case of continuous simulation data, this involved creating an annual maximum series from the flow peak data along with the Weibull plotting position (Equation 3.12) to determine the flows associated with certain return periods. For design storms, as mentioned previously, the return period of the rainfall intensity used to generate the design storm is assumed to be the same as the return period of the resulting peak flow (the fundamental assumption of design storms).

To account for the differences in drainage area between the two single basins, the resulting peak flows were normalized by dividing the peak by drainage area. The resulting peak flows were then expressed in mm/hr.

The results are given in Tables B7 and B8 of Appendix B, for the rural (basin 101) and urban (basin 106) basins respectively. The results are presented with several different error measures: Root Mean Squared Error (RMSE), Mean Relative Error (MRE), and Mean Absolute Relative Error (MARE). RMSE is simply the square root of the MSE, which is calculated as the mean of all the squared residuals between the true (continuous simulation) and modeled (design

storm) data. It is a commonly used and useful statistic, as it provides an error measurement in the same units as the variable being examined. The other two error measures use the Relative Error statistic:

Relative Error = (True Value – Modeled Value) / True Value (Equation 4.1)

MRE is simply the mean of Equation 4.1 taken for the five data points used to evaluate each design storm type. MARE is similar, except that the absolute value of the result of Equation 4.1 is used when taking the mean. Thus the MRE measure takes sign into account: a negative MRE indicates the design storm overestimates peak flows overall, while a positive MRE indicates the design storm underestimates peak flows overall. MARE ignores the sign and gives an overall measure of how well the design storm modeled flows compare to the continuous simulation values. Both are expressed as percentages. Standard deviation was not used as an error measure in this case, since the mean peak flow would not be that meaningful, nor would the spread of the residuals from this value.

4.1.1 BASIN AND DESIGN STORM TYPE

Numerous observations can be drawn from the results presented in Tables B7 and B8 of Appendix B. First, there is clearly a wide range in the performance of the various design storm types. MARE values ranged from 9.58% to 84.97% for the rural basin, and 9.57% to 70.05% for the urban basin. Clearly some design storm types performed extremely poorly. The different assumptions and methods involved in the development of the various design storm models translate into very different output results and errors. Many of the errors for the longer storms are due to the shortcomings of longer durations, as discussed in Section 4.1.2. The results suggest that it is necessary to verify the appropriateness of a particular design storm before applying it, as the resulting errors can be very significant.

Different design storms also appear to work better for different basin types. An arbitrary threshold MARE of 20% was chosen to separate well-performing design storms from poorly performing storms (an exception was made for one storm with a slightly higher MARE, but a low RMSE). By applying this threshold to the results summarized in Tables B7 and B8 of Appendix B, we find 6 design storms that perform well overall for the rural basin, and 7 design storms that perform well overall for the urban basin. These results are given below in Table 4.1.

Table 4.1: Results of Single Basin Analysis for well-performing storms

	Storm Name	Storm Duration (hrs)	RMSE (mm/hr)	MRE (%)	MARE (%)
Rural Basin 101	AES 10%	12	1.13	-12.14%	15.16%
	Alternating Block	12	1.13	3.36%	19.82%
	Huff Q3	6	1.03	13.81%	20.96%
	Huff Q4	6	0.88	0.87%	15.01%
	Huff Q4	12	1.04	9.58%	9.58%
	SCS Type II	24	0.69	15.45%	15.45%
Urban Basin 106	AES 10%	12	3.21	-17.84%	17.84%
	Alternating Block	3	3.71	-18.58%	19.07%
	Huff Q3	6	1.61	5.16%	9.57%
	Huff Q4	6	2.18	10.66%	11.95%
	SCS Dimensionless	6	1.81	7.87%	10.88%
	SCS Type II	24	1.89	-5.49%	10.22%
	Triangular	3	1.67	3.49%	9.79%

As can be seen in Table 4.1, certain storm types performed well for both basin types: the AES 10% 12 hour storm, Huff 3rd and 4th quartile 6 hour storms, and the SCS Type II 24-hour storm all performed well in both cases. These results are illustrated graphically in frequency distributions given in Figures 4.1 (Rural Basin) and 4.2 (Urban Basin) below. The continuous simulation data are fit with a logarithmic trendline, which plots linearly on the semi-logarithmic axes.

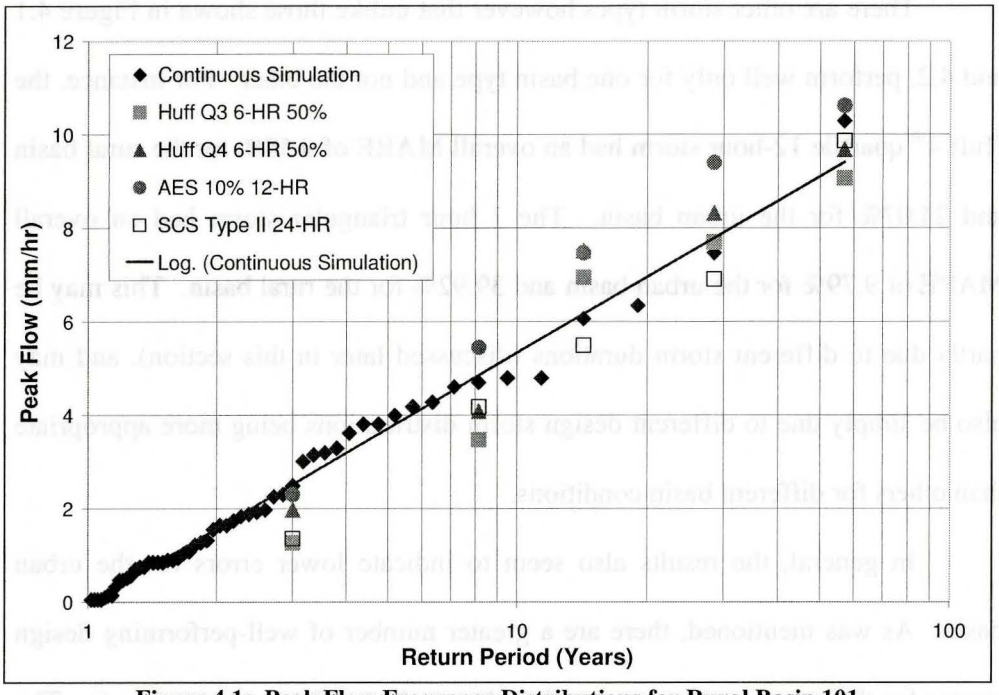

Figure 4.1: Peak Flow Frequency Distributions for Rural Basin 101

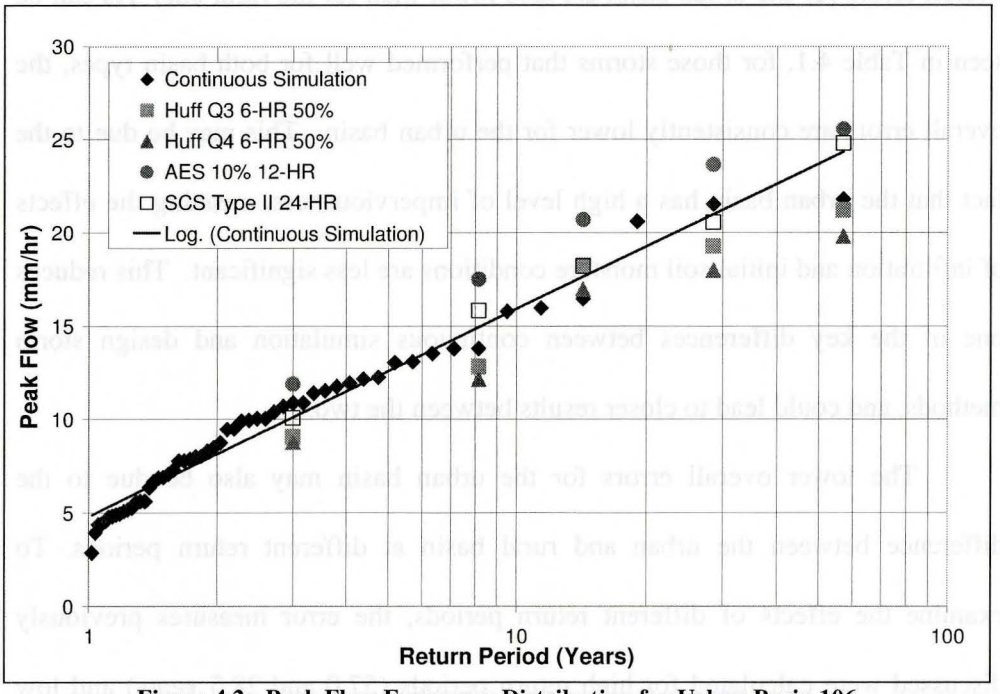

Figure 4.2: Peak Flow Frequency Distribution for Urban Basin 106

There are other storm types however that unlike those shown in Figure 4.1 and 4.2, perform well only for one basin type and not the other. For instance, the Huff 4th quartile 12-hour storm had an overall MARE of 9.58% for the rural basin and 24.07% for the urban basin. The 3 hour triangular storm had an overall MARE of 9.79% for the urban basin and 39.92% for the rural basin. This may be partly due to different storm durations (discussed later in this section), and may also be simply due to different design storm distributions being more appropriate than others for different basin conditions.

In general, the results also seem to indicate lower errors for the urban basin. As was mentioned, there are a greater number of well-performing design storms for the urban basin as opposed to the rural one (7 as compared to 6). The overall errors for the urban basin are also lower than for the rural one. As can be seen in Table 4.1, for those storms that performed well for both basin types, the overall errors are consistently lower for the urban basin. This may be due to the fact that the urban basin has a high level of imperviousness, meaning the effects of infiltration and initial soil moisture conditions are less significant. This reduces one of the key differences between continuous simulation and design storm methods, and could lead to closer results between the two.

The lower overall errors for the urban basin may also be due to the difference between the urban and rural basin at different return periods. To examine the effects of different return periods, the error measures previously discussed were calculated for high return periods (57.0 and 28.5 years) and low

return periods (8.1 and 3.0 years) separately for both basins for all of the design storms initially used (Tables B7 and B8). The previously used error threshold of an MARE below 20% was applied to identify well-performing design storms. The results are summarized below in Table 4.2.

Table 4.2: Performance of design storms at high and low return periods

	Number of Design Storms Below Threshold (MARE < 20%)	
	High Return Periods (57.0 and 28.5 years)	Low Return Periods (8.1 and 3.0 years)
Rural Basin 101	9	3
Urban Basin 106	8	7

As can be seen, design storms do not model low return period peak flows well for the rural basin. Table 4.2 shows that the urban and rural basins have approximately the same number of well performing storms at high return periods, but the rural basin has very few well performing storms at low return periods. This may explain why the rural basin has higher overall average errors for all return periods. The failure of design storms at low return periods for the rural basin may again be due to the increased role of infiltration and soil moisture conditions for that case. At lower return periods, peak flows may be more strongly affected by soil moisture parameters, leading to a larger discrepancy between continuous simulation and design storm methods.

Overall, design storms appear more likely to underestimate peak flows as compared to continuous simulation. Tables B7 and B8 show very few storms with an overall negative MRE – only 2 of the 18 storms (11%) for the rural basin,

and only 6 of the 18 (33%) for the urban one have a negative value. If the analysis is reduced to those storms identified as performing well (Table 4.1), then only 1 of the 6 storms (17%) overestimates for the rural basin, while 3 of the 7 storms (43%) overestimates for the urban basin. In general then, design storms appear more likely to underestimate peak flows as compared to continuous simulation with the antecedent moisture conditions used in this section. Rural basins appear much more likely to underestimate, while urban basins appear to roughly equally over- and under-estimate.

4.1.2 DESIGN STORM DURATION

Consideration of design storm duration is an important factor in ensuring accurate results. General wisdom is that the storm duration should be at least as long as the time of concentration in order to ensure that the complete basin is contributing to flow. Table 4.3 (below) presents the results of Tables B7 and B8 separated and averaged out by design storm duration.

Table 4.3: Summary of all design storms by duration

	Storm Duration (Hours)	RMSE (mm/hr)	MRE (%)	MARE (%)
Rural Basin 101	3	1.93	32.04%	33.29%
	6	1.66	24.03%	29.78%
	12	2.50	34.18%	40.43%
	24	2.76	36.81%	46.22%
Urban Basin 106	3	2.69	-7.54%	14.43%
	6	3.08	6.85%	17.42%
	12	6.00	21.87%	34.19%
	24	7.13	21.23%	40.53%

As Table 4.3 shows, based on RMSE and MARE values, the most appropriate storm duration for the rural basin is a 6 hour storm, while for the urban basin the most appropriate duration is a 3 hour storm. The results also appear to be in keeping with the time of concentration rule. The rural basin has a time of concentration of 3.98 hours, thus a 3 hour storm would generally be considered to be inappropriate, as it would not provide sufficient time for the entire basin to contribute and an adequate peak flow to be reached. Thus, the next highest storm duration which is above the time of concentration, 6 hours, gives the lowest overall errors. Likewise, for the urban basin with a time of concentration of 1.60 hours, the next highest storm duration of 3 hours gives the lowest errors. Similarly, if one examines the results of Table 4.1, we can see that the most appropriate storms for the rural basin have durations of 6 and 12 hours, while for the urban basins, the most appropriate storms have durations of 3 and 6 hours. Thus, the use of the time of concentration as a guide to the selection of design storm duration seems appropriate.

Another conclusion that can be drawn from Table 4.3 is that design storms with longer durations tend to have higher errors (of all types) than those with shorter durations. The results may be somewhat affected by the unequal number of storms in each time category (two 3-hour storms, five 6-hour storms, seven 12-hour storms and four 24-hour storms), however the general trend appears to be valid. In fact, the increasingly positive MRE with increasing duration seems to suggest that storms with longer durations underestimate peak flows by a greater

amount. In other words, longer duration design storms have lower peak flows than shorter duration storms. This is due to the fact that the majority of the storms used in the analysis are set as cumulative distributions, as well as that the same rainfall time increment (hourly) was used for all storms. When a shorter duration is used, the distribution is broken up into coarser incremental pieces, which results in higher incremental rainfall intensities as each piece covers a greater change in cumulative rainfall. When longer durations are used, the distribution is divided fairly finely, resulting in less sudden changes in the hyetograph, and thus a lower peak rainfall intensity. This is also due to the nature of depth-duration-frequency curves with increasing duration. Although depth always increases with duration, the rate of increase is significantly less with increased durations. Thus a longer duration storm has only a marginally larger depth than a shorter duration storm, with much finer incremental changes. This results in storms with progressively lower rainfall peaks, and thus lower runoff peaks.

An exception to the above observation is the alternating block storm, which does not use a fixed distribution. The alternating block storm uses all of the average intensities for all of the given durations. Thus alternating block storms of all durations contain the most intense n-hour periods within their distribution (where n varies from 1 hour to the chosen storm duration). Therefore, the alternating block storm actually tends to progressively overestimate as longer duration storms are chosen. This can be seen by viewing the MRE for these

storms in Tables B7 and B8 – it becomes increasingly negative with increasing duration.

Other exceptions to these general observations about design storm durations are the SCS Type-II 24 hour storm and the AES 10% 12-hour storm. As was shown, these two storms perform well for both basin types and have longer durations. However, these storm types have artificially long durations. In both cases (particularly the AES 10% storm) much of the total duration involves period with very small amounts of precipitation, particularly after the peak intensity, which would have little effect on resulting peak flows.

Storm duration should therefore be a serious consideration for all design storm distributions, however consideration should be given to other factors such as the type of storm (fixed distribution or purely IDF-based), and whether or not the duration assigned to the storm is indicative of the true duration. Rainfall time increment should also be a consideration, however it was not taken into account in this study – an hourly increment was used for both design storm and continuous simulation inputs.

4.2 SOIL MOISTURE ANALYSIS

In the previous analysis, an initial moisture condition of 0.2 S was assumed, in keeping with the standard SCS method. However, a more thorough analysis is warranted to determine whether or not this is in fact a valid

assumption. The initial moisture condition is an unimportant factor for continuous simulation, as the soil moisture level is continuously calculated throughout the year. Thus, the specified initial moisture condition for a continuous simulation run is not likely to be the moisture condition prior to the annual maximum flow. For design storms however it is critical, as it is the starting moisture level, which has a large effect on the magnitude and timing of the peak flow. Along with outflow data, HEC-HMS also outputs additional data, including the soil moisture deficit. Thus, the soil moisture deficit data from the continuous simulation runs of the previous section were analyzed in a few different ways in order to determine both the validity of the SCS assumption, as well as the effect of different initial moisture conditions on the results.

Three different methods were employed to estimate more accurate soil moisture conditions. As a first method, the continuous simulation calculated soil moisture deficit data were averaged out for each year of the simulation (April to October). These results were then averaged to obtain an overall average soil moisture deficit for each basin type.

As a second method, soil moisture deficits were averaged out only for those months where large rainfall events were more likely to occur (since we are only really interested in estimating initial moisture conditions prior to large peak outflow producing storms). To determine this, the annual maximum series of peak outflows for both the rural and urban basin were examined to determine

during which months the peak flows occurred. The results are given in histogram in Figure 4.3 below.

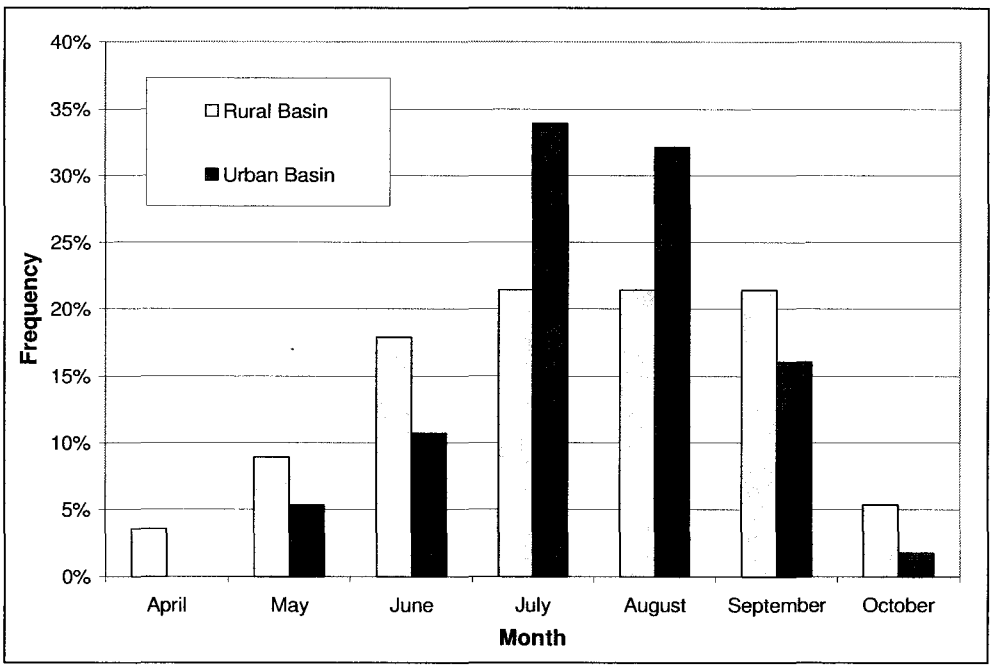

Figure 4.3: Histogram of Months containing peak flows

As can be seen from Figure 4.3, the majority of peak flows occurred during the months of June-September for both basin types. Therefore, the average of all of the moisture deficit values for June-September for both basin types were calculated.

A third method of analyzing soil moisture deficits was also employed. Rather than averaging out overall initial moisture conditions as in the previous two methods, this method attempts to capture the soil moisture conditions prior to the peak flow producing storm from each year of the simulation. To do so, the beginning of the peak producing rainfall storm must be determined so that the soil moisture deficit can be found at that point. Rather than employing an arbitrary

method to determine this point, an event-based approach to storm discretization was employed.

The event-based approach has been credited to numerous authors, including Guo and Adams (1998), who used the approach to develop analytical frequency distributions of the rainfall event characteristics. In this approach, rainfall periods are separated based on a specific time period without rainfall, called the minimum interevent time definition (IETD). If two rainfall periods are separated by a time interval greater than or equal to the IETD, they are considered separate rainfall events. If the time between two rainfall periods is less than the IETD, they are considered to be part of a single event. The choice of IETD is very important in determining the properties of the resulting rainfall events. Typically the IETD is greater than the basin t_c to ensure that runoff from one rainfall event does not carry over to the next one. This is not as important in this case, since we are only interested in determining the beginning of one rainfall event. Kauffman (1987) showed that for Toronto rainfall data, increases in the IETD above 6 hours do not result in significant changes to the annual number of events, which suggests this is a stable value to use. As can be seen from Table B4, this value is also greater than the t_c value for either the rural or urban basin. Thus, 6 hours was used as an IETD for rainfall discretization.

Using this approach, the beginning point of each annual peak causing rainfall event was defined, and the soil moisture deficit value at this point found. These annual values were then averaged out for both basins to obtain overall pre-

storm moisture deficit averages. The results of this method, along with the other two moisture deficit estimate methods, are given below in Table 4.4. It should be noted that the results for IETD values other than 6 hours yielded very similar results.

Table 4.4: Summary of different antecedent soil moisture conditions

Estimate Method	Rural Basin 101			Urban Basin 106		
	Initial Moisture Deficit Estimate (mm)	Difference (mm)	Relative Difference (%)	Initial Moisture Deficit Estimate (mm)	Difference (mm)	Relative Difference (%)
SCS Method	26.4			19.2		
Overall Average	18.8	-7.6	28.8	17.5	-1.7	8.9
Summer Average	23.2	-3.2	12.1	22.6	3.4	-17 7
Pre-Storm (IETD) Average	13.8	-12.6	47.8	26.9	7 7	-40.1
AVERAGE	**18.6**	**-7.8**	**29.6**	**22.3**	**3.1**	**-16.3**

A few observations can be made on the results of Table 4.4. With respect to the overall average method, it can be seen that values are quite close for both the urban and rural basin – 17.5 mm and 18.8 mm respectively Similarly for the summer average method, values are quite close for the two basin types (22.6 and 23.2 mm respectively), slightly higher than the overall average method. This is expected because of the higher evapotranspiration rates of the summer months. In both cases, values were reasonably close to the SCS method values, with the highest difference being 7.6 mm. The IETD average method resulted in much more significant differences between basin types and from the SCS method results. As opposed to all the other methods examined, the urban basin has a higher deficit than the rural basin (much more so in fact – almost twice the value). This is likely due to the fact that in many years, the peak flow for the urban and

rural basin occur at different times. Different infiltration rates and maximum soil deficits for the two basin types likely have some effect, but the major difference is likely due to the difference in imperviousness. If conditions are dry, a major storm for a rural basin may be used up replenishing the soil moisture deficit, and result in little runoff. Because a large portion of the urban basin is impervious, that portion of the rainfall will become runoff, regardless of the soil moisture deficit. Thus large peak flows may result, even though the soil moisture deficit is large. For the rural basin with little to no imperviousness, peak flows are only likely to occur when the soil moisture deficit is low, and most of the rainfall will become runoff. This may explain the difference in moisture deficit values using the IETD average approach.

Thus, after examining the results of Table 4.4, it can be seen that the SCS method for estimating initial moisture conditions seems to give reasonable values in comparison to other average methods. The average difference between the various initial soil moisture estimation methods discussed in this section and the SCS method is only approximately 5 mm. However, the sensitivity of continuous simulation and design storm results to this parameter should still be evaluated.

To test the effect of initial moisture conditions on continuous simulation results, the two basin models were partially re-run with the moisture deficit estimates of Table 4.4. In addition to these average deficit estimates, two extreme cases were also considered: a fully saturated soil (initial deficit = 0) and a very dry soil (initial deficit = 50 mm). Rather than re-running all 56 years of the

continuous simulation for both basins, only the years corresponding to the key return period peak flows (i.e., 57.0, 28.5, 14.3, 8.1, and 3.0 year return periods) were used. This is a simplification to reduce computation, as resulting differences in flows may slightly alter return periods. However, rainfall records from the same year of simulation are still being compared, which in itself allows for a reasonable comparison.

The results of this analysis can be seen in Tables B9 and B10 of Appendix B for the Rural and Urban basins respectively. As can be seen from the results, changing initial moisture conditions has very little impact on continuous simulation peak flows. For the rural basin, only one difference is observed in peak flows (peak flow for 1944 with very dry conditions) – all other conditions result in identical flows, including the fully saturated condition. For the urban basin, differences can be seen with the results of the 1941 simulation year. Each of the different methods predicts a slightly different peak flow than was seen with the SCS method, however overall differences are fairly small, with MARE values less than 2%. The exception is again the fully dry condition, which results in a significant decrease in the predicted peak for the 1941 storm, and a larger MARE value (6.09%). Thus, it appears that with the exception of the very dry condition, moisture deficit values have little impact on continuous simulation results. Given the continuous tracking of moisture deficits, and long simulation times (since, as seen in Figure 4.3, most peak flows occur in the summer months, long after the start of the year), it appears that any initial difference in moisture deficits is

generally counteracted before the occurrence of the annual peak flow causing rainfall. This is usually due to long low-intensity rainfalls at the beginning of continuous simulation runs. These rainfalls replenish the soil moisture deficit, and do not result in runoff from the pervious portion of the basin if, as given in Equation 3.1, the rate of rainfall is less than the constant rate of infiltration. Thus, two basins with different moisture deficits eventually reach the same condition, and will give identical peak flows when a higher intensity storm occurs later in the simulation year. Differences between moisture estimate methods appear only to occur when the basin is subjected to shorter or more intense rainfalls soon after the start of each simulation year. Using any of the average moisture deficit methods, or assuming fully saturated initial conditions yields very similar results in the continuous simulation model.

Of more importance is the effect of varying initial moisture conditions on design storm results, given that it is indeed the initial moisture deficit, unlike the continuous simulation runs where the moisture deficit is continuously calculated. To examine the effect of the initial moisture deficit on design storm results, the models were re-run using the previously discussed moisture deficit estimates. Rather than re-running the analysis for the full range of design storms seen in Tables B7 and B8, only those design storms identified as performing well in both scenarios (as discussed in Section 4.1.1) were used – namely the Huff 50% Q3 and Q4 6-hour storms, the AES 10% 12-hour storm, and the SCS Type-II 24-hour storm. This was done to avoid unnecessary calculations for poorly performing

design storms. The results of this new design storm analysis are given in two different forms for the Rural and Urban basins respectively.

Tables B11 and B12 compare the results within design storm moisture estimate methods to the original continuous simulation results. The errors are therefore calculated with respect to the original continuous simulation results. It should be noted that this is not strictly correct, as the proper comparison would be to re-run the continuous simulation for each moisture estimate method, and then use this as the basis of comparison for each of the different methods. However as was seen in Tables B9 and B10, varying initial moisture conditions has very little effect on continuous simulation results. Thus the original continuous simulation results can be assumed to be a good basis of comparison for all design storm moisture estimate methods. The averages of the overall results of Tables B11 and B12 are summarized below in Table 4.5.

Table 4.5: Average errors for design storm results with varying antecedent moisture conditions

	Initial Moisture Condition Method	RMSE (mm/hr)	MRE (%)	MARE (%)
Rural Basin 101	SCS Method	0.93	4.50%	16.64%
	Overall Average	1.44	-20.68%	20.91%
	Summer Average	0.98	-6.70%	14.84%
	Pre-Storm (IETD) Average	1.63	-29.11%	29.11%
	Fully Saturated	2.46	-45.40%	45.40%
	Very Dry	4.15	71.52%	71.52%
Urban Basin 106	SCS Method	2.22	-1.88%	12.39%
	Overall Average	2.26	-2.83%	12.50%
	Summer Average	2.22	1.11%	12.41%
	Pre-Storm (IETD) Average	2.25	4.85%	12.42%
	Fully Saturated	2.61	-6.54%	14.50%
	Very Dry	4.66	27.02%	27.02%

Several observations can be drawn from the results summarized in Table 4.5. First, we can see that the rural basin is much more susceptible to changes in the initial moisture condition. Overall errors are much higher and show a greater range in values for the rural basin (average MARE values of 14.84 to 71.52%) as compared to the urban one (MARE values of 12.39 to 27.02%). Given the rural basin's dependence on the pervious portion of the basin to generate peak flows (and urban basin's high imperviousness) this seems to be a logical conclusion. Second, some observations can be made about the performance of the various moisture estimates. It appears that the SCS estimate method and the two average methods (Overall Average and Summer Average) were the most successful methods. These three methods had the lowest MAREs for both basin types – the SCS and Summer Average method in particular had the lowest errors. The other three moisture estimates were much less successful. The very dry condition in particular resulted in larger underestimates of peak flows, indicated by high positive MRE values. The fully saturated condition results in high overestimates for the rural basin (negative MRE), and a slight overestimation for the urban basin (again, for the reasons previously suggested). This suggests that extreme values are generally inappropriate for an estimate of design storm initial moisture conditions – an average value is more appropriate. An alternative approach, the IETD method, gave good results for the urban basin, but high errors and overestimates for the rural basin. Given the inconsistency in the results, and the difficulty in obtaining moisture deficit estimates using the IETD method, this is

likely not a feasible method of estimating moisture deficits. The most appropriate methods appear to be the SCS method and the summer average method, given their low overall errors. These methods may also be simpler to implement – the SCS method simply requires an estimate of the curve number for the basin (or an estimate of max potential storage), while the summer average method appears to give a relatively constant deficit regardless of basin type (approximately 23 mm).

CHAPTER 5: MULTIPLE BASIN COMPARISON

With the analysis of single basins complete, it is now possible to examine more complex watershed systems. Specifically, the watershed system originally shown in Figure 3.3 will be examined. To examine the effects of increasingly complex watershed systems, the watershed will be evaluated at several different nodal points: junctions A05, A08, A14, and A29, which is the outlet of the entire watershed. These nodal points are highlighted below in Figure 5.1

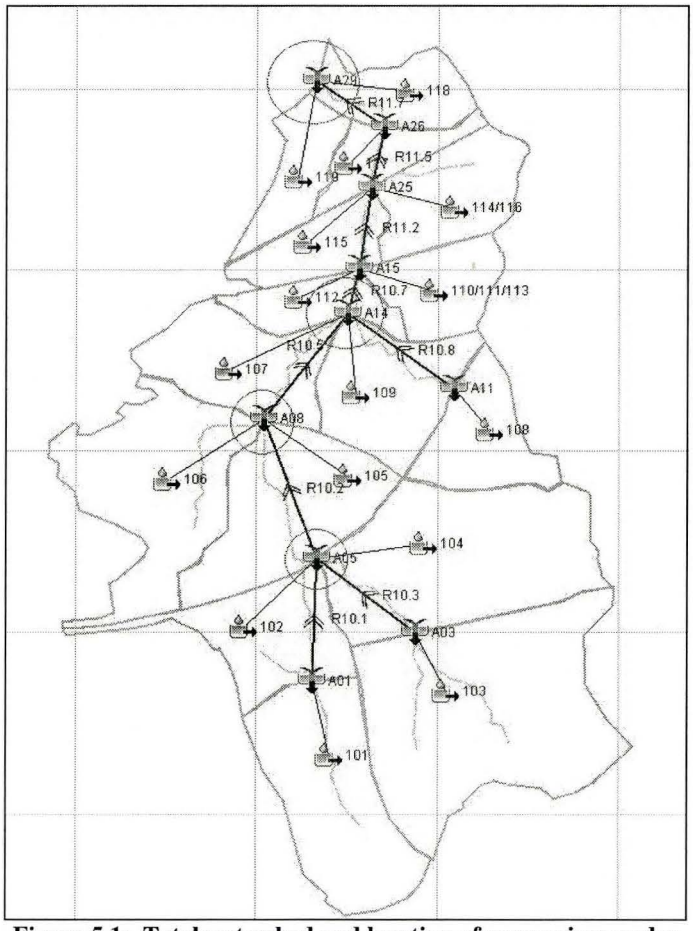

Figure 5.1: Total watershed and location of comparison nodes

These points were chosen to attempt to evenly represent the watershed. A05 was chosen as the first point as it is the first available nodal point on the main branch of the creek. The subsequent points have roughly the same increase in drainage area, as can be seen in Table B13 of Appendix B.

The watershed analysis again used the basin parameters and methods described in Chapter 3. Note that results are again normalized by drainage area., thus results are again presented in mm/hr rather than m^3/s to ensure a consistent comparison. The choice of specific design storms and moisture conditions was based on the analysis of the previous chapter. As discussed, two different moisture conditions were shown to be appropriate for both single basin types – the original SCS assumption, and the summer average method. Four different design storm types were also shown to have fairly low errors regardless of basin type: the AES 10% 12 hour storm, Huff 3^{rd} and 4^{th} quartile 6 hour storms, and the SCS Type II 24-hour storm. Thus these storms and moisture estimate methods were used for the design storm approach. For the continuous simulation method, the analysis was only completed using the SCS initial moisture assumption. This is also based on the results of the previous chapter, in particular Tables B9 and B10 of Appendix B, which showed very little change in continuous simulation results by changing initial moisture conditions.

The results are presented in several different ways. Tables B14 and B15 of Appendix B show the results of the multiple basin analysis sorted and averaged by nodal point, moving downstream. Table B14 gives the results using the SCS

moisture deficit estimate, while Table B15 gives the results using the summer average method. The average errors at the different nodal points are summarized below in Table 5.1.

Table 5.1: Summary of average errors at different nodal points by initial moisture deficit estimate method

Initial Moisture Deficit Estimate Method	Nodal Point	RMSE (mm/hr)	MRE (%)	MARE (%)
SCS Method	A05	0.84	-4.96%	11.88%
	A08	0.70	-8.04%	10.70%
	A14	0.72	-6.69%	10.98%
	A29	0.59	-5.91%	11.35%
Summer Average Method	A05	0.91	-3.35%	13.43%
	A08	0.61	-1.32%	9.88%
	A14	0.66	-4.27%	10.54%
	A29	0.56	-4.56%	11.08%

As can be seen in Table 5.1, both methods appear to give fairly close results. Both the average RMSE and MARE show very small variations between the different nodal points. For the SCS method results, overall RMSE values vary only from 0.59 to 0.84, while overall MARE values range only from 10.70 to 11.88%. Results from the Summer Average method appear to show similar results with a slightly larger range, with overall RMSE values ranging from 0.56 to 0.91, while overall MARE values range from 9.88 to 13.43%. A clear trend is not immediately apparent from these results, given the relatively small variations in error magnitudes, and the fact that errors both increase and decrease as the analysis moves downstream. Error values do appear to decrease slightly from

A05 to the outlet at A29, but there are both increases and decreases evident – it is not a steady decline.

In order to try and identify a clearer pattern, the results of the previously discussed tables were sorted by storm type. The results for the SCS moisture deficit method are given below in Figures 5.2 and 5.3 for the RMSE and the MARE respectively With the exception of the AES 10% design storm, the results of all the storms and overall average were very similar for the Summer Average moisture deficit method, and were therefore not included.

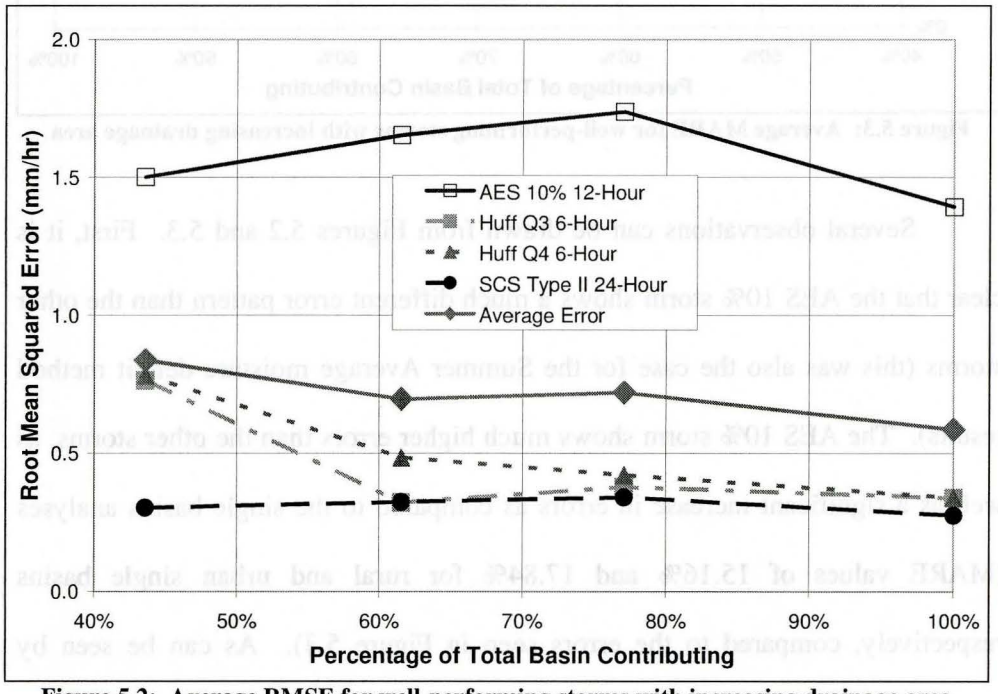

Figure 5.2: Average RMSE for well-performing storms with increasing drainage area

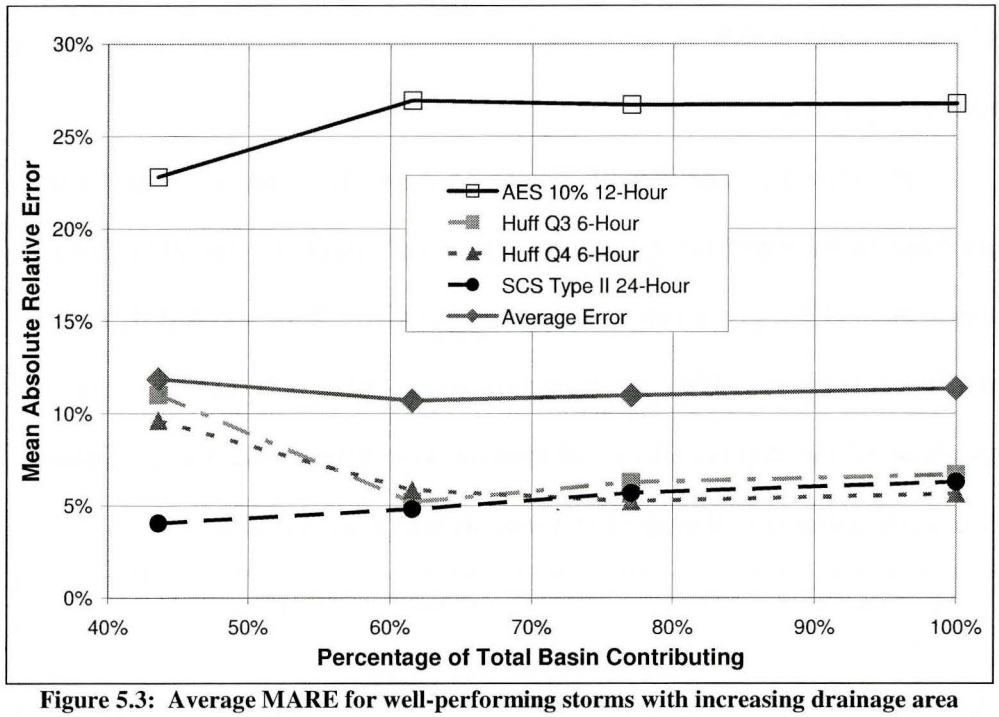

Figure 5.3: Average MARE for well-performing storms with increasing drainage area

Several observations can be drawn from Figures 5.2 and 5.3. First, it is clear that the AES 10% storm shows a much different error pattern than the other storms (this was also the case for the Summer Average moisture deficit method results). The AES 10% storm shows much higher errors than the other storms, as well as a significant increase in errors as compared to the single basins analyses (MARE values of 15 16% and 17.84% for rural and urban single basins respectively, compared to the errors seen in Figure 5.3). As can be seen by examining the MRE values of the single basin analysis (-12.14% and 17.84% for the rural and urban basins respectively) as well as the MRE values of Table B14, the AES 10% storm consistently overestimates peaks, increasingly so with increasing drainage area. This is likely due to the storm distribution itself. As

mentioned in the previous chapter, the rapidly peaking nature of this storm means that it is essentially a 3-hour storm. Thus, a 12-hour depth is being fit into a 3-hour distribution, which would naturally lead to peak flow overestimates. This suggests that storms should be slightly more evenly distributed, with the total depth spread over a longer duration, and perhaps with a delayed peak.

The trends for the other design storms and the overall average appear to be more consistent. As can be seen in Figure 5.2, the RMSE decreases slightly overall as the percentage of the total basin contributing increases. It is not a steady decrease however, with storms showing both increases and decreases. However, the overall trend is to lower RMSE with increasing contributing basin area. It should be noted however that RMSE may not be an appropriate error measure for comparison in this case, given that the overall magnitude of peak flows changes as the analysis moves downstream (peak flows in units of mm/hr appear to generally decrease with increasing contributing area). Because the RMSE is not a relative error measure, the results and the observed trend may not be reliable – they may simply be following the overall trend in values.

Figure 5.3 shows the results from a relative error measure, the MARE. The results are somewhat similar to those using RMSE, however, the MARE appears to actually increase slightly rather than decrease - it appears to reach more of a constant value as contributing basin area increases. It is therefore difficult to draw any clear pattern from the previous figures. In general, overall errors do appear to decrease slightly as the percentage of the total contributing area

increases. Figure 5.3 suggests that this error decrease may eventually cease though, whereby errors remain relatively constant with increases in basin complexity. Errors may in fact increase slightly. This suggests that design storm and continuous simulation method results compare more favourably as the size and complexity of the watershed being modeled increase, to a certain limiting size or complexity.

This last conclusion also appears to be supported by comparing the results of single basin analysis to results seen in this section. Comparing the results of Tables B14 and B15 to the previous single basin results (the SCS Method and Summer Average method data in Tables B11 and B12), we can see that average error measures are much higher for the single basins. The rural basin (101) had average MARE values of 16.64% and 14.84% for the SCS and Summer Average methods respectively. The urban basin (106) had average MARE values of 12.39 and 12.41% for the SCS and Summer Average methods respectively. With the exception of the AES 10% storm, the error measures for the single basins are higher than those seen at all the different nodal points in the multiple basin analysis.

In order to further verify the previous results and observations, the analysis was repeated with storms that did not meet the error threshold previously used to identify well-performing storms (MARE < 20% for both single basin types). In this case, the error threshold was raised to 30%. Thus, those storms with MARE values between 20 and 30% for both single basins (Tables B7 and

B8) were used. This criterion resulted in the identification of four design storms. Alternating block 3, 6, and 12 hour design storms, and the Huff 4th quartile 12-hour design storm. Given the previous discussion of the appropriateness of RMSE as an error measure in this case, and the observed similarities between SCS and Summer average moisture deficit methods, the analysis was only performed using the MARE as an error measure for SCS method results. The results are shown below in Figure 5.4.

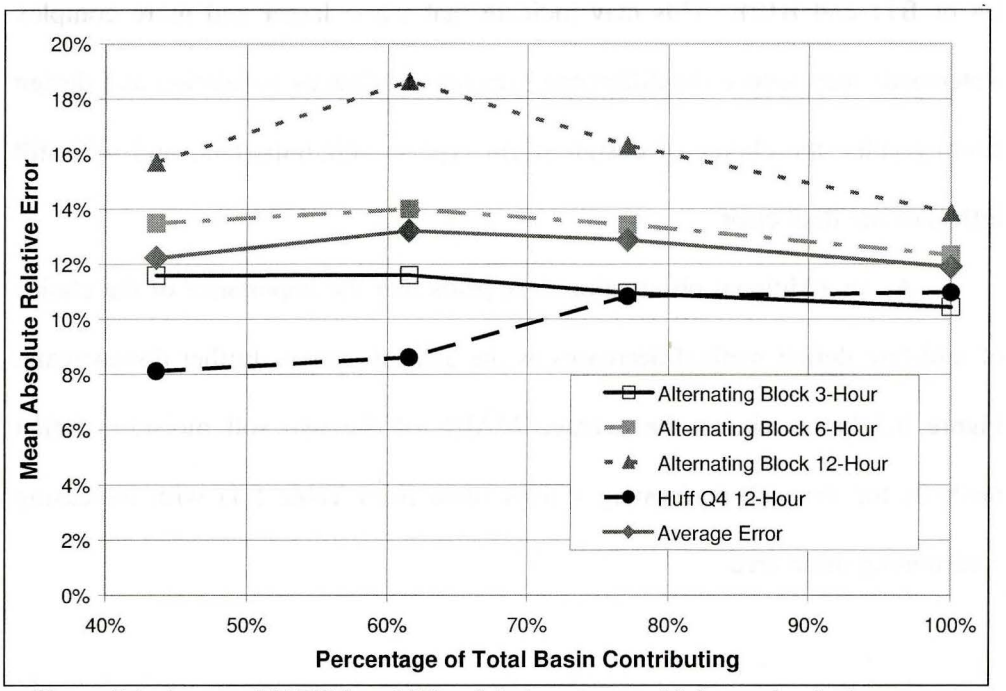

Figure 5.4: Average MARE for additional design storms with increasing drainage area

The results of Figure 5.4 appear to share similarities with Figure 5.3. There is a small overall decrease in error for most storms with increasing contributing area. The exception is the Huff Q4 12-hour storm, which actually shows a consistent, if slight, increase in error as the analysis moves downstream.

It is unclear why this storm shows an increase in error. In general, errors also appear to again converge towards a somewhat constant condition, with closer MARE values. With the full watershed contributing, the errors for these storms are still higher than those observed with the well-performing design storms in Figure 5.3. Also, in keeping with a previous observation, it should be noted that the errors seen in Figure 5.4 at all nodal points are less than those for either of the single basin tests using the SCS initial moisture deficit method (see Tables B7 and B8 or B11 and B12). This may indicate that while larger and more complex watersheds may reduce the difference between continuous simulation and design storm results, the choice of design storm type is still important, and will still influence the final error.

As an additional observation, it appears that the importance of the choice of moisture deficit method decreases as the analysis moves further downstream. Figure 5.5 below shows the average MARE of the two soil moisture deficit methods for the well-performing storms (data from Table 5.1) with increasing contributing basin area.

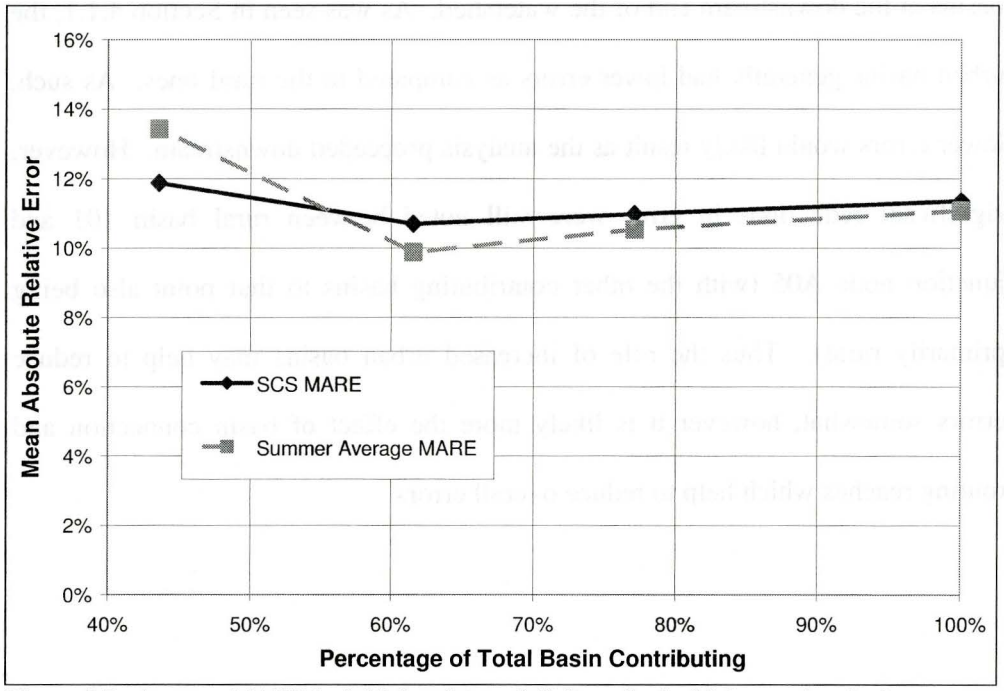

Figure 5.5: Average MARE by initial moisture deficit method with increasing drainage area

As can be seen from Figure 5.5, average errors for the two methods converge as contributing basin area increases. This suggests that design storm results are much less sensitive to initial moisture deficit conditions in larger watershed systems.

In general, it appears that larger and more complex watershed models tend to reduce the differences in results from different design storms and initial moisture conditions, to a certain degree. This may be due to two causes. First, it may be that the effect of the system itself is to reduce differences. The effect of basin connections and routing reaches may tend to average out or blur differences between results based on different methods. Second, in the case of this particular basin, it is possible that the reduction is due to the higher proportion of urbanized

basins at the downstream end of the watershed. As was seen in Section 4.1.1, the urban basins generally had lower errors as compared to the rural ones. As such, lower errors would likely result as the analysis proceeded downstream. However, significant reductions in error were still noted between rural basin 101 and junction node A05 (with the other contributing basins to that point also being primarily rural). Thus the role of increased urban basins may help to reduce errors somewhat, however it is likely more the effect of basin connection and routing reaches which help to reduce overall errors.

CHAPTER 6: DETENTION POND ANALYSIS

As a further comparison of design storm and continuous simulation methodologies, the effect of a simple detention basin will be evaluated. In order to simplify the analysis and more clearly examine the effects of a detention pond, the case of only a single basin discharging into a detention pond will be investigated. Since detention ponds are typically employed to help control outflow from urbanized areas, the single urban basin used in previous sections (Basin 106) will be employed. Thus, the setup in this chapter will involve a single urban basin feeding into a detention pond. The resulting peak flows outletting from the pond modeled by both continuous simulation and design storm methodologies will then be examined. Only the SCS initial moisture deficit method will be employed in the analysis, since that parameter is not the focus of the analysis in this section. In keeping with previous sections, all results are presented in basin area-normalized units (mm/hr for outflow, and mm for storage).

Outflow from a reservoir or detention pond in HEC-HMS is solved for using the finite difference version of the continuity equation. Since inflow is known at all times, it remains to calculate storage and outflow at each time step. If storage and outflow are related through a rating curve, and the initial condition of either storage or discharge at t=0 is known, then outflows from the pond can be found. Thus before the analysis can be started, the properties of the detention

basin must be determined. HEC-HMS allows the user to either specify the particulars of the reservoir structure (spillways, pumps, orifices, etc.) and have the program calculate the outflow rating curve for the structure, or to input the curve directly. In our case, a simpler detention pond is desired, thus it is easier to input the rating curve directly.

As a first detention pond, a linear type will be employed – one with a linear storage-discharge function. Such a function would be an approximation of a detention basin with a weir-type outlet only. It is assumed that the pond is a dry one, therefore the intercept of the rating curve can be assumed to be zero (zero storage = zero outflow). Thus it only remains to determine the slope. The detention pond was sized such that it would roughly attenuate peak flows by 50%. In order to determine the necessary function slope to achieve this, different values were tested in HEC-HMS using the SCS Type-II 24-hour design storm. The SCS Type-II storm was chosen for use given its excellent performance in the single basin analysis, as well as its longer duration and large peak. Using this design storm, it was found that an appropriate linear rating function was

Outflow (mm/hr) = Storage (mm) x 0.54 (Equation 6.1)

The above storage-outflow function yielded an average peak flow reduction of 52% for the SCS Type-II storms. To use Equation 6.1 in HEC-HMS,

the units must be converted to m^3/s for discharge and 1000 m^3 for storage, which simply changes the slope to 0.15 instead of 0.54.

In addition to the above linear storage-discharge function, a second non-linear function was also generated in order to provide a comparison and examine what differences may result. To make this function realistic, actual detention pond calculations were used to generate it. A trapezoidal detention pond was used to calculate storage volumes, while discharges were based on a lower orifice outlet combined with a higher overflow weir Parameters (such as weir length, orifice area, and coefficients) were then adjusted to give a storage-discharge function roughly comparable to the previously calculated linear one. The resulting non-linear function, along with the original linear one, are shown below in Figure 6.1

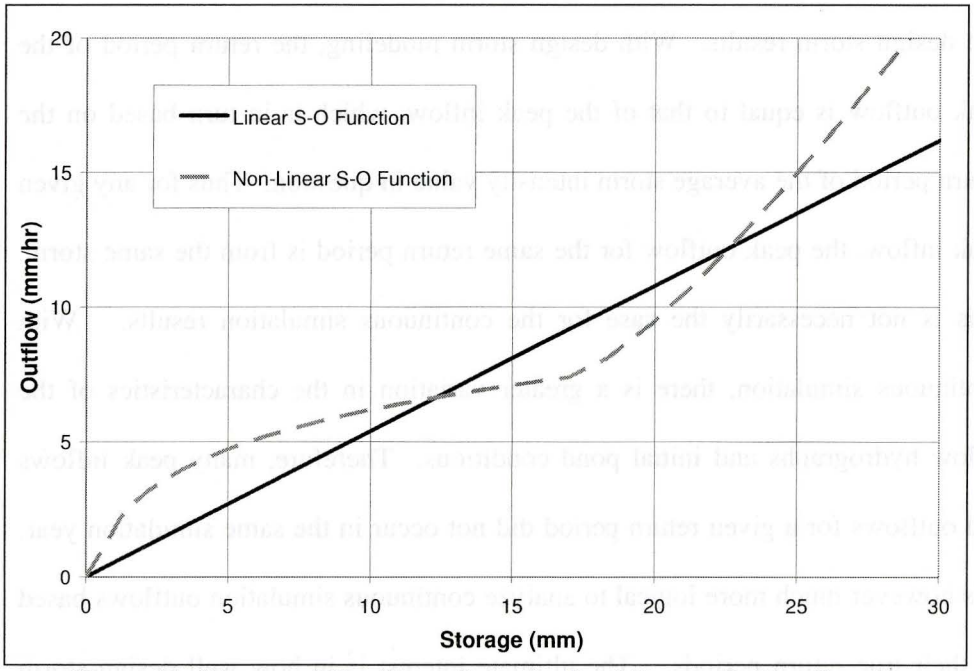

Figure 6.1: Linear and Non-Linear Detention Pond Storage-Outflow Functions

As can be seen from Figure 6.1, the two functions compare reasonably well to one another overall, while still providing clear differences at different storage levels.

As noted previously, an initial assumption of known storage or outflow must be given. As an initial condition for the analysis, inflow was assumed to be equal to outflow for both design storm and continuous simulation models. Given the previous assumption of a dry pond (zero intercept for the storage-discharge function) and the low initial flows in both cases, this is likely a reasonable assumption.

The detention pond analysis again used the basin parameters, methods, and error measures described in previous chapters. Before discussing the results in detail, it is worth noting a slight discrepancy between continuous simulation and design storm results. With design storm modeling, the return period of the peak outflow is equal to that of the peak inflow, which is in turn based on the return period of the average storm intensity value in question. Thus for any given peak inflow, the peak outflow for the same return period is from the same storm. This is not necessarily the case for the continuous simulation results. With continuous simulation, there is a greater variation in the characteristics of the inflow hydrographs and initial pond conditions. Therefore, many peak inflows and outflows for a given return period did not occur in the same simulation year. It is however much more logical to analyze continuous simulation outflows based on their true return periods. The ultimate interest is in how well design storm

results can model the overall continuous simulation outflows, which is much better represented by using the true outflow return period, rather than the return period of the peak inflow.

The results of the analysis in terms of peak outflow are presented in detail in Tables B16 and B17 of Appendix B. Table B16 presents the results for those storms identified in previous sections as performing very well (MARE < 20% for both single basin tests of Chapter 4), while Table B17 presents the results for those storms which performed less well (20% < MARE < 30% for both single basin tests of Chapter 4). Along with the previously used error measures, average peak reduction (APR) was also calculated, which gives the overall average reduction in peak inflow as compared to peak outflow using the same method. These values are given Table B18. The results of tables B16 and B17 are summarized below in Table 6.1.

Table 6.1: Summary of average design storm MARE values for detention pond peak flows

Storm Name	Average MARE for Design Storm Outflows		
	Basin 106	Linear Pond	Non-Linear Pond
AES 10% 12-Hr	17.84%	26.97%	38.32%
Huff Q3 6-Hr	9.57%	4.58%	5.13%
Huff Q4 6-Hr	11.95%	4.67%	4.46%
SCS Type II 24-Hr	10.22%	6.83%	6.71%
Alternating Block 3-Hr	19.07%	10.24%	11.07%
Alternating Block 6-Hr	22.07%	13.50%	16.59%
Alternating Block 12-Hr	25.30%	16.69%	20.06%
Huff Q4 12-Hr	24.07%	10.13%	15.21%

The results appear to be similar for almost all design storms. In almost all cases, errors between design storm and continuous simulation results significantly

decreased after being routed through the detention pond. This is clearly seen by comparing MARE values from inflow to outflows from both the linear and non-linear detention pond, which showed very similar decreases in errors. The MARE is again the most appropriate error measure for comparison (as compared to RMSE), as it takes into account the relative difference in peak flow magnitudes from inflow to outflow.

The only exception to this trend is again the AES 10% 12-Hour design storm, for which errors actually increased significantly. As can be seen in Table B16, the MARE for the inflow (outflow from Basin 106) was 11.27%, while the MARE for the outflow from the linear basin was 26.97% and 38.32% from the non-linear basin. It is unclear why errors increase so dramatically. It may be due to the rapid and sharp peaking nature of this storm, which might result in less attenuation through a detention basin than a centre-peaking or late-peaking storm, as the other storms are. As can be seen in Table B18, the peak outflows from the AES 10% storm are reduced less by both the detention ponds than the continuous simulation results (for the linear pond, 45% APR from continuous simulation compared to 41% from the AES 10% storm, for the non-linear pond, 49% APR from continuous simulation compared to 41% from the AES 10% storm). Given that the inflow already consistently overestimated peaks, less of a reduction in peaks through the detention pond would only increase this overestimation and associated errors.

As mentioned, for all other storms the trend is a substantial decrease in errors after being routed through the pond. These results were true for both the linear and non-linear detention ponds. If the AES 10% storm results are omitted, the average MARE for the well-performing storms drops from 10.58% for the inflow to 5.36% for the linear pond outflow and 5.43% for the non-linear pond outflow. Errors between continuous simulation and design storm results are therefore nearly halved after being routed through the pond. Similar results are seen for those storms which performed less well (Table B17 of Appendix B). The average MARE for these storms goes from 22.62% for the inflow to 12.64% for the linear pond outflow and 15.73% for the non-linear pond outflow.

In terms of differences between the two ponds tested, the two ponds performed almost equally in terms of error reductions. Average MARE values for the two outflows were roughly equal. Although overall errors were comparable, differences are apparent in the overall peak reduction. Comparing values of APR in Table B18, it can be seen that the non-linear pond reduces outflow peaks by a greater amount than the linear pond. The non-linear detention pond also shows more variability at different return periods than the linear detention basin. Figure 6.2 below illustrates the variation in peak reduction at different return periods for the SCS Type-II 24 hour design storm. Plots for other storms were similar.

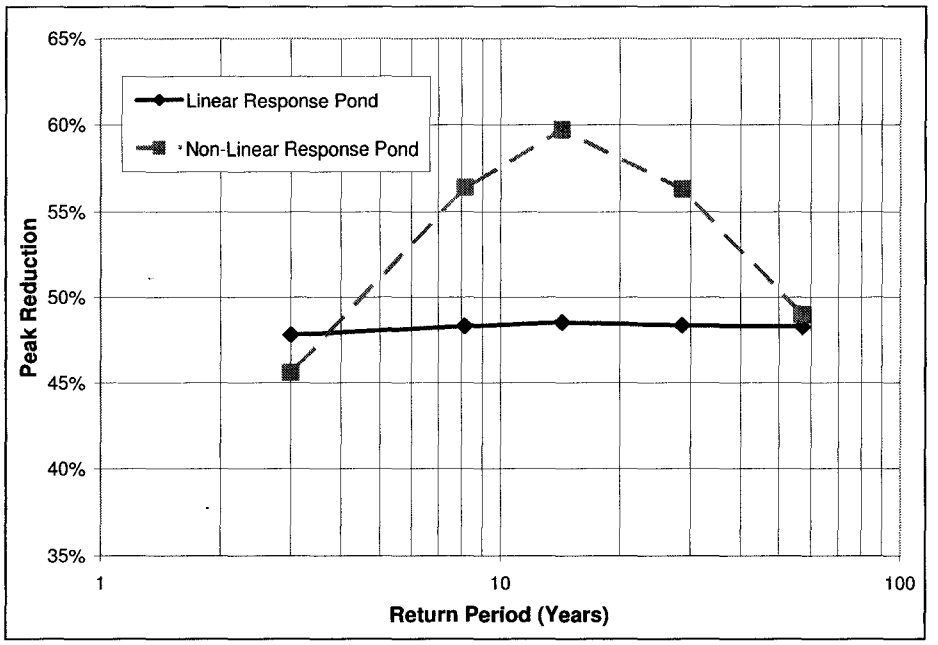

Figure 6.2: Variation in Peak Reduction for SCS Type-II storm through different detention basins

As can be seen from Figure 6.2, the linear response pond provides essentially even peak reduction at all return periods. The non-linear response pond however provides varying peak reduction depending on the return period (and therefore the volume and intensity) of the storm. This is simply due to the nature of the storage-outflow relationship shown in Figure 6.1. For storms in the mid-range of the function, the non-linear basin has more storage for the same outflow as compared to the linear function. As such, the non-linear basin can more greatly attenuate and reduce peaks. Differences in peak reduction at varying return periods are also seen in the continuous simulation results for the linear detention pond as well as the non-linear detention pond. This is likely due more to the earlier observation that peak inflow and outflow may not necessarily occur

in the same year, thus it is not strictly a one-to-one function as the design storm results are. These overall differences suggest that consideration should be given to the peak reduction statistic. Despite very similar overall errors (such as the MARE) the two detention basins provide different individual and overall peak reductions as determined by design storm and continuous simulation results. If a specific peak reduction is specified, certain design storms may over or under-estimate the reduction, especially at different return periods if the pond is non-linear.

In general though, this chapter illustrated that differences in peak flow estimation between design storm and continuous simulation methods are greatly reduced by the effects of detention ponds (with the exception of the AES 10% storm). It is possible that the hydrograph translation and attenuation effects of the detention basin serve to reduce differences between continuous simulation and design storm results. This might also support the postulate of the previous chapter that basin connections, and routing reaches in particular (which translate and attenuate hydrographs) blur the differences between the two methods. Reductions may also be due to the fact that differences between design storm and continuous simulation methods in initial pond conditions are not as significant as the initial moisture conditions in previous comparisons. After most storms, the outflow of the pond calculated in continuous simulation will eventually drop to the inflow value, meaning that the initial conditions for subsequent storms are the same as for the design storm run (inflow=outflow).

CHAPTER 7: SUMMARY AND CONCLUSIONS

7.1 SUMMARY

This thesis has attempted to undertake a thorough and in-depth comparison of design storm and continuous simulation methods in estimating peak flow frequency distributions. As was suggested in Chapter 2, previous studies on the subject have failed to address a number of issues, such as a wider variety of design storm and basin types, as well as complex watershed systems and detention ponds. This thesis was intended to address these shortcomings, and expand research on the comparison of these two approaches. Several findings and observations have resulted from this work.

In the single-basin comparison of Chapter 4, a single urban and a single rural basin were used as an initial basis for comparing design storm and continuous simulation methods. It was found that errors between design storm and continuous simulation methods were much more prominent with the rural basin, particularly for lower return period storms. In general, it appears design storms are more likely to underestimate peak flows, as indicated by generally positive average MRE values. This was particularly true for rural basins. Several different design storm distributions were found to work well with both basin types: the AES 10% 12-hour storm, Huff 3rd and 4th quartile 6-hour storms, and the SCS Type-II 24-hour storm. Suitable storm durations were found to be longer

than the time of concentration of the basin. The most appropriate duration may vary, depending on the storm distribution. Longer duration storms are generally worse, as most are fixed distribution storms which result in lower peaks due to declining depths and finer storm discretization. Initial moisture conditions were found to be unimportant for continuous simulation results, given its continuous accounting of soil moisture deficits. Initial moisture conditions had a larger effect on the rural basin using the design storm method. The urban basin was relatively insensitive to changes in initial moisture conditions using the design storm approach, with the exception of the very dry condition. In general, average moisture deficit methods were found to be the most appropriate for basins of both types. Specifically, the SCS method and the summer average method were found to have the lowest errors.

Chapter 5 focused on the differences between design storm and continuous simulation results on a complex watershed system. Errors in the comparison appear to decrease as more basins are added and the watershed becomes more complex. The choice of design storm was still found to be an important consideration however, as the relatively constant error value at the outlet was still dependent on the original accuracy of the storm. The AES 10% storm displayed a significant increase in error as the watershed system became more complex – this may be due to the storm's tendency to over-estimate, and its rapidly peaking nature. The importance of the design storm initial moisture deficit was found to become less significant as the analysis became more complex as well.

Chapter 6 compared design storm and continuous simulation methods for a linear and a non-linear detention basin, with inflow from the single urban basin tested previously. Differences between peak flows estimated by the two methods were found to be significantly decreased at the outlet of the detention basin. Errors were roughly halved for most storms, with the exception of the AES 10% storm. This storm resulted in significant increases in error from the detention pond, possibly for the reasons previously mentioned (tendency to overestimate and rapid peak). Variation was also found in the peak reduction of the various storms, which suggests that the selection of an appropriate storm is necessary to properly match the peak reduction of continuous simulation. A variation in peak reduction was also found for different return period storms for the non-linear basin, even though overall errors and average peak reductions were very close to those of the linear detention basin.

7.2 CONCLUSIONS AND FUTURE RESEARCH

As was discussed in Chapter 2, the design storm concept has limitations. The assumption of equal return periods for rainfall and runoff is false, given that neither possesses a unique frequency. Despite this, the design storm continues to be used in practice. This thesis has demonstrated that its use in estimating flood frequency distributions is conditionally justified, despite these theoretical shortcomings. It appears that in practice, when appropriate parameters were

chosen, design storm results compare favourably with continuous simulation results. Given the design storm approach's simplicity, it is therefore frequently the first choice for water resources engineers in estimating flood frequency distributions. The following considerations should however be made:

1. The choice of design storm distribution is still very important. A poorly chosen distribution will lead to high errors regardless of the error reductions seen in more complex watersheds or detention ponds. An appropriate distribution representative of the local precipitation patterns should be chosen. In this thesis, Huff 50% 3rd and 4th quartile storms, the SCS Type-II 24-hour storm, and short duration Alternating-block storms were found to give the best results.
2. The use of average values for design storm parameters appears to yield consistently good results regardless of basin type or watershed complexity. As such, using average values for initial moisture deficits and perhaps even for design storm durations (i.e. the average duration of flood producing storms) tends to result in lower errors. This is appropriate not only for single basins, but for more complex watershed systems as well.
3. The results of this thesis should only be interpreted for the usage of design storms in estimating flood frequency distributions. This work did not consider other applications, such as estimating runoff event

volume. Design storms may well be ill-equipped to model other such parameters.

It should also be noted that this work considered continuous simulation results to be the better estimate of flood frequency distributions. As noted earlier, this is not necessarily always the case. There are certain design situations in which continuous simulation is not the appropriate modeling tool, and other approaches should be considered. One of the key problems with continuous simulation not considered in this work is the simplifying assumption of stationary watershed and climate conditions. This assumption means that the flood frequency distribution created by continuous simulation is not indicative of the true distribution when the watershed or the climate conditions are changing. Although necessary for this study, this shortcoming can potentially be overcome by appropriately adjusting land use parameters throughout the simulation – perhaps running the simulation for several shorter time periods rather than one long period. An alternative solution is to use a worst-case scenario, such as assuming land usage in accordance with final development plans.

The stationary climate assumption is questionable given recent research on global climate change. For design storm models, this can be accounted for by using updated IDF curves, which place a heavier emphasis on more recent rainfall events or utilize climate model results to estimate the anticipated shift in rainfall intensities. Continuous simulation models can also attempt to account for this by

focusing on more recent rainfall data. There is also the possibility of using climate model generated rainfall data within a continuous simulation model. However, current climate models do not output the spatial or temporal resolution necessary for accurate hydrologic modeling.

There are a number of other different avenues for future research on this subject – areas that this thesis was not able to examine. The analysis in this thesis should be repeated with other hydrologic modeling methods to determine what effects this would have. Perhaps a more complex continuous simulation soil moisture tracking method should be used, as well as a more non-linear infiltration and loss method (such as a Horton-type equation), in order to determine what differences might result. Even larger and more complex watersheds should also be tested. The effect of varying the rainfall time step should also be examined – 15 minute data instead of the hourly data used in this study. It would also be interesting to include more actual recorded streamflow data into the study to better verify the long-term performance of both approaches. The work in this thesis could also be expanded to examine other parameters, in particular runoff volume and time parameters.

REFERENCES

Adams, B. J., and Howard, C. D. D. (1986). "Design Storm Pathology". *Canadian Water Resources Journal.* 11(3), 49-55.

Akan, A. O. and Houghtalen, R. J. (2003). *Urban Hydrology, Hydraulics, and Stormwater Quality.* John Wiley and Sons Inc., Hoboken, NJ.

ASCE Task Committee on Glossary of Hydraulic Modeling. (1982). "Modeling Hydraulic Phenomena: A Glossary of Terms". *Journal of the Hydraulics Division*, 108(HY7), 845-52.

Beaudoin, P., Rousselle, J., and Marchi, G. (1983). "Reliability of the Design Storm Concept in Evaluating Runoff Peak Flow". *Water Resources Bulletin*, 19(3), 483-7.

Clarke, R. T. (1973). *Mathematical Models in Hydrology.* Food and Agriculture Organization of the United Nations, Rome, Italy.

Crawford, N. H., and Linsley, R. K. (1966). "Digital simulation in hydrology: the Stanford Watershed Simulation Model IV". *Department of Civil Engineering of Stanford University.* Technical Report no. 39.

Fleming, G. (1979). *Deterministic Models in Hydrology.* Food and Agriculture Organization of the United Nations, Rome, Italy.

Guo, Y. and Adams, B. J. (1998). "Hydrologic analysis of urban catchments with event-based probabilistic models". *Water Resources Research*, 34(12), 3421-31.

Hjelmfelt, A. T. (1985). "Negative Outflows from Muskingum Flood Routing". *J. Hydraulic Engineering ASCE*, 111(6), 1010-4.

Hogg, W. D. (1980). "Time Distribution of Short Duration Storm Rainfall in Canada". *Proceedings, Canadian Hydrology Symposium*, 80, 53-63.

Horton, R. E. (1940). "An Approach Toward a Physical Interpretation of Infiltration-Capacity". *Soil Science Society of America Proceedings.* 5, 399-417.

Huff, F. A. (1967). "Time Distribution of Rainfall in Heavy Storms". *Water Resources Research*, 3(4), 1007-19.

James, W. (1994). "Why Design Storm Methods have become Unethical". *Hydraulic Engeering: proceedings of the 1994 conference,* 2, 1203-7.

Kauffman, G. M.. (1987). *A Comparison for analytical and simulation models for drainage system design: SUDS versus STORM* (M.A.Sc. Thesis). University of Toronto, Toronto, Ontario.

Keifer, C. J. and Chu, H. H. (1957). "Synthetic Storm Pattern for Drainage Design". *Proceedings of the American Society of Civil Engineers*, Paper 1332, 1-25.

LeFever Kee, J., Paulanka, B. J., and Purnell, L. D. (2004). *Handbook of Fluid, Electrolyte, and Acid-Base Imbalances 2nd Edition.* Delmar Learning, Clifton Park NY.

Linsley, R., and Crawford, N. (1974). "Continuous Simulation Models in Hydrology". *Geophysical Research Letters*, 1(1), 59-62.

Maidment, D. R. (editor). (1992). *Handbook of Hydrology.* McGraw-Hill Inc., New York, NY.

Marsalek, J. (1978). "Research on the Design Storm Concept". *ASCE Urban Water Resources Research Program.* Technical Memorandum No. 33.

Marsalek, J., and Watt, W. E. (1984). "Design storms for urban drainage design". *Canadian Journal of Civil Engineering,* 11, 574-84.

McCarthy, G. T. (1938). "The Unit Hydrograph and Flood Routing". Unpublished manuscript presented at a Conference of the North Atlantic Division, U.S. Army Corps of Engineers, June 24.

McCuen, R. H., Wong, S. L., and Rawls, W. J. (1984). "Estimating Urban Time of Concentration". *Journal of Hydraulic Engineering*, 110(7), 887-904.

McCuen, R. H. (2005). *Hydrologic Analysis and Design 3rd Edition.* Pearson Prentice Hall, Upper Saddle River NJ.

Medina, M. A. (1986). "Use of Continuous Simulation Versus the Design Storm Concept for Water Quality". *Water Forum 1986: world water issues in evolution: proceedings of the conference.* 949-57.

Mulvaney, T. J. (1850). "On the use of self-registering rain and flood gauges in making observations of the relation of rainfall and flood discharges in a given catchment". *Proc. Inst. Of Civil Engineers of Ireland*, 4, 18-31.

Natural Resource Conservation Service. (2005). *Earth Dams and Reservoirs: Technical Release 60.* U.S. Department of Agriculture, Washington, DC.

Nnadi, F. N., Kline, F. X., Wray Jr., H. L., and Wanielista, M. P. (1999). "Comparison of Design Storm Concepts using Continuous Simulation with Short Duration Storms". *Journal of the American Water Resources Association,* 35(1), 61-72.

Packman, J. C., and Kidd, C. H. (1980). "A Logical Approach to the Design Storm Concept". *Water Resources Research*, 16(6), 994-1000.

Petrovic, J., and Despotovic, J. (1998). "Historical Rainfall for Urban Storm Drainage Design". *Water Science and Technology*, 37(11), 105-11.

Philips Planning and Engineering Limited. (1987). *Master Drainage Plan – Town of Ancaster.* Philips Planning and Engineering Limited, Burlington, Ontario.

Philips Planning and Engineering Limited. (2004). *City of Hamilton Criteria and Guidelines for Stormwater Infrastructure Design - Draft.* Philips Planning and Engineering Limited, Burlington, Ontario.

Ponce, V. M. (1989). *Engineering Hydrology: Principles and Practice.* Prentice Hall, Englewood Cliffs NJ.

Priestley, C.H.B., and R.J. Taylor. (1972). "On the assessment of surface heat flux and evaporation using large-scale parameters". *Monthly Weather Review*, 100(2), 81-92.

Seddon, J. A. (1900). "River Hydraulics". *Transactions ASCE*, 43, 179-229.

Sherman, L. K. (1932). "Stream-Flow from Rainfall by the Unit-Graph Method". *Eng. News-Rec.*, 108, 501-5.

Singh, V. P. (1988a) *Hydrologic Systems Volume I: Rainfall-Runoff Modeling*. Prentice Hall, Eaglewood Cliffs, NJ.

Singh, V. P. (1988b). *Hydrologic Systems Volume II: Watershed Modeling*. Prentice Hall, Eaglewood Cliffs, NJ.

Skaggs, R.W., and Khaleel, R. (1982). *Infiltration, Hydrologic modeling of small Watersheds*. American Society of Agricultural Engineers, St. Joseph, MI.

Soil Conservation Service. (1964). . *National Engineering Handbook: Chapter 10: Estimation of Direct Runoff from Storm Rainfall*. U.S. Department of Agriculture, Washington, DC.

Soil Conservation Service. (1972a). *National Engineering Handbook: Chapter 16: Hydrographs*. U.S. Department of Agriculture, Washington, DC.

Soil Conservation Service. (1972b). *National Engineering Handbook Chapter 15: Travel Time, Time of Concentration and Lag*, U.S. Department of Agriculture, Washington, DC.

Soil Conservation Service. (1986). *Urban Hydrology for Small Watersheds: Technical Release 55*. U.S. Department of Agriculture, Washington, DC.

Trenberth, K. E. (1999). "Conceptual framework for changes of extremes of the hydrologic cycle with climate change." *Climatic Change*, 42(1), 327-339.

United States Army Corps of Engineers. (2000). *Hydrologic Modeling System HEC-HMS Technical Reference Manual.* Hydrologic Engineering Center, Davis, CA.

Urbonas, B. (1979). "Reliability of Design Storms in Modelling". *International Symposium on Urban Storm Runoff.* 1-13.

Viessman Jr., W., and Lewis, G. L. (2003). *Introduction to Hydrology 5th Edition.* Pearson Prentice Hall, Upper Saddle River NJ.

Vukmirovic, V. and Despotovic, J. (1984). "Statistical methods of storm analysis". *Water Science and Technology,* 16(8/9), 85-92.

Wenzel Jr., H. G., and Voorhees, M. L. (1984). "An Evaluation of Urban Design Storm Sensitivity". *Water Science and Technology*, 16, 219-36.

Yen, B. C. and Chow V. T. (1980). "Design Hyetographs fro Small Drainage Structures". *Journal of the Hydraulics Division ASCE*, 106(HY6), 1055-76.

Yen, B. C. and Chow V. T. (1983). *Local Design Storm, Val. II: Report No FHWA/RD-82-064.* Federal Highway Administration, Washington, DC.

Zhengji Zhuge. (2005). *Inclusion of Flood Routing in the Analytical Probabilistic Model* (M.A.Sc Thesis). McMaster University, Hamilton, ON.

APPENDIX A: SYMBOLS AND NOTATION

A: Watershed area

B: Channel surface width

CN: SCS curve number

f_c: Constant rate of infiltration

i: Rainfall intensity

i_{avg}: Average rainfall intensity

i_p: Peak rainfall intensity

I: Inflow

I_a: Initial abstraction

IDF: Intensity-Duration-Frequency

$IETD$: Inter-Event Time Definition

K: Muskingum storage time constant

K_r: Baseflow recession constant

L: Hydraulic length

L_r: Reach length

$MARE$: Mean Absolute Relative Error

MRE: Mean Relative Error

O: Outflow

p: Precipitation

pe_t: Excess precipitation at time t

P: Excess precipitation

q_0: Initial discharge

q_p: Peak discharge

q_t: Discharge at time t

Q: Flow or runoff

Q_p: Peak flow

r: Advanceness of storm hyetograph

R^2: Coefficient of determination

RMSE: Root Mean Square Error

S: Maximum potential soil moisture retention

S_p: Average watershed slope

S_r: Storage

t_c: Time of concentration

t_d: Storm duration

t_l: Lag time

t_p: Time to hydrograph peak from beginning

T: Return period

U: Unit Hydrograph ordinate

UH: Unit Hydrograph

v_w: Flood wave velocity

V: Runoff volume

V_p: Rainfall volume

X: Muskingum weighting factor

y: Water depth

Δx: Distance step

Δt: Time step

APPENDIX B: ADDITIONAL TABLES

Table B1: Assumed soil infiltration rates

SCS Soil Type	SCS Transmission Rate (in/hr)	Assumed Infiltration Rate (in/hr)	Assumed Infiltration Rate (mm/hr)
A	0.30 - 0.45	0.38	9.65
AB		0.30	7.62
B	0.15 - 0.30	0.23	5.84
BC		0.15	3.81
C	0.05 - 0.15	0.10	2.54
CD		0.05	1.27
D	0.00 - 0.05	0.03	0.76

Table B2: Sub-catchment soil type percentages

		Percentage Soil Classification							
Sub-Catchment	Area (ha)	A	AB	B	BC	C	CD	D	Resulting Infiltration Rate (mm/hr)
101	76.6	60	8	10	22				7.8
102	44.4	52	11		37				7.3
103	137.4	45	17	8	13	17			7.0
104	101.7	32	34		31	3			6.9
105	67.3	56	21		23				7.9
106	81.4	77			23				8.3
107	48.1	68	8		24				8.1
108	33.8	69	26		5				8.8
109	46.3	13	56		31				6.7
110/111/113	31.8		83		17				7.0
112	22.7	28	11	26	35				6.4
114/116	35.2		75		25				6.7
115	21.5	19	12	46	23				6.3
117	21.5		34	26	40				5.6
118	29.7		41		17		42		4.3
119	27.0	5		90	5				5.9

Table B3: Lake Evaporation data

Month	April	May	June	July	August	September	October	Total
Lake Evaporation (mm/day)	2.5	3.4	4.1	4.3	3.5	2.2	0.9	
# of Days per month	30	31	30	31	31	30	31	
Monthly Evaporation (mm/mth)	75.0	105.4	123.0	133.3	108.5	66.0	27.9	639.1

Table B4: Basin times

Sub-Catchment	Area (ha)	CN (AMC-II)	Measured Longest Length (ft)	Average Slope of Watershed (ft/ft or m/m)	Time of Conc. (t_c in hours)	Min. Time Step (min)	0.13 * t_c (min)	0.17 * t_c (min)
101	76.6	65.8	4286	0.0041	3.9814	41.6	31.1	40.6
102	44.4	72.2	2929	0.0108	1.5139	15.8	11.8	15.4
103	137.4	66.9	4519	0.0055	3.4634	36.2	27.0	35.3
104	101.7	78.2	5269	0.0062	2.6843	28.0	20.9	27.4
105	67.3	71.7	3427	0.0145	1.5015	15.7	11.7	15.3
106	81.4	72.6	4369	0.0180	1.6007	16.7	12.5	16.3
107	48.1	59.2	3720	0.0155	2.1514	22.5	16.8	21.9
108	33.8	72.5	2607	0.0099	1.4275	14.9	11.1	14.6
109	46.3	62.6	3086	0.0234	1.3838	14.4	10.8	14.1
110/111/113	31.8	73.6	2597	0.0171	1.0517	11.0	8.2	10.7
112	22.7	66	2691	0.0221	1.1687	12.2	9.1	11.9
114/116	35.2	79.4	2753	0.0127	1.0765	11.2	8.4	11.0
115	21.5	78.8	3084	0.0137	1.1578	12.1	9.0	11.8
117	21.5	80	2106	0.0202	0.6777	7.1	5.3	6.9
118	29.7	82.2	2928	0.0202	0.8228	8.6	6.4	8.4
119	27.0	82.3	3371	0.0311	0.7391	7.7	5.8	7.5

Table B5: Reach routing parameters

Reach Number	Reach Length (m)	K (hrs)	X	1 - X	Δt (hrs)	0.5 Δt / K	K / Δt	Number of Subreaches
R10.1	600	0.62	0.05	0.95	0.17	0.135	3.70	4
R10.2	998	1.03	0.05	0.95	0.17	0.081	6.16	6
R10.3	766	0.79	0.05	0.95	0.17	0.106	4.73	5
R10.5	880	0.91	0.05	0.95	0.17	0.092	5.43	5
R10.7	366	0.38	0.05	0.95	0.17	0.221	2.26	2
R10.8	780	0.80	0.05	0.95	0.17	0.104	4.81	5
R11.2	510	0.52	0.05	0.95	0.17	0.159	3.15	3
R11.5	369	0.38	0.05	0.95	0.17	0.220	2.28	2
R11.7	499	0.51	0.05	0.95	0.17	0.162	3.08	3

Table B6: Final basin parameters

Sub-Catchment	Area (km^2)	CN (AMC-II)	Assumed Initial Deficit 0.2 *S* (mm)	Maximum Storage *S* (mm)	% Impervious
101	0.766	65.8	26.4	132.0	1.0
102	0.444	72.2	19.6	97.8	36.0
103	1.374	66.9	25.1	125.7	0.0
104	1.017	78.2	14.2	70.8	12.7
105	0.673	71.7	20.1	100.3	35.7
106	0.814	72.6	19.2	95.9	50.3
107	0.481	59.2	35.0	175.1	17.3
108	0.338	72.5	19.3	96.3	43.3
109	0.463	62.6	30.4	151.8	17.3
110/111/113	0.318	73.6	18.2	91 1	35.4
112	0.227	66.0	26.2	130.8	0.0
114/116	0.352	79.4	13.2	65.9	34.9
115	0.215	78.8	13.7	68.3	17.3
117	0.215	80.0	12.7	63.5	44.0
118	0.297	82.2	11.0	55.0	27.0
119	0.270	82.3	10.9	54.6	50.7

Table B7: Results of Single-basin comparison for Rural Basin 101

Storm Name	Storm Duration (hrs)	Peak Outflow (mm/hr) for Specified Return Period (years)					RMSE (mm/hr)	MRE (%)	MARE (%)
		57.0	28.5	14.3	8.1	3.0			
CONTINUOUS SIMULATION		**10.29**	**7.47**	**6.06**	**4.70**	**2.49**	**0.00**	**0.00%**	**0.00%**
AES 10%	12	10.62	9.40	7.47	5.45	2.30	1.13	-12.14%	15.16%
AES 30%	12	5.36	4.51	3.20	1.88	0.19	3.30	57.46%	57.46%
Alternating Block	3	7.71	6.96	6.44	4.14	0.42	1.53	24.17%	26.65%
Alternating Block	6	8.08	7.94	6.81	4.65	0.75	1.32	14.72%	22.19%
Alternating Block	12	8.60	8.18	7.38	5.17	1.46	1.13	3.36%	19.82%
Alternating Block	24	10.48	8.88	8.27	6.44	1.55	1.47	-11.28%	26.37%
Huff Q3	6	9.07	7.71	6.96	3.48	1.27	1.03	13.81%	20.96%
Huff Q3	12	6.20	5.31	3.95	2.54	0.56	2.62	45.38%	45.38%
Huff Q3	24	2.82	1.46	0.94	0.42	0.09	5.33	84.97%	84.97%
Huff Q4	6	9.68	8.32	7.52	4.09	1.97	0.88	0.87%	15.01%
Huff Q4	12	8.04	7.19	5.92	4.65	2.02	1.04	9.58%	9.58%
Huff Q4	24	5.22	3.48	2.82	2.11	0.52	3.54	58.10%	58.10%
SCS Dimensionless	6	6.72	5.50	4.89	2.07	0.56	2.39	42.77%	42.77%
SCS Dimensionless	12	5.36	4.46	3.34	2.11	0.38	3.22	54.61%	54.61%
SCS Type II	24	9.87	6.91	5.50	4.18	1.36	0.69	15.45%	15.45%
Triangular	3	6.34	5.87	5.22	2.77	0.38	2.33	39.92%	39.92%
Triangular	6	6.34	5.17	4.56	1.83	0.38	2.68	47.98%	47.98%
Triangular	12	2.91	2.26	1.32	0.52	0.09	5.05	81.00%	81.00%

Table B8: Results of Single-basin comparison for Urban Basin 106

Storm Name	Storm Duration (hrs)	Peak Outflow (mm/hr) for Specified Return Period (years)					RMSE (mm/hr)	MRE (%)	MARE (%)
		57.0	28.5	14.3	8.1	3.0			
CONTINUOUS SIMULATION		**21.80**	**21.54**	**16.45**	**13.80**	**10.88**	**0.00**	**0.00%**	**0.00%**
AES 10%	12	25.56	23.66	20.70	17.51	11.90	3.21	-17.84%	17.84%
AES 30%	12	12.78	11.68	10.00	8.18	5.22	7.54	43.83%	43.83%
Alternating Block	3	26.27	24.32	20.74	18.57	10.75	3.71	-18.58%	19.07%
Alternating Block	6	26.67	25.30	21.23	19.19	11.14	4.24	-22.07%	22.07%
Alternating Block	12	27.11	25.47	21.71	19.72	11.85	4.64	-25.30%	25.30%
Alternating Block	24	28.75	26.23	22.64	20.96	12.03	5.68	-30.75%	30.75%
Huff Q3	6	21.23	19.28	18.27	12.83	9.07	1.61	5.16%	9.57%
Huff Q3	12	12.96	11.90	10.30	8.54	5.48	7.29	42.09%	42.09%
Huff Q3	24	7.56	5.79	5.00	4.16	3.01	12.14	70.05%	70.05%
Huff Q4	6	19.81	18.00	16.98	12.16	8.80	2.18	10.66%	11.95%
Huff Q4	12	16.54	15.26	13.31	11.28	7.65	4.33	24.07%	24.07%
Huff Q4	24	11.99	9.60	8.45	7.25	4.47	8.80	51 10%	51.10%
SCS Dimensionless	6	20.96	18.84	17.69	12.34	8.71	1.81	7.87%	10.88%
SCS Dimensionless	12	17.29	16.01	13.80	11.41	7.39	3.90	22.38%	22.38%
SCS Type II	24	24.81	20.57	18.22	15.83	10.08	1.89	-5.49%	10.22%
Triangular	3	20.57	19.72	18.62	14.15	8.80	1.67	3.49%	9.79%
Triangular	6	15.43	13.89	13.05	8.98	6.24	5.58	32.61%	32.61%
Triangular	12	8.27	7.47	6.32	5.13	3.54	11.07	63.85%	63.85%

Table B9: Comparison of different moisture deficits for continuous simulation run on Rural Basin 101

Initial Moisture Estimate Method	Peak Outflow (mm/hr) for Specified Original Return Period (years) and Simulation Year					RMSE (mm/hr)	MRE (%)	MARE (%)
	57.0 (1968)	28.5 (1954)	14.3 (1960)	8.1 (1970)	3.0 (1944)			
SCS Method	**10.29**	**7.47**	**6.06**	**4.70**	**2.49**	**0.00**	**0.00%**	**0.00%**
Overall Average	10.29	7.47	6.06	4.70	2.49	0.00	0.00%	0.00%
Summer Average	10.29	7.47	6.06	4.70	2.49	0.00	0.00%	0.00%
Pre-Storm (IETD) Average	10.29	7.47	6.06	4.70	2.49	0.00	0.00%	0.00%
Fully Saturated	10.29	7.47	6.06	4.70	2.49	0.00	0.00%	0.00%
Very Dry	10.29	7.47	6.06	4.70	0.99	0.67	12.08%	12.08%

Table B10: Comparison of different moisture deficits for continuous simulation run on Urban Basin 106

Initial Moisture Estimate Method	Peak Outflow (mm/hr) for Specified Original Return Period (years) and Simulation Year					RMSE (mm/hr)	MRE (%)	MARE (%)
	57.0 (1941	28.5 (1968)	14.3 (1986)	8.1 (1951	3.0 (1992)			
SCS Method	**21.80**	**21.54**	**16.45**	**13.80**	**10.88**	**0.00**	**0.00%**	**0.00%**
Overall Average	22.16	21.54	16.45	13.80	10.88	0.16	-0.32%	0.32%
Summer Average	20.83	21.54	16.45	13.80	10.88	0.44	0.89%	0.89%
Pre-Storm (IETD) Average	19.64	21.54	16.45	13.80	10.88	0.97	1.99%	1.99%
Fully Saturated	22.16	21.54	16.72	13.80	10.88	0.20	-0.65%	0.65%
Very Dry	15.17	21.54	16.45	13.80	10.88	2.97	6.09%	6.09%

Table B11: Comparison of Design Storm results using different antecedent moisture conditions for Rural Basin 101

Storm Name	Initial Moisture Condition Method	Peak Outflow (mm/hr) for Specified Return Period (years)					RMSE (mm/hr)	MRE (%)	MARE (%)
		57.0	28.5	14.3	8.1	3.0			
CONTINUOUS SIMULATION		**10.29**	**7.47**	**6.06**	**4.70**	**2.49**	**0.00**	**0.00%**	**0.00%**
AES 10%	SCS Method	10.62	9.40	7.47	5.45	2.30	1.13	-12.14%	15.16%
Huff Q3	SCS Method	9.07	7.71	6.96	3.48	1.27	1.03	13.81%	20.96%
Huff Q4	SCS Method	9.68	8.32	7.52	4.09	1.97	0.88	0.87%	15.01%
SCS Type II	SCS Method	9.87	6.91	5.50	4.18	1.36	0.69	15.45%	15.45%
AVERAGE	**SCS Method**						**0.93**	**4.50%**	**16.64%**
AES 10%	Overall Average	12.13	10.86	8.93	6.91	3.57	2.41	-40.15%	40.15%
Huff Q3	Overall Average	10.10	8.93	8.27	4.79	2.49	1.19	-11.22%	11.95%
Huff Q4	Overall Average	10.25	9.07	8.41	5.22	2.91	1.31	-17.53%	17.72%
SCS Type II	Overall Average	10.67	8.46	7.14	5.78	2.77	0.84	-13.80%	13.80%
AVERAGE	**Overall Average**						**1.44**	**-20.68%**	**20.91%**
AES 10%	Summer Average	11.28	10.01	8.08	6.06	2.82	1.64	-23.82%	23.82%
Huff Q3	Summer Average	9.68	8.32	7.57	4.04	1.79	0.93	2.42%	16.87%
Huff Q4	Summer Average	10.10	8.79	8.04	4.56	2.35	1.07	-7.94%	12.13%
SCS Type II	Summer Average	10.57	7.61	6.20	4.84	1.93	0.30	2.54%	6.52%
AVERAGE	**Summer Average**						**0.98**	**-6.70%**	**14.84%**
AES 10%	Pre-Storm (IETD) Average	11.98	10.81	8.98	7.05	3.95	2.45	-43.53%	43.53%
Huff Q3	Pre-Storm (IETD) Average	10.34	9.12	8.46	5.45	3.38	1.40	-22.77%	22.77%
Huff Q4	Pre-Storm (IETD) Average	10.39	9.16	8.51	5.50	3.57	1.46	-24.85%	24.85%
SCS Type II	Pre-Storm (IETD) Average	10.67	8.46	7.38	6.34	3.81	1.21	-25.28%	25.28%
AVERAGE	**Pre-Storm (IETD) Average**						**1.63**	**-29.11%**	**29.11%**
AES 10%	Fully Saturated	15.56	14.29	12.31	10.20	6.58	5.66	-105.32%	105.32%
Huff Q3	Fully Saturated	10.39	9.16	8.51	5.45	3.52	1.45	-24.27%	24.27%
Huff Q4	Fully Saturated	10.39	9.16	8.51	5.50	3.57	1.46	-24.85%	24.85%
SCS Type II	Fully Saturated	10.67	8.46	7.38	6.34	4.04	1.26	-27.17%	27.17%
AVERAGE	**Fully Saturated**						**2.46**	**-45.40%**	**45.40%**
AES 10%	Very Dry	5.78	4.61	2.77	0.89	0.14	3.45	62.36%	62.36%
Huff Q3	Very Dry	4.28	2.91	2.30	0.14	0.14	4.41	74.56%	74.56%
Huff Q4	Very Dry	5.36	4.04	3.38	0.42	0.14	3.66	64.68%	64.68%
SCS Type II	Very Dry	4.42	1.60	0.28	0.14	0.14	5.07	84.48%	84.48%
AVERAGE	**Very Dry**						**4.15**	**71.52%**	**71.52%**

Table B12: Comparison of Design Storm results using different antecedent moisture conditions for Urban Basin 106

Storm Name	Initial Moisture Condition Method	Peak Outflow (mm/hr) for Specified Return Period (years)					RMSE (mm/hr)	MRE (%)	MARE (%)
		57.0	28.5	14.3	8.1	3.0			
CONTINUOUS SIMULATION		**21.80**	**21.54**	**16.45**	**13.80**	**10.88**	**0.00**	**0.00%**	**0.00%**
AES 10%	SCS Method	25.56	23.66	20.70	17.51	11.90	3.21	-17.84%	17.84%
Huff Q3	SCS Method	21.23	19.28	18.27	12.83	9.07	1.61	5.16%	9.57%
Huff Q4	SCS Method	19.81	18.00	16.98	12.16	8.80	2.18	10.66%	11.95%
SCS Type II	SCS Method	24.81	20.57	18.22	15.83	10.08	1.89	-5.49%	10.22%
AVERAGE	**SCS Method**						**2.22**	**-1.88%**	**12.39%**
AES 10%	Overall Average	25.74	23.84	20.87	17.69	12.16	3.38	-19.12%	19.12%
Huff Q3	Overall Average	21.23	19.33	18.27	13.05	9.33	1.51	4.31%	8.72%
Huff Q4	Overall Average	19.81	18.00	16.98	12.25	8.89	2.15	10.37%	11.66%
SCS Type II	Overall Average	24.81	20.57	18.53	16.14	10.39	2.00	-6.89%	10.48%
AVERAGE	**Overall Average**						**2.26**	**-2.83%**	**12.50%**
AES 10%	Summer Average	25.16	23.26	20.26	17.03	11.32	2.81	-14.80%	14.80%
Huff Q3	Summer Average	20.96	18.84	17.69	12.16	8.36	1.93	8.78%	11.79%
Huff Q4	Summer Average	19.77	17.91	16.89	11.94	8.49	2.31	11.78%	12.85%
SCS Type II	Summer Average	24.77	19.81	17.47	15.04	9.33	1.83	-1.30%	10.20%
AVERAGE	**Summer Average**						**2.22**	**1.11%**	**12.41%**
AES 10%	Pre-Storm (IETD) Average	24.63	22.64	19.64	16.28	10.61	2.26	-10.60%	11.57%
Huff Q3	Pre-Storm (IETD) Average	20.39	18.27	17.07	11.45	7.70	2.40	12.84%	14.34%
Huff Q4	Pre-Storm (IETD) Average	19.59	17.69	16.63	11.59	8.09	2.54	13.71%	14.14%
SCS Type II	Pre-Storm (IETD) Average	23.97	19.06	16.72	14.33	8.58	1.81	3.45%	9.61%
AVERAGE	**Pre-Storm (IETD) Average**						**2.25**	**4.85%**	**12.42%**
AES 10%	Fully Saturated	27.33	25.39	22.47	19.28	13.71	4.89	-29.11%	29.11%
Huff Q3	Fully Saturated	21.32	19.37	18.31	13.40	10.04	1.36	2.32%	6.84%
Huff Q4	Fully Saturated	19.86	18.00	17.03	12.34	9.11	2.09	9.74%	11.14%
SCS Type II	Fully Saturated	24.81	20.57	18.53	16.45	11.37	2.08	-9.12%	10.93%
AVERAGE	**Fully Saturated**						**2.61**	**-6.54%**	**14.50%**
AES 10%	Very Dry	20.03	17.87	14.64	11.68	8.76	2.40	14.22%	14.22%
Huff Q3	Very Dry	15.35	13.05	11.94	8.71	6.94	5.92	33.90%	33.90%
Huff Q4	Very Dry	16.85	14.59	13.40	8.27	6.55	5.13	30.68%	30.68%
SCS Type II	Very Dry	18.40	13.31	11.10	10.00	7.34	5.19	29.28%	29.28%
AVERAGE	**Very Dry**						**4.66**	**27.02%**	**27.02%**

Table B13: Summary of watershed comparison nodes

Basin Point	Contributing Area (km^2)	Percentage of Total Area Contributing	Incremental Increase in Drainage Area (km^2)
A29	8.264	100.00%	1.894
A14	6.370	77.08%	1.282
A08	5.088	61.57%	1.487
A05	3.601	43.57%	

Table B14: Results of full watershed comparison using SCS initial moisture deficit estimate

Storm Name	Basin Point	Peak Outflow (mm/hr) for Specified Return Period (years)					RMSE (mm/hr)	MRE (%)	MARE (%)
		57.0	28.5	14.3	8.1	3.0			
CONTINUOUS SIMULATION	**A05**	**10.25**	**8.01**	**6.16**	**4.96**	**2.98**	**0.00**	**0.00%**	**0.00%**
AES 10%	A05	11.15	9.99	8.22	6.37	3.54	1.50	-22.82%	22.82%
Huff Q3	A05	9.30	8.05	7.39	4.39	2.57	0.76	2.82%	11.03%
Huff Q4	A05	9.64	8.39	7.71	4.64	2.81	0.78	-2.35%	9.63%
SCS Type II	A05	9.98	7.44	6.25	5.08	2.78	0.30	2.53%	4.05%
AVERAGE	**A05**						**0.84**	**-4.96%**	**11.88%**
CONTINUOUS SIMULATION	**A08**	**8.62**	**7.06**	**6.52**	**4.74**	**3.48**	**0.00**	**0.00%**	**0.00%**
AES 10%	A08	10.17	9.30	7.99	6.61	4.29	1.65	-26.94%	26.94%
Huff Q3	A08	8.35	7.44	6.95	4.69	3.13	0.32	0.44%	5.20%
Huff Q4	A08	8.71	7.79	7.29	4.97	3.42	0.48	-5.26%	5.85%
SCS Type II	A08	8.58	7.04	6.20	5.36	3.30	0.32	-0.42%	4.82%
AVERAGE	**A08**						**0.70**	**-8.04%**	**10.70%**
CONTINUOUS SIMULATION	**A14**	**8.86**	**7.18**	**6.72**	**4.88**	**3.49**	**0.00**	**0.00%**	**0.00%**
AES 10%	A14	10.56	9.64	8.23	6.73	4.18	1.74	-26.71%	26.71%
Huff Q3	A14	8.63	7.70	7.17	4.72	3.09	0.38	0.67%	6.28%
Huff Q4	A14	8.78	7.85	7.35	4.93	3.30	0.42	-2.67%	5.25%
SCS Type II	A14	8.96	7.18	6.22	5.28	3.09	0.34	1.96%	5.70%
AVERAGE	**A14**						**0.72**	**-6.69%**	**10.98%**
CONTINUOUS SIMULATION	**A29**	**7.18**	**5.92**	**5.18**	**3.90**	**2.79**	**0.00**	**0.00%**	**0.00%**
AES 10%	A29	8.53	7.77	6.61	5.38	3.31	1.39	-26.77%	26.77%
Huff Q3	A29	6.94	6.19	5.76	3.77	2.48	0.34	0.46%	6.69%
Huff Q4	A29	6.96	6.22	5.82	3.87	2.59	0.34	-1.22%	5.66%
SCS Type II	A29	7.07	5.63	4.87	4.13	2.43	0.28	3.88%	6.30%
AVERAGE	**A29**						**0.59**	**-5.91%**	**11.35%**

Table B15: Results of full watershed comparison using summer average moisture deficit estimate

Storm Name	Basin Point	Peak Outflow (mm/hr) for Specified Return Period (years)					RMSE (mm/hr)	MRE (%)	MARE (%)
		57.0	28.5	14.3	8.1	3.0			
CONTINUOUS SIMULATION	**A05**	**10.25**	**8.01**	**6.16**	**4.96**	**2.98**	**0.00**	**0.00%**	**0.00%**
AES 10%	A05	11.24	10.06	8.26	6.35	3.19	1.52	-20.87%	20.87%
Huff Q3	A05	9.49	8.20	7.51	4.27	2.20	0.84	4.65%	14.39%
Huff Q4	A05	9.89	8.60	7.90	4.65	2.60	0.87	-2.61%	11.66%
SCS Type II	A05	10.32	7.60	6.30	4.99	2.22	0.39	5.42%	6.82%
AVERAGE	**A05**						**0.91**	**-3.35%**	**13.43%**
CONTINUOUS SIMULATION	**A08**	**8.62**	**7.06**	**6.52**	**4.74**	**3.48**	**0.00**	**0.00%**	**0.00%**
AES 10%	A08	9.60	8.74	7.46	6.11	3.88	1.15	-17.98%	17.98%
Huff Q3	A08	8.07	7.10	6.58	4.21	2.76	0.47	7.39%	7.94%
Huff Q4	A08	8.59	7.60	7.06	4.59	3.06	0.39	-0.04%	6.30%
SCS Type II	A08	8.54	6.72	5.84	4.97	2.94	0.43	5.37%	7.32%
AVERAGE	**A08**						**0.61**	**-1.32%**	**9.88%**
CONTINUOUS SIMULATION	**A14**	**8.86**	**7.18**	**6.72**	**4.88**	**3.49**	**0.00**	**0.00%**	**0.00%**
AES 10%	A14	10.25	9.35	7.97	6.52	4.08	1.50	-22.97%	22.97%
Huff Q3	A14	8.49	7.53	7.01	4.57	2.97	0.38	3.26%	6.91%
Huff Q4	A14	8.73	7.76	7.22	4.77	3.19	0.38	-0.62%	5.60%
SCS Type II	A14	9.09	7.08	6.11	5.17	3.00	0.39	3.26%	6.68%
AVERAGE	**A14**						**0.66**	**-4.27%**	**10.54%**
CONTINUOUS SIMULATION	**A29**	**7.18**	**5.92**	**5.18**	**3.90**	**2.79**	**0.00**	**0.00%**	**0.00%**
AES 10%	A29	8.36	7.62	6.48	5.28	3.27	1.27	-24.53%	24.53%
Huff Q3	A29	6.89	6.11	5.68	3.70	2.41	0.33	1.99%	7.12%
Huff Q4	A29	6.97	6.20	5.77	3.81	2.54	0.33	-0.39%	6.03%
SCS Type II	A29	7.22	5.60	4.83	4.06	2.34	0.30	4.70%	6.64%
AVERAGE	**A29**						**0.56**	**-4.56%**	**11.08%**

Table B16: Detention Pond Peak Flows for well-performing storms

Storm Name	Outflow Source	Peak Outflow (mm/hr) for Specified Return Period (years)					RMSE (mm/hr)	MRE (%)	MARE (%)
		57.0	28.5	14.3	8.1	3.0			
CONTINUOUS SIMULATION	**Basin 106**	**21.80**	**21.54**	**16.45**	**13.80**	**10.88**	**0.00**	**0.00%**	**0.00%**
AES 10%	Basin 106	25.56	23.66	20.70	17.51	11.90	3.21	-17.84%	17.84%
Huff Q3	Basin 106	21.23	19.28	18.27	12.83	9.07	1.61	5.16%	9.57%
Huff Q4	Basin 106	19.81	18.00	16.98	12.16	8.80	2.18	10.66%	11.95%
SCS Type II	Basin 106	24.81	20.57	18.22	15.83	10.08	1.89	-5.49%	10.22%
AVERAGE	**Basin 106**						**1.97**	**-0.23%**	**10.75%**
CONTINUOUS SIMULATION	**Linear Pond**	**12.60**	**10.84**	**10.39**	**7.25**	**5.71**	**0.00**	**0.00%**	**0.00%**
AES 10%	Linear Pond	15.26	14.06	12.25	10.30	7.08	2.53	-26.97%	26.97%
Huff Q3	Linear Pond	12.74	11.59	10.97	7.65	5.48	0.47	-3.03%	4.58%
Huff Q4	Linear Pond	12.83	11.63	10.97	7.83	5.66	0.52	-4.36%	4.67%
SCS Type II	Linear Pond	12.83	10.61	9.38	8.18	5.26	0.66	1.00%	6.83%
AVERAGE	**Linear Pond**						**1.05**	**-8.34%**	**10.76%**
CONTINUOUS SIMULATION	**Non-Lin. Pond**	**12.69**	**9.73**	**8.76**	**6.59**	**5.75**	**0.00**	**0.00%**	**0.00%**
AES 10%	Non-Lin. Pond	17.20	15.26	12.25	8.98	6.46	3.76	-38.32%	38.32%
Huff Q3	Non-Lin. Pond	12.65	10.70	9.64	6.68	5.53	0.60	-3.45%	5.13%
Huff Q4	Non-Lin. Pond	12.69	10.66	9.55	6.68	5.62	0.55	-3.53%	4.46%
SCS Type II	Non-Lin. Pond	12.65	8.98	7.34	6.90	5.48	0.74	4.83%	6.71%
AVERAGE	**Non-Lin. Pond**						**1.41**	**-10.12%**	**13.65%**

Table B17: Detention Pond Peak Flows for adequately-performing storms

Storm Name	Outflow Source	Peak Outflow (mm/hr) for Specified Return Period (years)					RMSE (mm/hr)	MRE (%)	MARE (%)
		57.0	28.5	14.3	8.1	3.0			
CONTINUOUS SIMULATION	**Basin 106**	**21.80**	**21.54**	**16.45**	**13.80**	**10.88**	**0.00**	**0.00%**	**0.00%**
Altern. Block 3-Hr	Basin 106	26.27	24.32	20.74	18.57	10.75	3.71	-18.58%	19.07%
Altern. Block 6-Hr	Basin 106	26.67	25.30	21.23	19.19	11.14	4.24	-22.07%	22.07%
Altern. Block 12-Hr	Basin 106	27.11	25.47	21.71	19.72	11.85	4.64	-25.30%	25.30%
Huff Q4 12-Hr	Basin 106	16.54	15.26	13.31	11.28	7.65	4.33	24.07%	24.07%
AVERAGE	**Basin 106**						**4.23**	**-10.47%**	**22.62%**
CONTINUOUS SIMULATION	**Linear Pond**	**12.60**	**10.84**	**10.39**	**7.25**	**5.71**	**0.00**	**0.00%**	**0.00%**
Altern. Block 3-Hr	Linear Pond	12.87	12.07	11.32	9.11	5.53	1.09	-9.00%	10.24%
Altern. Block 6-Hr	Linear Pond	13.18	12.83	11.63	9.51	5.79	1.48	-13.50%	13.50%
Altern. Block 12-Hr	Linear Pond	13.44	12.91	11.90	9.82	6.15	1.68	-16.69%	16.69%
Huff Q4 12-Hr	Linear Pond	10.84	10.00	8.71	7.39	5.09	1.19	9.40%	10.13%
AVERAGE	**Linear Pond**						**1.36**	**-7.45%**	**12.64%**
CONTINUOUS SIMULATION	**Non-Lin. Pond**	**12.69**	**9.73**	**8.76**	**6.59**	**5.75**	**0.00**	**0.00%**	**0.00%**
Altern. Block 3-Hr	Non-Lin. Pond	13.14	11.76	10.53	7.30	5.75	1.26	-11.07%	11.07%
Altern. Block 6-Hr	Non-Lin. Pond	13.58	12.91	11.06	7.61	5.84	1.86	-16.59%	16.59%
Altern. Block 12-Hr	Non-Lin. Pond	14.06	13.05	11.50	7.87	6.01	2.10	-20.06%	20.06%
Huff Q4 12-Hr	Non-Lin. Pond	9.24	7.87	7.08	6.50	5.22	1.92	15.21%	15.21%
AVERAGE	**Non-Lin. Pond**						**1.79**	**-8.13%**	**15.73%**